
Theses and Dissertations

Summer 2011

Rationale design of polymeric siRNA delivery systems

NaJung Kim
University of Iowa

Copyright 2011 NaJung Kim

This dissertation is available at Iowa Research Online: <http://ir.uiowa.edu/etd/1237>

Recommended Citation

Kim, NaJung. "Rationale design of polymeric siRNA delivery systems." PhD (Doctor of Philosophy) thesis, University of Iowa, 2011. <http://ir.uiowa.edu/etd/1237>.

Follow this and additional works at: <http://ir.uiowa.edu/etd>



Part of the [Biomedical Engineering and Bioengineering Commons](#)

RATIONAL DESIGN OF POLYMERIC SIRNA
DELIVERY SYSTEMS

by
NaJung Kim

An Abstract

Of a thesis submitted in partial fulfillment of the
requirements for the Doctor of Philosophy degree
in Biomedical Engineering
in the Graduate College of
The University of Iowa

July 2011

Thesis Supervisor: Associate Professor Aliasger K. Salem

ABSTRACT

Regulation of gene expression using small interfering RNA (siRNA) is a promising strategy for research and treatment of numerous diseases. However, siRNA cannot easily cross the cell membrane due to its inherent instability, large molecular weight and anionic nature. For this reason, a carrier that protects, delivers and unloads siRNA is required for successful gene silencing. The goal of this research was to develop a potential siRNA delivery system for *in vitro* and *in vivo* applications using cationic polymers, chitosan and polyethylenimine (PEI), poly(ethylene glycol) (PEG), mannose, and poly(D,L-lactic-co-glycolic acid) (PLGA). Furthermore, the delivery system was constructed in two different ways to explore the effect of mannose location in the structure. In the first approach, mannose and PEG were directly conjugated to the chitosan/PEI backbone, while mannose was connected to the chitosan/PEI backbone through PEG spacer in the second approach. First, the ability of modified chitosan polymers to complex and deliver siRNA for gene silencing was investigated. Despite the modified chitosan polymers successfully formed nanoplexes with siRNA, entered target cells and reduced cytotoxicity of unmodified chitosan, they showed limited gene silencing efficiency. For this reason, modified PEIs were examined to improve *in vitro* gene knockdown. The modified PEI polymers also complexed with siRNA and facilitated endocytosis of the nanoplexes. In addition, the modifications reduced inherent cytotoxicity of unmodified PEI without compromising the gene silencing efficiency on both mRNA and protein levels. Interestingly, we found that complexation of siRNA with PEI-PEG-mannose resulted in higher cell uptake and gene silencing than complexes made with mannose-PEI-PEG. Finally, the effect of sustained release of the mannosylated pegylated PEI/siRNA nanoplexes on gene silencing was tested by encapsulating the nanoplexes within PLGA microparticles. The modified PEIs enhanced the entrapment efficiency of siRNA into the particles and resulted in reduced initial burst

followed by sustained release. Incorporating the modified PEIs increased cellular uptake of siRNA, whereas it did not enhance *in vitro* gene knockdown efficiency due to the sustained release properties. The modified PEIs reduced the *in vitro* cytotoxicity and *in vivo* hepatotoxicity of the PLGA microparticles. In addition, encapsulating the nanoplexes into PLGA microparticles further reduced the cytotoxicity of PEI. Throughout the study, the second structure was proven more efficacious than the first structure in cellular uptake, gene silencing, siRNA encapsulation, and sustained release. We have developed novel polymeric siRNA delivery systems that enhance delivery efficiency and cellular uptake of siRNA. They have great potential for utility as a long-acting siRNA delivery system in biomedical research.

Abstract Approved:

Thesis Supervisor

Title and Department

Date

RATIONAL DESIGN OF POLYMERIC SIRNA
DELIVERY SYSTEMS

by
NaJung Kim

A thesis submitted in partial fulfillment of the
requirements for the Doctor of Philosophy degree
in Biomedical Engineering
in the Graduate College of
The University of Iowa

July 2011

Thesis Supervisor: Associate Professor Aliasger K. Salem

Copyright by
NAJUNG KIM
2011
All Rights Reserved

Graduate College
The University of Iowa
Iowa City, Iowa

CERTIFICATE OF APPROVAL

PH.D. THESIS

This is to certify that the Ph.D. thesis of

NaJung Kim

has been approved by the Examining Committee
for the thesis requirement for the Doctor of Philosophy
degree in Biomedical Engineering at the July 2011 graduation.

Thesis Committee: _____
Aliasger K. Salem, Thesis Supervisor

Nicole M. Grosland

Joon B. Park

Tae-Hong Lim

Mark A. Behlke

To my dearest grandmothers

ACKNOWLEDGMENTS

First, I am indefinitely indebted to my advisor Dr. Aliasger Salem for his wholehearted help throughout the development of my research. This work has been achieved solely for his guidance. He has always led me to point the right direction for the project. I owe my deep gratitude to Dr. Joon Park for his unconditional support and inspiration without which this work would have never been fulfilled. His insight has been invaluable to the progress of this study. I am truly grateful to Dr. Nicole Grosland for her willing support and advice whenever asked. Special thanks go to Dr. Mark Behlke for the continuous experimental support and valuable discussion. The molecular work completed in the IDT research lab has been critical to this study. I sincerely thank Dr. Tae-Hong Lim for keeping me maintain the engineering perspectives.

I thank all members of the Salem Lab including former members, Dr. Janjira Intra, Dr. Treniece Terry, Dr. Jessica Graham, Dr. Aiman Abbas, Dr. Yogita Krishnamachari, and Megan Pearce for their help in my early years in the lab. Dahai Jiang has collaborated with me in the joint project. Dr. Caitlin Lemke has been unfailingly kind enough to volunteer herself on the grand finale of my research, which could have never been completed without her help. Dr. Sean Geary, Vijaya Joshi, Dennison John, Sheetal D'mello, Kristan Sorenson, and Amaraporn Wongrakpanich have been pleasant to work with and helpful in every way they can. I have earned a valuable asset knowing and befriending all of them.

I wish to express my gratitude to Dr. Scott Rose, Kim Lennox, Ashley Jacobi, and Ashley Dvorak for helping me at the IDT research lab. Their expertise, helpful discussion and unlimited support on molecular work have fulfilled my research. I am also very appreciative of the staff at the Central Microscopy Research Facility, especially Jean Ross, Kathy Walters, and Chantal Allamargot, for lending their expertise in the completion of the research and sharing passion towards the research using microscopy.

My friends have helped me through my graduate program with their friendship and compassion. Some of them have supported me from Korea by phone calls and international care packages filled with love and snacks. Some have accompanied me surviving through the life in Iowa as graduate students, which could not be diminished. Their motivation and encouragement have challenged me to work harder.

Finally, I wish to express my profound thanks to my family for their endless love and prayers. My father always heartens me with books and music to become whoever I want to be. I receive from him the positive force to strive through hardships. The ultimate inspiration comes from my mother who enlightens me through her efforts to show me the right path. It is her devotion and wisdom that constantly drives me to do my best in every aspect of my life. I am truly blessed to have them as my parents. My heartfelt thanks also go to my stepparents, grandparents, and my siblings, for their immeasurable love and help. My family has given me emotional, financial and every other form of support to assist me in accomplishing my goal. They have never hesitated to provide me with whatever I requested, even when it was laughable. Their enduring love and faith have strengthened me along the way and sculpted me into a scientist. I am pleased to finally join the family tradition of PhDs.

ABSTRACT

Regulation of gene expression using small interfering RNA (siRNA) is a promising strategy for research and treatment of numerous diseases. However, siRNA cannot easily cross the cell membrane due to its inherent instability, large molecular weight and anionic nature. For this reason, a carrier that protects, delivers and unloads siRNA is required for successful gene silencing. The goal of this research was to develop a potential siRNA delivery system for *in vitro* and *in vivo* applications using cationic polymers, chitosan and polyethylenimine (PEI), poly(ethylene glycol) (PEG), mannose, and poly(D,L-lactic-co-glycolic acid) (PLGA). Furthermore, the delivery system was constructed in two different ways to explore the effect of mannose location in the structure. In the first approach, mannose and PEG were directly conjugated to the chitosan/PEI backbone, while mannose was connected to the chitosan/PEI backbone through PEG spacer in the second approach. First, the ability of modified chitosan polymers to complex and deliver siRNA for gene silencing was investigated. Despite the modified chitosan polymers successfully formed nanoplexes with siRNA, entered target cells and reduced cytotoxicity of unmodified chitosan, they showed limited gene silencing efficiency. For this reason, modified PEIs were examined to improve *in vitro* gene knockdown. The modified PEI polymers also complexed with siRNA and facilitated endocytosis of the nanoplexes. In addition, the modifications reduced inherent cytotoxicity of unmodified PEI without compromising the gene silencing efficiency on both mRNA and protein levels. Interestingly, we found that complexation of siRNA with PEI-PEG-mannose resulted in higher cell uptake and gene silencing than complexes made with mannose-PEI-PEG. Finally, the effect of sustained release of the mannosylated pegylated PEI/siRNA nanoplexes on gene silencing was tested by encapsulating the nanoplexes within PLGA microparticles. The modified PEIs enhanced the entrapment efficiency of siRNA into the particles and resulted in reduced initial burst

followed by sustained release. Incorporating the modified PEIs increased cellular uptake of siRNA, whereas it did not enhance *in vitro* gene knockdown efficiency due to the sustained release properties. The modified PEIs reduced the *in vitro* cytotoxicity and *in vivo* hepatotoxicity of the PLGA microparticles. In addition, encapsulating the nanoplexes into PLGA microparticles further reduced the cytotoxicity of PEI. Throughout the study, the second structure was proven more efficacious than the first structure in cellular uptake, gene silencing, siRNA encapsulation, and sustained release. We have developed novel polymeric siRNA delivery systems that enhance delivery efficiency and cellular uptake of siRNA. They have great potential for utility as a long-acting siRNA delivery system in biomedical research.

TABLE OF CONTENTS

LIST OF TABLES	xi
LIST OF FIGURES	xii
CHAPTER 1: INTRODUCTION AND BACKGROUND	1
Gene Therapy.....	1
Gene Therapy with RNAi	1
Small interfering RNA (siRNA).....	2
Viral Gene Delivery.....	3
Non-viral Gene Delivery.....	4
Chitosan.....	4
Polyethylenimine (PEI)	6
Poly(ethylene glycol) (PEG)	7
Mannose	8
Poly(D,L-lactic-co-glycolic acid) (PLGA).....	9
Targeted siRNA Delivery	10
Summary and Objectives	10
CHAPTER 2: MATERIALS AND METHODS	16
Polymer/siRNA Nanoplex Preparation.....	16
Size Distribution and Surface Morphology Observation by Scanning Electron Microscopy (SEM)	17
SiRNA Retardation Analysis by Ethidium Bromide Gel Electrophoresis	18
Intracellular Trafficking by Confocal Laser Scanning Microscopy	18
<i>In Vitro</i> Gene Knockdown Analysis by Luciferase Protein Expression.....	19
<i>In Vitro</i> Gene Knockdown Analysis by Real-Time Polymerase Chain Reaction (PCR).....	19
Cytotoxicity Evaluation using MTS Assay	21
Flow Cytometry and FACS Analysis	21
Animal Care and Handling	22
<i>In Vivo</i> Gene Knockdown Analysis in Mouse Model	22

CHAPTER 3 : SIRNA DELIVERY SYSTEM COMPOSED OF CHITOSAN,
POLY(ETHYLENE GLYCOL) AND MANNOSE28

Introduction.....	28
Materials and Methods.....	29
Materials.....	29
Pegylation and Mannosylation of Chitosan.....	29
Confirmation of Pegylation and Mannosylation.....	30
Quantification of Mannose Content.....	31
Cell Culture.....	31
Amplification and Purification of pDNA.....	31
Preparation of Chitosan/siRNA Nanoplexes.....	32
Size Distribution and Surface Morphology Analysis.....	32
SiRNA Retardation Ability.....	33
Intracellular Trafficking.....	33
<i>In vitro</i> Gene Knockdown Efficiency on Protein Expression.....	33
Cytotoxicity Evaluation.....	34
Statistical Analysis.....	35
Results.....	35
Pegylation and Mannosylation of Chitosan are Verified.....	35
Mannose Quantity is Determined.....	35
Nanoplexes are Spherical and Coarse in Appearance.....	36
Modified Chitosan Polymers Complex and Retard siRNA Migration.....	36
Modified Chitosan/siRNA Nanoplexes are Endocytosed by RAW264.7 Cells.....	37
Modifications of Chitosan Do Not Reduce Gene Knockdown Efficiency.....	37
Modifications of Chitosan Reduce Cytotoxicity.....	38
Discussion.....	38

CHAPTER 4 : SIRNA DELIVERY SYSTEM COMPOSED OF
POLYETHYLENIMINE, POLY(ETHYLENE GLYCOL) AND MANNOSE57

Introduction.....	57
Materials and Methods.....	58
Materials.....	58
Pegylation and Mannosylation of PEI.....	58
Confirmation of Pegylation and Mannosylation.....	59
Quantification of Mannose Content.....	59
Cell Culture.....	59
Amplification and Purification of pDNA.....	59
Preparation of PEI/siRNA Nanoplexes.....	59
Size Distribution and Surface Morphology Analysis.....	60
SiRNA Retardation Ability.....	60
Intracellular Trafficking.....	60

<i>In Vitro</i> Gene Knockdown Efficiency on mRNA Expression	60
<i>In Vitro</i> Gene Knockdown Efficiency on Protein Expression	61
Cytotoxicity Evaluation	61
Statistical Analysis.....	61
Results.....	61
Pegylation and Mannosylation of PEI are Verified	61
Mannose Quantity is Determined	62
Nanoplexes are Spherical and Coarse in Appearance.....	62
Modified PEI Polymers Complex and Retard siRNA Migration	63
Modified PEI/siRNA Nanoplexes are Endocytosed by RAW264.7 Cells	64
Modifications of PEI Improve Gene Knockdown Efficiency.....	64
Modifications of PEI Significantly Reduce Toxicity.....	66
Discussion	66

CHAPTER 5: THERAPEUTIC PLGA MICROPARTICLES INCORPORATING THE MODIFIED PEI/SIRNA NANOPLEXES.....88

Introduction.....	88
Materials and Methods.....	89
Materials	89
Preparation of Modified PEI/siRNA Nanoplexes-Loaded PLGA Microparticles	89
Evaluating Encapsulation Efficiency (EE)	90
Evaluating EE using Fluorescent PLGA Microparticles	90
Size Distribution and Surface Morphology Analysis	91
<i>In Vitro</i> Release Profile of siRNA from PLGA Microparticles.....	91
Intracellular Trafficking.....	92
Construction of EGFP-Expressing HEK293 Cell Line	92
Evaluating <i>In Vitro</i> Gene Knockdown Efficiency	93
Cytotoxicity Evaluation	93
Evaluating <i>In Vivo</i> Gene Knockdown Efficiency in Mouse Model	93
Liver toxicity Evaluations by AST and ALT Serum Concentrations	95
Statistical Analysis.....	95
Results.....	95
Incorporating Modified PEIs Enhances EE of siRNA into PLGA Microparticles	95
PLGA Microparticles have Smooth Surface and Sufficient Size for Cellular Uptake	96
Sustained Release Profile is Improved by Incorporating Modified PEI.....	97
PLGA Microparticles are Endocytosed at 24 hours Post-Transfection	97
Incorporating Modified PEI Do Not Enhance <i>In Vitro</i> Gene Knockdown Efficiency	98
PLGA Microparticles Display Very Low <i>In Vitro</i> Cytotoxicity	99

Incorporating Modified PEI Do Not Improve <i>In Vivo</i> Gene Knockdown Efficiency in Mouse Model	99
PLGA Microparticles Display No Significant Hepatotoxicities.....	100
Discussion	101
CHAPTER 6: CONCLUSIONS AND FUTURE DIRECTIONS	136
REFERENCES	140

LIST OF TABLES

Table 3-1:	Molecular structures of two different constructs using chitosan, PEG, and mannose, and schematics of nanoplexes once complexed with siRNA	43
Table 3-2:	Chitosan/PEG molar ratio and mannose content of the various modified chitosan (CS) polymers	44
Table 4-1:	Molecular structures of two different constructs using PEI, PEG, and mannose, and schematics of nanoplexes once complexed with siRNA	72
Table 4-2:	PEI/PEG molar ratio and mannose content of the various modified PEI polymers.....	73
Table 4-3:	Hydrodynamic size and zeta potential of the modified PEI polymer/siRNA nanoplexes	74
Table 5-1:	The effect of modified PEI incorporation on the encapsulation efficiency of the PLGA microparticles	110
Table 5-2:	The mouse injection groups used to evaluate <i>in vivo</i> gene delivery efficiency of the various PLGA microparticle formulations in comparison to polymer/siRNA nanoplexes	110

LIST OF FIGURES

Figure 1-1:	Schematic of a RNA interference (RNAi) process	12
Figure 1-2:	Molecular structures of chitosan, polyethylenimine (PEI), poly(ethylene glycol) (PEG), mannose, and poly(D,L-lactic-co-glycolic acid) (PLGA).....	14
Figure 2-1:	Map of psiCHECK TM -2 vector encoding two reporter genes, firefly and Renilla luciferase, for quantitative RNAi studies	24
Figure 2-2:	Principle of real-time polymerase chain reaction (PCR) process using Taqman probe.....	26
Figure 3-1:	¹ H NMR spectra of the modified chitosan polymers confirming the presence of chitosan, PEG, and mannose in each construct	45
Figure 3-2:	Scanning Electron Microscopy (SEM) images demonstrating the effect of pegylation and mannosylation on the size distribution and surface morphology of the modified chitosan/siRNA nanoplexes	47
Figure 3-3:	The effect of pegylation and mannosylation on siRNA retardation ability of the modified chitosan polymers using ethidium bromide agarose gel electrophoresis	49
Figure 3-4:	Confocal microscope images demonstrating the effect of pegylation and mannosylation on cellular uptake and intracellular localization of the modified chitosan/siRNA nanoplexes in RAW264.7 cells.....	51
Figure 3-5:	The effect of pegylation and mannosylation on luciferase gene knockdown efficiency of the modified chitosan/siRNA nanoplexes in RAW264.7 cells.....	53
Figure 3-6:	The effect of pegylation and mannosylation on cytotoxicity of the modified chitosan/siRNA nanoplexes in RAW264.7 cells.....	55
Figure 4-1:	¹ H NMR spectra of the modified PEI polymers confirming the presence of PEI, PEG, and mannose in each construct.....	75
Figure 4-2:	Scanning Electron Microscopy (SEM) images demonstrating the effect of pegylation and mannosylation on the size distribution and surface morphology of the modified PEI/siRNA nanoplexes.....	78

Figure 4-3:	The effect of pegylation and mannosylation on siRNA retardation ability of the modified PEI polymers using ethidium bromide agarose gel electrophoresis	80
Figure 4-4:	Confocal microscope images demonstrating the effect of pegylation and mannosylation on cellular uptake and intracellular localization of the modified PEI/siRNA nanoplexes in RAW264.7 cells	82
Figure 4-5:	The effect of pegylation and mannosylation on gene knockdown efficiency of the modified PEI/siRNA nanoplexes demonstrated for luciferase protein and HPRT mRNA expression in RAW264.7 cells	84
Figure 4-6:	The effect of pegylation and mannosylation on cytotoxicity of the modified PEI/siRNA nanoplexes in RAW264.7 cells	86
Figure 5-1:	Microparticle formulation technique using double emulsion, solvent evaporation method.....	111
Figure 5-2:	Map of pEGFP-C1 vector encoding enhanced green fluorescence protein (EGFP) utilized for <i>in vitro</i> gene knockdown study.....	113
Figure 5-3:	EGFP stably expressing HEK293 cells constructed for <i>in vitro</i> gene knockdown study	115
Figure 5-4:	Confocal microscopy images and flow cytometry analyses demonstrating the effect of the modified PEI incorporation into the PLGA microparticles on encapsulation efficiency of Cy3-labeled fluorescent RNA	117
Figure 5-5:	Scanning Electron Microscopy (SEM) images demonstrating the effect of the modified PEI incorporation on the size distribution and surface morphology of the various PLGA microparticles	119
Figure 5-6:	The effect of the modified PEI incorporation on <i>in vitro</i> release profile of siRNA from the polymer/siRNA nanoplexes-loaded PLGA microparticles in PBS, pH 7.4.....	121
Figure 5-7:	Confocal microscope images demonstrating the effect of the modified PEI incorporation on cellular uptake and intracellular localization of the PLGA microparticles	123
Figure 5-8:	The effect of the modified PEI incorporation on <i>in vitro</i> gene knockdown efficiency of the PLGA microparticles in EGFP-HEK293 cells	125

Figure 5-9:	The effect of the modified PEI incorporation on cytotoxicity of the PLGA microparticles in HEK293 cells.....	127
Figure 5-10:	Analyzing the quality and quantity of the total RNA from the mouse organs administrated with the PLGA microparticles.....	129
Figure 5-11:	The effect of the modified PEI incorporation in PLGA microparticles on <i>in vivo</i> gene knockdown efficiency in mouse model.....	132
Figure 5-12:	The effect of the modified PEI incorporation in PLGA microparticles on hepatotoxicity in mouse model.....	134

CHAPTER 1: INTRODUCTION AND BACKGROUND

Gene Therapy

The idea of regulating gene expression for the treatment of genetic disorders emerged decades ago. Gene therapy aimed to transfer a functional gene to replace or repair a defected gene for the treatment of a disease. Introducing functional genes as a treatment for a disease was first established when the first gene therapy clinical trial for adenosine deaminase (ADA) deficiency via a viral carrier succeeded.¹ Encouraged by the success of this trial, another clinical trial for the treatment of melanoma was conducted and proven safe.² It resulted in numerous subsequent clinical trials primarily for treating cancer such as melanoma, ovarian carcinoma, sarcoma, brain tumor and lung cancer.³⁻¹⁰ There is tremendous potential for the application of gene therapy to inherited or acquired genetic disorders including cancer, AIDS, cardiopathies, and neurologic disorders.¹¹ For example, gene therapies are being developed to treat cancer using strategies such as restricting proliferation of cancer cells, regulating angiogenesis, and stimulating an immune response to attack cancerous cells. These strategies can be used in combination with surgery, chemotherapy, or hormone therapy. There are, as with the development of any drug, issues of gene target selection, route of administration, dosing and, in particular, the scaling-up from preclinical models to clinical trials.¹²

Gene Therapy with RNAi

Gene therapy using RNA interference (RNAi) machinery has a significant potential for treatment of various diseases, as well as a tool for biomedical research.^{13, 14} RNAi is a natural cellular mechanism by which a specific mRNA is targeted for degradation with the purpose of decreasing the synthesis of the encoded protein.^{15, 16} It was discovered that long double-stranded RNAs (dsRNAs) reduced the translation of complementary mRNAs in *Caenorhabditis elegans*.¹⁷ Since the discovery, dsRNAs have been applied in research to take advantage of RNAi by inhibiting specific genes.^{18, 19} In

addition to RNAi, long dsRNAs cause antiviral immune responses in higher organisms, such as induction of type 1 interferon (IFN) and IFN-stimulated genes.²⁰ Therefore, siRNAs, the shortened form of dsRNAs, are utilized in place of dsRNAs and stimulate RNAi with significantly reduced antiviral immune responses.²¹ It has been used in various research fields for diagnostic or therapeutic purposes.^{22, 23}

RNAi relies on an intracellular multistep process. (Figure 1-1) RNA can be introduced into cells in various forms such as by itself, dsRNA, short-hairpin RNA (shRNA), or plasmid DNA (pDNA). When introduced as pDNA or shRNA, it is transcribed and processed into dsRNA. Then the dsRNA is cut by an endoribonuclease called Dicer into smaller siRNAs.^{24, 25} Then, siRNAs enter the multi-protein cluster, RNA induced silencing complex (RISC).²⁶ By recognizing the least stable 5' end of the double strand, RNA helicase in the RISC unwinds double-stranded siRNA into single strands. One strand of the duplex (the passenger strand) is cleaved and discarded. The other strand (the guide strand) is retained and directs a sequence-specific hybridization to the target mRNA which has the complementary sequence to the guide strand.²⁷⁻²⁹ This process leads to the specificity of the RNAi silencing. The target mRNA is cleaved by RISC and rapidly degraded due to its unprotected ends.³⁰⁻³² The RISC is recycled for subsequent rounds leading this process to the selective silencing in the target mRNA, which in turn results in decreased expression of the target gene. Selectively silencing post-transcriptional mRNA by RNAi represents a promising new approach for the inhibition of gene expression *in vitro* and *in vivo*.¹⁷

Small interfering RNA (siRNA)

SiRNA, 21-27 base-pair (bp) double-stranded RNA, plays a crucial role in initiating the RNAi mechanism.^{21, 33, 34} Synthetic siRNA drugs are built to mimic natural siRNAs and take advantage of the natural RNAi system in a consistent and predictable manner. Since siRNA enters the RNAi pathway at a later stage than long dsRNA or

shRNA does, siRNA is less likely to cause adverse side effects.^{35,36} However, the delivery of siRNA has faced a few challenges. Its backbone contains an extra hydroxyl group which, unlike DNA, makes RNA more vulnerable to hydrolysis by serum nucleases. Nucleases cleave along the phosphodiester backbone and lead to rapid degradation of the nucleic acids in plasma and cytoplasm. This process results in a shorter half-life of the nucleic acids.³⁷ Furthermore, siRNA cannot passively diffuse through the cellular membrane by itself due to its inherent instability, large molecular weight (about 13kDa), and polyanionic nature.³⁸⁻⁴³ Because of these limitations, native siRNA has low delivery efficiencies.^{14,44} To overcome this challenge, both viral and non-viral carriers have been developed to facilitate siRNA delivery.^{16,45} There are several requirements to be a good candidate for siRNA delivery. It should be able to (i) bind and condense siRNA protecting against enzymatic degradation,⁴⁶ guide siRNA to target cells and facilitate intracellular uptake, followed by (iii) escape from the lysosome into the cytosol, (iv) and finally promote efficient gene silencing.⁴⁷

Viral Gene Delivery

To transfer genes efficiently into the cells, two types of techniques are utilized; viral and non-viral vectors.⁴⁸ Viral vectors are universal tools in molecular biology that are used to deliver genetic materials into cells. Viral vectors capitalize on the molecular mechanism of virus to transport their genomes inside the cells.⁴⁹ Reliable viral vectors should have very little effect on the physiology of the infected cell to ensure the replication of the inserted genomes. Numerous clinical trials for AIDS vaccines utilize viral vectors as carriers.⁵⁰⁻⁵⁴ Viral vectors result in a strong transfection efficiency because viruses are programmed to recognize certain cells and insert their DNA into them. Since they are originated from pathogenic viruses, viral vectors are modified to minimize the risk of handling and adverse effects. Viral vectors are based on a variety of viruses such as retrovirus, adeno-associated virus (AAV), adenovirus, herpes simplex

virus (HSV), lentivirus, human cytomegalovirus (CMV), Epstein-Barr virus (EBV), poxvirus, negative-strand RNA virus (influenza virus), alphavirus, and herpesvirus saimiri.^{11, 55} Viral vectors such as adenoviruses and retroviruses have been proven very effective as delivery systems.⁵⁶

However, there are issues associated with immunogenicity and potential oncogenicity of viral vectors due to their inherent instability.⁵⁷ Concerns about inadvertent gene expression changes following random integration into the host genome still remain.^{58, 59} Difficulties in large-scale production of viruses limit the practical application.⁶⁰ For these reasons, non-viral vectors such as liposomes or polymer complexes have been harnessed to deliver genes with reduced adverse effects and limitation of production relative to viral vectors.

Non-viral Gene Delivery

Non-viral carriers have been of interest for siRNA delivery because they are easy to handle and they generate reduced specific immune responses relative to viral carriers. The potential for large-scale production also favors non-viral delivery of siRNA. Countless studies on DNA delivery have proven that cationic polymers as carriers are effective *in vitro* and *in vivo* gene expression. However, the extra vulnerability of RNA to enzymatic degradation has more challenges to cationic polymer-mediated RNA transfer than it does to conventional pDNA delivery. Moreover, due to the difference in structure and size of siRNA from that of pDNA, the different formulation parameters need to be optimized in regards to the physical and biological features of the polymer/siRNA polyplexes.⁴⁷

Chitosan

Chitosan is obtained from deacetylation of chitin, which is found abundantly in crustaceans and fungi. It is a natural cationic polysaccharide in neutral or basic pH conditions composed of beta (1–4) linked D-glucosamine (GlcN; D-unit) and N-acetyl-D-

glucosamine units (GlcNAc; A-unit).⁶¹ (Figure 1-2A) The pKa of these amino groups is about 6.5, allowing the majority of them to be protonated at pH 5.5 and therefore solubilized in an acidic solution.⁶² In the physiological environment, chitosan can be digested either by lysozymes or by chitinases in human intestine and in the blood.⁶²⁻⁶⁴ The primary amines in the chitosan backbone become positively charged in an aqueous acidic solution. This process enables chitosan to bind to negatively charged siRNA via electrostatic interactions and spontaneously form nano-sized complexes.⁶⁵ Chitosan nanoplex condenses and protects encapsulated genes from nuclease degradation as a three-dimensional carrier.⁶⁶ It is neutralized, positively charged at physiological pH, and hydrophobic chitosan becomes insoluble. This unique property ensures nanoparticles formed at low pH to remain physically stable at body pH without chemical crosslinking.⁶⁷ Moreover, its protonable amino groups help endosomal escape by buffering acidification. Chitosan is a good candidate in a variety of biomedical applications including controlled release, tissue engineering, weight loss supplement, and wound dressing, etc.⁶⁸⁻⁷⁰ In particular, chitosan has great potential in gene delivery due to the nucleic acid binding affinity and biocompatibility.^{46, 71-73}

The molecular weight of chitosan influences the physicochemical properties and *in vitro* gene silencing efficiency of chitosan/siRNA nanoplexes. Nanoplex should be stable for extracellular siRNA protection; however, disassembly of the nanoplex is required to release siRNA for subsequent interaction with RISC. A balance between these two prerequisites is to be optimized.⁴⁷ Lower molecular weight chitosan (110kDa) formed smaller complexes with siRNA compared to higher molecular weight chitosan (270kDa).⁷⁴ Chitosan molecules that had 5-10 times (64.8-170kDa) the length of siRNA (13.36kDa) could form stable complexes with siRNA through electrostatic interactions resulting in high gene silencing efficiency. In contrast, low molecular weight chitosan (10kDa) could not complex and compact siRNA into stable particles, resulting in large aggregates and very little knockdown.⁷⁵ Therefore, higher molecular weights of chitosan

is a significant factor for gene knockdown using siRNA delivery. The concentration of chitosan also affects the properties of the complexes. The mean particle size and surface charge of chitosan/siRNA complexes are increased proportionally to the increased concentration of chitosan.⁷⁴ A high degree of deacetylation has been reported to increase net positive charge of polymer building a greater siRNA binding capacity.⁷⁵ Chitosan forms smaller complexes with siRNA prepared at higher N/P ratios over 50 (N/P ratio represents the ratio of amino groups (N) in chitosan to phosphate groups (P) in siRNA)⁷⁶ and results in improved gene silencing efficiency relative to chitosan/siRNA complexes prepared at lower N/P ratios.⁷⁵

Polyethylenimine (PEI)

Polyethylenimine (PEI) is a synthetic cationic polymer that has been investigated as a potential non-viral delivery vehicle for oligonucleotides, siRNA and plasmid DNA *in vitro* and *in vivo*.^{44, 59, 77-85} It is one of the most densely charged polymers, because one third of the atoms are nitrogen and one sixth of these nitrogen atoms carry a positive charge at physiological pH. (Figure 1-2B) The protonable amino group at every third atom provides two important properties of PEI. First, PEI can condense nucleic acids and form positively charged complexes by electrostatic interactions. The other is effective buffering capacity of PEI at most pH.^{82, 86} As a result, it enables the proton sponge effect over a wide range of pH. After being endocytosed, PEI buffers the acidification within the endosome causing endosomal chloride accumulation. This leads to osmotic swelling and rupture, which allows for endosomal escape of the PEI/siRNA polyplexes.⁸⁰ The cationic PEI comes in two forms: linear and branched. Linear PEI provides efficient gene delivery on account of the less condense complex, which enables faster dissociation of the cargo than branched PEI.⁸⁷ Linear PEI is less cytotoxic than branched PEI.⁸⁸ Branched PEI has a ratio of primary:secondary:tertiary amine groups close to 1:1:1, which allows the branched PEI more buffering capacity relative to linear PEI.^{89, 90}

Branched PEI with higher molecular weights has shown great success for *in vitro* transfections since it condenses nucleic acids more efficiently than the linear PEI.^{91, 92}

Although the cationic polymer PEI has promising potential as a gene delivery vehicle, it is also associated with higher toxicity compared to other non-viral vectors.^{44, 82, 93-96} Toxicity and transfection efficiency of PEI depend on its molecular weight. When PEI has higher molecular weight and degrees of branching, it condenses siRNA more strongly causing higher delivery efficiency and higher toxicity.^{92, 97-100} Low molecular weight polycations have shown less cytotoxicity, but they are less efficient at transfecting cells.¹⁰¹ Finding a suitable size of PEI can balance delivery efficiency and toxicity. Cytotoxicity of PEI triggers cell death through both necrosis and apoptosis.^{100, 102, 103} The toxicity can be reduced by chemical modification with hydrophilic moieties like poly(ethylene glycol) (PEG).^{83, 84, 104-108}

The characteristics of PEI/siRNA complexes depend on the charge ratio of PEI to siRNA. In order for the nucleic acid to condense, approximately 90% of its charged groups must be neutralized by the positive charge from the amine group in PEI, requiring an N/P ratio of at least 2 to 3. The PEI/siRNA complexes with a higher charge ratio give better transfection efficiency, but also show higher toxicity. The additional presence of PEI aids in the release of the complex from the endosome; however, excessive PEI may also cause membrane permeabilization.^{109, 110}

Poly(ethylene glycol) (PEG)

To overcome transient gene expression and reduce the toxicity of the carrier, chemical modifications are utilized.^{106, 111, 112} They include coupling of the carrier to other macromolecules like poly(ethylene glycol) (PEG) (Figure 1-2C), either alone or in combination with a ligand for tissue or cell specific targeting.^{113, 114} Introducing PEG to the surface of nanoparticles creates a hydrophilic layer around it. This PEG layer minimizes the adsorption of opsonin proteins by steric repulsion, which blocks and

delays the first step in the opsonization process. This results in an increased serum half-life, lower immunogenicity, and lower toxicity of the particles.^{115, 116} A surface PEG chain larger than 2 kDa is able to significantly delay the recognition of the particle by the immune system. This minimum molecular weight is due to the inflexibility of shorter PEG chains. Moreover, as the molecular weight increases above 2 kDa, the half-life of the pegylated particles in circulation increases.¹¹⁷⁻¹²⁰ PEG is a non-biodegradable polymer that can be secreted primarily through renal excretion with the molecular weight smaller than 5 kDa. PEG bigger than 5 kDa can be secreted through the fecal route. Altering the size of the PEG used can change pharmacokinetic activity of drugs. It is preferably accumulated in the liver and spleen. It is approved by the FDA for internal use due to its nontoxic and non-immunogenic characteristics.¹²¹⁻¹²³

Mannose

Specific ligands can bind to target cell surface receptors and promote receptor-mediated endocytosis.¹²⁴ Mannose is often used as a ligand that binds mannose receptors on cells to aid in the endocytosis of the carriers and increase the gene delivery efficacy. (Figure 1-2D)¹²⁵ The mannose receptor is expressed on antigen presenting cells (APCs; dendritic cells, macrophages) and liver endothelial cells.¹²⁶⁻¹²⁸ APC-targeted vaccines have strong potential to guide exogenous antigens into vesicles that process the antigen for major histocompatibility complex (MHC) class I and class II presentation.¹²⁹ In this process, the mannose receptor plays a key role in innate and adaptive immune responses.^{130, 131} The mannose receptor is also expressed on the surface of glial cells in the brain; astrocytes and microglia can be turned into immune-competent cells.¹³² A number of studies have shown that mannosylated nanoparticles enter Raw264.7 cells via receptor-mediated endocytosis.^{124, 133-135} Mannose-PEI/DNA complexes have been shown more efficient in gene expression than PEI/DNA complex.¹³⁶ Chitosan-

mannose/DNA microspheres enhanced serum antibody and cytotoxic T lymphocyte (CTL) responses through targeted dendritic cell overactivation compared to naked DNA.¹³⁷ Chitosan-mannose/DNA complexes showed higher transfection efficiency relative to chitosan/DNA complexes through a mannose-mediated receptor-specific endocytosis mechanism in mouse peritoneal macrophages.^{138, 139}

Poly(D,L-lactic-co-glycolic acid) (PLGA)

Poly(D,L-lactic-co-glycolic acid) (PLGA) is a biocompatible and biodegradable polymer that has an FDA approval for human use.¹⁴⁰ It has been extensively studied for encapsulation and controlled delivery of drugs.¹⁴¹⁻¹⁴³ PLGA is a biodegradable polymer because it is hydrolyzed in the body to produce the original monomers, lactic and glycolic acids, that can be metabolized through the citric acid cycle.¹⁴⁴ (Figure 1-2E) PLGA polymers can be converted into insoluble microparticles that can be loaded with therapeutic molecules. PLGA microparticles of appropriate size are reported to be efficiently taken up by mouse and human dendritic cells (DCs), and slowly hydrolyzed to induce prolonged antigen stimulation.¹⁴⁵ The PLGA microparticles have advantages in protection and sustained release of the cargo. These are of particular interest for siRNA therapy due to the inherent susceptibility of siRNA to serum nuclease hydrolysis.¹⁴⁶ SiRNA-loaded PLGA particles have shown *in vitro* gene knockdown capacities.¹⁴⁷ PLGA particles can carry siRNA by two different methods: (1) siRNA can be encapsulated inside the particles, (2) or adsorbed onto the surface of the modified PLGA particles via electrostatic interactions. The PLGA particles in the latter method could have cationic charges on the surface by chemical modification.¹⁴⁸ In regards to formulation development, it is challenging to efficiently encapsulate high amounts of hydrophilic macromolecules like siRNA into uniform PLGA particles. This difficulty in loading of siRNA into PLGA particles can be attributed to the hydrophobic nature of

PLGA and the absence of electrostatic interaction between siRNA and PLGA. One way to improve encapsulation of nucleic acids is to add a cationic excipient to the PLGA matrix such as PEI.¹⁴⁹ Another way to improve encapsulation of nucleic acids is to utilize double emulsion-solvent evaporation method which enables relatively high encapsulation efficiencies for water-soluble drugs. The loading efficiency and particle size can be optimized with careful control over the formulation parameters such as surfactant concentration and stirring speed.

Targeted siRNA Delivery

The key to a successful siRNA delivery is to protect siRNA in serum and transport siRNA into the target tissue.^{15, 150} Target specificity can reduce random non-specific cellular uptake of siRNA and improve tissue and cell specific endocytosis. To achieve these goals, ligand-mediated cell binding is adapted to the carriers. Many cells including tumor cells have unique antigens or receptors on their surface. With proper ligands that specifically recognize these surface molecules, therapeutic siRNAs can bind to their receptors and enter the target cells. The use of cell type-specific ligands improves the efficiency, specificity and safety of the delivery system.¹⁵¹ The specificity and efficiency of ligand-mediated delivery systems minimizes nonspecific immune activation or systemic toxicity.¹⁵² Ligand conjugation, such as mannose, on the surface of non-viral delivery vehicles can alter the transport and enhance the permeability of drugs.¹⁵³ Many studies have shown that mannose, as a cell binding ligand, enhances gene delivery. Its receptors are overexpressed on the surface of antigen presenting cells, such as dendritic cells and macrophages, and liver endothelial cells.¹²⁶⁻¹²⁸

Summary and Objectives

To summarize, the goal of this research is to develop an efficient non-viral vector system for *in vitro* and *in vivo* siRNA delivery. Clinical trials have shown the prospects of siRNA for a research and therapeutic tool because its strong ability to induce RNAi.

To achieve efficient siRNA transfer, both viral and non-viral vectors have been successfully utilized for efficient siRNA transfer. Viral vectors promise delivery efficiencies, but their safety is still in controversy. For this reason, non-viral vectors such as cationic polymers and lipids have increasingly researched gene therapy due to the lower potential immunogenicity. In this research, we designed a siRNA delivery system using combinations of chitosan, PEI, PEG and mannose to capitalize on their respective advantages. Cationic polymers such as chitosan and PEI condense anionic siRNA through electrostatic interactions thereby protecting siRNA from enzymatic degradation with no chemical conjugation and carry it to destination. PEG can provide another layer of protection by steric shielding and prolonging serum half-life. The mannose ligand can be utilized as a cell binding ligand to increase target cell specific endocytosis. Moreover, the polymer modification was carried out using two different structures to investigate the effect of mannose location in the polymer construct. The first structure has mannose and PEG directly conjugated to the cationic polymer backbone. The other structure has mannose indirectly linked to the cationic polymer via a PEG spacer. Therefore, the performance of modified polymers and the effect of the structure of the construct on siRNA delivery efficiency is evaluated. Initially, modified polymers is characterized and assessed for *in vitro* delivery efficiency. Mannosylated pegylated chitosans are discussed first in chapter 3 followed by mannosylated pegylated PEIs in Chapter 4. In Chapter 5, PLGA microparticles are utilized to improve delivery efficiency of cationic polymer/siRNA nanoplexes for *in vivo* delivery.

Figure 1-1: Schematic of a RNA interference (RNAi) process. siRNA can be introduced into cells as pDNA, shRNA, dsRNA, or by itself. When it is introduced as pDNA, shRNA, or dsRNA, it is transcribed and then processed into siRNA. siRNA joins the multi-protein cluster, RNA induced silencing complex (RISC). RNA helicase in the RISC unwinds double-stranded siRNA into single strands by recognizing the least stable 5' end of siRNA. The single stranded (guidance) siRNA binds to a mRNA which has complementary sequence to the guidance siRNA. Then the target mRNA is cleaved by RISC and rapidly degraded. RISC is recycled for subsequent rounds resulting in decreased expression of the target gene. (Adapted from ¹⁶)

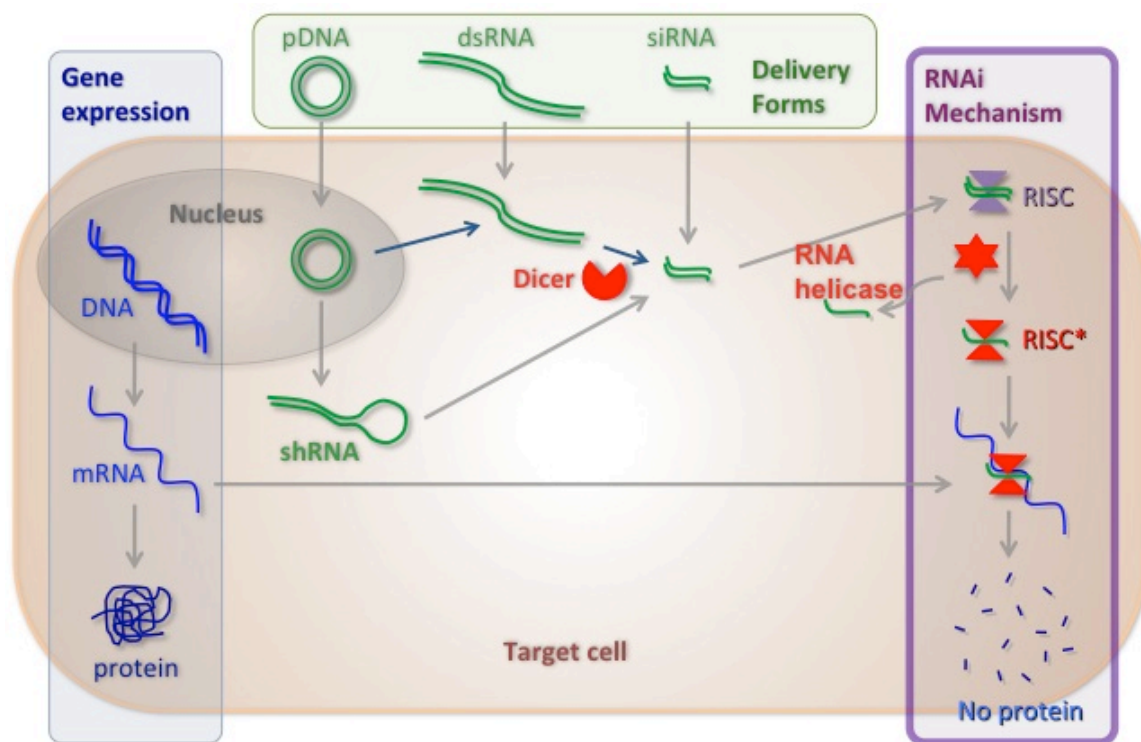
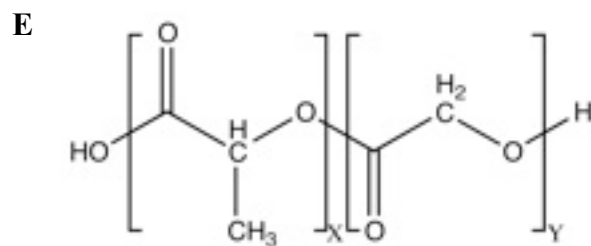
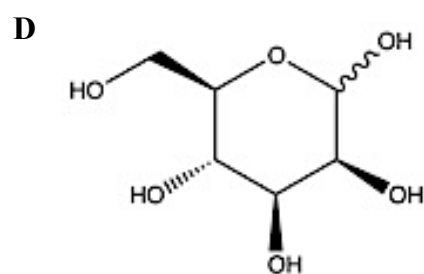
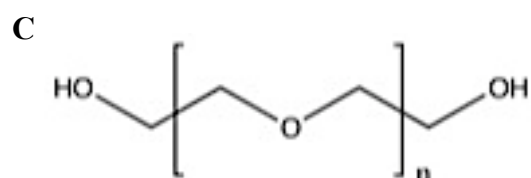
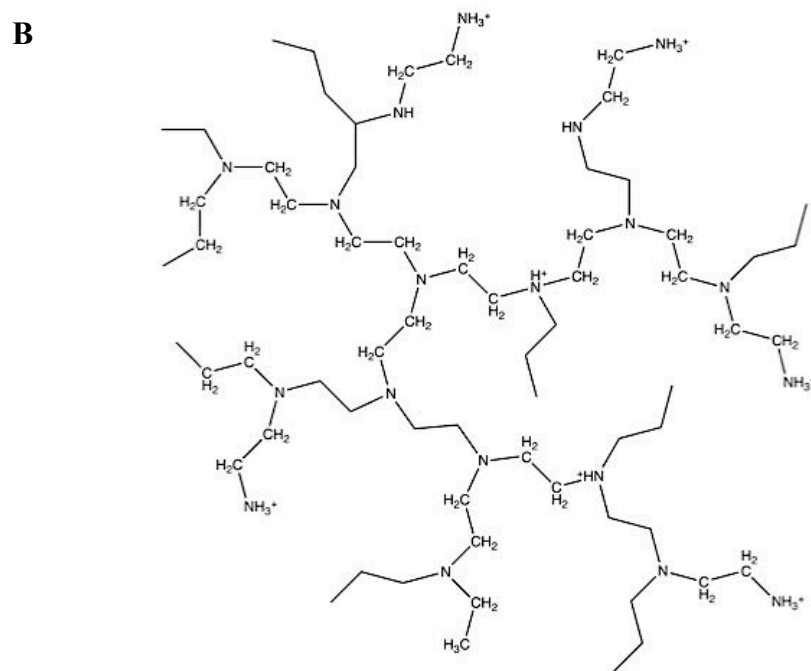
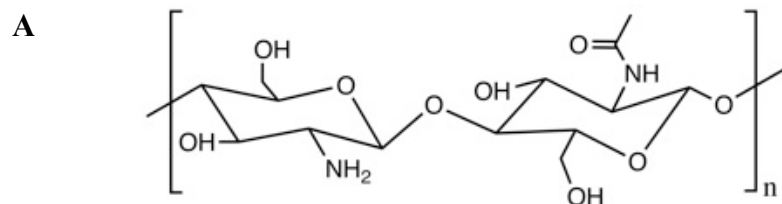


Figure 1-2: Molecular structures of chitosan, polyethylenimine (PEI), poly(ethylene glycol) (PEG), mannose, and poly(D,L-lactic-co-glycolic acid) (PLGA). A. Chitosan, B. Branched Polyethylenimine (PEI), C. Poly(ethylene glycol) (PEG), D. Mannose, E. Poly(D,L-lactic-co-glycolic acid) (PLGA), x is the number of units of lactic acid, and y is the number of units of glycolic acid.



CHAPTER 2: MATERIALS AND METHODS

The background of each experimental method and the principles behind them are discussed in this chapter. Developing polymeric siRNA delivery systems with cationic polymers was carried out in a joint project in collaboration with Dahai Jiang (College of Pharmacy, University of Iowa).

Polymer/siRNA Nanoplex Preparation

In order to test the gene delivery capacity of the polymer formulations, the polymers were complexed with siRNAs. As introduced in the previous chapter, the cationic backbone polymers, chitosan and PEI, are positively charged in solution. With sufficient presence of cationic polymers, they form self-assembled complexes and condense negatively charged siRNA when mixed.¹⁵⁴ This condensation offers certain levels of protection to siRNA against nuclease digestion.¹⁵⁵ The extent of condensation between polymer and siRNA is decided by the polymer:siRNA charge ratio, also called the N/P ratio.¹⁵⁶ It represents the ratio of nitrogen in cationic polymer to phosphate in nucleic acid. By means of affecting condensation, the N/P ratio also affects the size of the polymer/siRNA complexes.¹⁵⁷ To calculate the amount of siRNA and the polymer needed for a predetermined N/P ratio, the mass per phosphate of 325 Da for siRNA, the mass per charge of 167 Da for chitosan, and the mass per charge of 43 Da for PEI were used. Before forming polymer/siRNA nanoplexes, stock solutions were prepared. All the solutions and buffers used in this research were prepared with nuclease-free deionized water to prevent degradation of siRNA. Chitosan and chitosan derivatives were dissolved in 1% acetic acid solution at the required concentration for each experiment. PEI and PEI derivatives were dissolved in nuclease-free deionized water. Lyophilized siRNAs were resuspended, annealed, and stored in Nuclease-Free Duplex Buffer (30mM HEPES, pH 7.5, 100mM Potassium Acetate, IDT, Coralville, IA).

To make polymer/siRNA nanoplexes, the polymer solution was dropped into the siRNA solution at a precalculated concentration. Then the mixture was immediately vortexed for 20 seconds followed by 30 minutes of incubation at room temperature. The polymer and siRNA assembled via electrostatic interaction into a condensed nanoplex and stabilized during the incubation period. All the experiments were carried out after the incubation period.

Size Distribution and Surface Morphology Observation by Scanning Electron Microscopy (SEM)

Scanning Electron Microscopy (SEM) enables us to examine the actual size and surface morphology of the complexes or particles. SEM utilizes high-energy electron beams to scan a sample and produce images. Interactions between the electron beams and the atoms on the surface of the sample produce signals, which gives high-resolution and three-dimensional images of the sample surface. It gives us information of surface topography, composition, and electrical conductivity. The samples must be electrically conductive at the surface. This prevents accumulation of electrostatic charge. Nonconductive specimens cause scanning faults and image artifacts. Therefore, the sample is usually coated with an ultrathin layer of electrically conductive material. This material was gold/palladium in our PLGA microparticles study. The samples were coated using low vacuum sputter coating. Coating also improves the resolution. Another method to improve conductivity of the sample is impregnation with osmium vapor. This approach was used in the chitosan and PEI samples. Since the polymer/siRNA complexes were nanoscale size range, they easily lose structural integrity because of the surface tension. We therefore used Nebulizer to spray-mount the samples on the silicon wafer to produce small droplets and prevent crushing of nanoplexes during the air-drying. A low voltage was maintained during imaging to prevent indentation on the surface of the nanoplexes or the microparticles from the electron beam. Imaging studies conducted in

this research were carried out at the Central Microscopy Research Facilities at the University of Iowa.

SiRNA Retardation Analysis by Ethidium Bromide Gel

Electrophoresis

A polymer needs to be able to strongly complex and condense siRNA for a effective siRNA delivery. To test the complexation capacity of the polymers, ethidium bromide agarose gel electrophoresis assays were used. This is a molecular biological technique that separates a mixed population of nucleic acids by size. Negatively charged DNA or RNA moves through an agarose gel matrix towards the positive end of an electric field. The smaller the molecules are, the farther they migrate through the pores of the gel.¹⁵⁸ Based on these fundamentals, we assume if the polymer complexes and condenses siRNA with enough strength, the migration of the siRNA would be retarded. Moreover, the degree of retardation would be directly proportional to the strength of complexation. Therefore, if the migration of complexed siRNA was not as far as that of naked siRNA, we concluded that this is the polymer holding the siRNA molecule and interfering with its migration. To make nucleic acid visible in the gel, dyes such as ethidium bromide (EtBr) are commonly used. Ethidium bromide intercalates into minor grooves of double-stranded nucleic acids and fluoresces under UV light.

Intracellular Trafficking by Confocal Laser Scanning

Microscopy

To investigate the intracellular fate of the polymer/siRNA delivery system, we chose to use confocal microscopy. Confocal microscopy is widely used for *in vitro* fluorescence images of cells and tissues. The technique is based on selective collection of light from focused planes in the sample. A beam of light is focused on a specific point in the sample using a low-power near-infrared laser. Light reflected from this point is collected through an aperture by a detector.^{159,160} It generates an integrated image of

multiple planes at a focal point with higher resolution than fluorescence microscopy. To visualize cells using confocal microscopy, fluorophores are generally used; for example, green fluorescence protein (GFP), DAPI (4',6-diamidino-2-phenylindole) and Cy3 as used in our studies. Imaging studies conducted in this research were carried out at the Central Microscopy Research Facilities at the University of Iowa.

In Vitro Gene Knockdown Analysis by Luciferase Protein

Expression

To quantify gene expression on protein level, a dual-luciferase method was chosen. This method allows an efficient detection of firefly and *Renilla* luciferase gene expressions. The method sequentially measures the luminescence from two proteins in a single sample. A psiCHECK™-2 vector (6.3kb) is specifically designed pDNA for RNAi experiment that was used to facilitate this experiment. (Figure 2-1) It has two different reporter genes, firefly (hluc+) luciferase and *Renilla* (hRluc) luciferase each with separate promoters, and a synthetic poly(A) sequence in between to reduce the potential for recombination events. This firefly reporter sequence has been specifically designed as a normalization reporter of intraplasmid transfection, thus the *Renilla* luciferase signal can be normalized to the internal control of firefly luciferase signal. We selectively knockdown *Renilla* luciferase gene by RLuc-S1 siRNA transfection, which encodes a complementary sequence for *Renilla* luciferase mRNA, and measured their expression levels. By comparing the protein expression of *Renilla* luciferase and firefly luciferase, we can calculate the relative expression and deduce the degree of gene silencing.

Gene Knockdown Analysis by Real-Time Polymerase

Chain Reaction (PCR)

To analyze gene expression more accurately on mRNA level, real-time PCR techniques were utilized. Unlike the standard PCR, the target DNA is amplified and the

amplified DNA is simultaneously measured allowing real-time quantification during each cycle in a real-time PCR setting. This results in a quantitative measurement of PCR products accumulated during the course of the reaction. The technique is also called as quantitative PCR (qPCR). The reactions are carried out in a thermocycler that permits measurement of a fluorescent detector molecule, which decreases post-processing steps and minimizes experimental error. This is most commonly achieved through the use of fluorescence probe sequences. These approaches require less RNA, detect a wider range of expression, and are more target specific than conventional PCR.¹⁶¹ This technique enables detection and quantification of more than one specific sequences in a sample, and the quantification may appear as an absolute number of copies or a relative amount when normalized to DNA input or additional normalizing genes. Frequently, qPCR is combined with reverse transcription to quantify the amount of mRNA.

We used a fluorescent detector molecule called Taqman probe, which consisted of a fluorophore covalently attached to the 5'-end of the oligonucleotide probe and a quencher at the 3'-end. The quencher molecule prevents the fluorescence from emitting when excited by the cycler's light source via fluorescence resonance energy transfer (FRET). As long as the fluorophore and the quencher are in close proximity, the quencher inhibits any fluorescence signals. During the PCR reaction, the Taqman probe anneals within a target DNA sequence that will be amplified by a specific set of primers. The primer attaches to the sequence, and enzyme called Taq polymerase extends the primer and makes the strand grow. As this strand grows, Taq polymerase degrades the probe, which releases the fluorophore away from the quencher allowing fluorescence of the fluorophore. Hence, fluorescence detected in the qPCR machine (thermal cycler) is directly proportional to the amount of fluorophore released and the amount of DNA template present in the reaction. (Figure 2-2) All the qPCR experiments were carried out at IDT research lab.

Cytotoxicity Evaluation using MTS Assay

To examine possible toxicity from our polymers, cell viability tests were carried out. We chose to use MTS (5-{3-(carboxymethoxy)phenyl}-3-(4,5-dimethyl-2-thiazolyl)-2-(4-sulfophenyl)-2H-tetrazolium inner salt) cell viability analysis. It is a colorimetric method of determining cytotoxicity or the number of viable cells in proliferation. As a part of metabolic activity, live cells reduce colorless or weakly colored MTS into colored derivatives known as soluble formazans. This byproduct dissolves in growth media allowing the measurement by UV spectrophotometer.¹⁶²

Flow Cytometry and FACS Analysis

Flow cytometry analysis was used for two different purposes in our study. First, to sort enhanced green fluorescence protein (EGFP) stably expressing HEK293 cells from regular HEK293 cells; and second, to identify the population of the PLGA particles loaded with fluorescence Cy3 siRNA. It is a technique for counting and examining microscopic particles in a stream of fluid and passing them by an electronic detection apparatus. It allows simultaneous multiparametric analysis of the physical and chemical characteristics of thousands of particles per second. The principle is that laser light is focused on a narrow stream of the cell suspension that passes cells through the detector one at a time. The detectors that measure the scattered light convert it into electrical pulses. An analog to digital converter allows the events to be plotted on a graphical scale, for viewing information about the chemical and physical structure of the cell. Based on the forward and side scatter of the light from the cells, the cell volume and shape are determined. Fluorescence Activated Cell Sorting (FACS) is a specialized type of flow cytometry that allows cells to be labeled with fluorochromes, and then from a mixed population, be separated into subpopulations based on the fluorescence and light scattering characteristics of the cell.

Animal Care and Handling

Before beginning any animal experiments, animal training and education were carried out through the University of Iowa's Office of Animal Resources.¹⁶³ The instruction included proper handling and restraint of mice, which minimizes stress on the animal and prevent aggression or defensive responses to handling. Animal experiments were conducted in accordance with the principles and procedures described in the University of Iowa's Guidelines for Care and Use of Experimental Animals. For all cases involving anesthesia, a ketamine/xylazine mixture was injected intraperitoneally (i.p.) to deliver 87.5 mg/kg ketamine and 2.5 mg/kg xylazine in a 100 μ l volume. This provided the animal with full anesthesia of approximately 20-30 minutes within a few minutes, then the animals returned to full consciousness and mobility within 2 hours.¹⁶⁴ To harvest organs, the mice were euthanized using CO₂ and death confirmed by cervical dislocation. Throughout the course of all experiments, the mice were monitored daily. Great care was taken to optimize formulations prior to the injection to minimize the number of animals necessary for each experiment while retaining significance.

In vivo Gene Knockdown Analysis in Mouse Model

In order to test the *in vivo* delivery efficiency of our microparticles, we used a C57/Black6 mouse model. There are several injection routes that were used in previous studies and clinical models. Subcutaneous (s.c.) injection directs the particles between the epidermis and dermal layers; intraperitoneal (i.p.) injections delivers particles directly into the peritoneum, and intravenous injections (i.v.) deliver directly into the bloodstream.^{164, 165} Given the possible toxicity from PEI and the relatively large size of the PLGA particles, we decided the intraperitoneal route of administration was the best method for the delivery of our particles.¹⁶⁶ At the same concentration of PEI, intraperitoneal administration showed the least toxicity when compare to other injection routes.¹⁶⁷ If the carrier size is under 1 μ m, an intravenous injection is possible because the

diameter of the smallest blood capillaries is 4 μ m. This carrier size is also desirable for intramuscular and subcutaneous route of administration because of the minimized irritant reactions. Nanoparticles in sizes ranging from 10 to 1000nm are acceptable for intravenous injection.¹⁶⁸ Because our particles displayed 2-4 μ m in the size range, intraperitoneal route was most appropriate to avoid possible adverse effects.

Figure 2-1: Map of psiCHECK™-2 vector encoding two reporter genes, firefly and *Renilla* luciferase, for quantitative RNAi studies¹⁶⁹

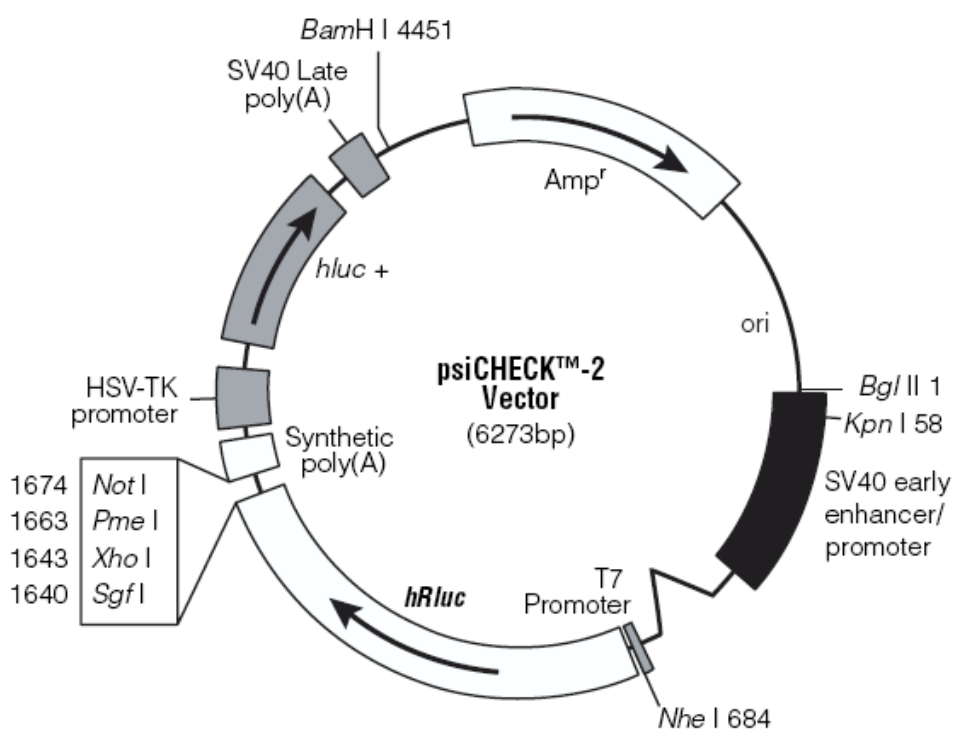
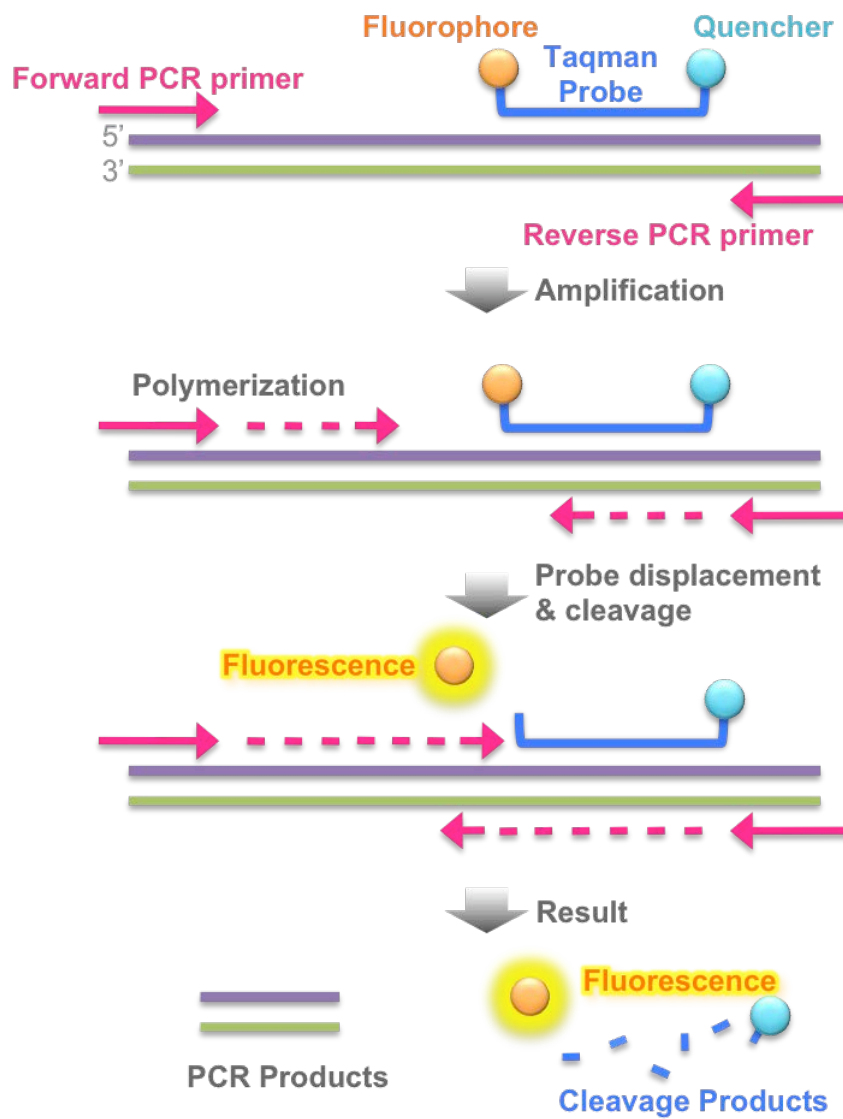


Figure 2-2: Principle of real-time polymerase chain reaction (PCR) process using Taqman probe (Adapted from ¹⁷⁰)



CHAPTER 3 : SIRNA DELIVERY SYSTEM COMPOSED OF CHITOSAN, POLY(ETHYLENE GLYCOL) AND MANNOSE

Introduction

To develop a non-viral delivery system for siRNA, we first selected chitosan due to its cationic characteristics and track record of low toxicity. As introduced in the chapter 1, chitosan (CS) is solubilized at acidic pH enabling electrostatic interactions with siRNA to form a complex. The complex formed at low pH is physically stable at body pH without chemical crosslinking because chitosan becomes insoluble at physiological pH.⁶⁷ This unique property of chitosan plays an important role in protecting siRNA. Furthermore, chitosan has nonimmunogenic and low toxic properties against degradation from components present in serum.⁶⁸⁻⁷⁰

Chitosan can be modified to enhance the delivery efficiency of siRNA.¹⁷¹ It is commonly conjugated with PEG and a cell binding ligand to improve serum stability and achieve higher delivery efficiency, respectively.^{172, 173} PEG provides steric hindrance on the surface of the nanoplexes and reduces adsorption of serum proteins. As a result, the PEG layer increases the serum half-life of the nanoplexes and reduces toxicity.^{115, 116} Specific ligands on the nanoplexes enables ligand-receptor specific interactions promoting in a receptor-mediated endocytosis.^{174,124} This process improves gene delivery efficiency by increasing the chance of endocytosis. Mannose ligands bind to mannose receptors that are overexpressed on the surface of the cells such as dendritic cells, macrophages, and liver endothelial cells, etc.¹²⁸ Mannose-conjugated chitosan has shown improved siRNA delivery efficiency by increasing cell binding to macrophages.¹³³

With the purpose of developing an efficient polymeric delivery system for siRNA, we designed and synthesized a set of modified polymers that incorporates chitosan, PEG, and mannose. Furthermore, to study the influence of the structure in the polymer formulation, the mannosylated pegylated chitosan delivery systems were designed in two

different constructs. In our first design, mannose and PEG chains were directly conjugated to the chitosan backbone. In the second design, mannose was conjugated to chitosan via a PEG chain. (Table 3-1) Both constructs were then characterized for their capacity to complex with siRNA, surface morphology and size, gene knockdown efficiency and toxicity to evaluate their potential as delivery vehicles.

Materials and Methods

Materials

Low molecular weight chitosan and α -D-mannopyranosylphenyl isothiocyanate (MPITC) were purchased from Sigma-Aldrich (St. Louis, MO). PEG 2 kDa with one amine terminus was from Creative PEGWorks (Winston Salem, NC). DMSO, glacial acetic acid and EDTA from Fisher Scientific (Pittsburgh, PA) were used. Maleic anhydride, toluene, glutaraldehyde 50%, methanol and sulfuric acid were purchased from Sigma-Aldrich (St. Louis, MO). Bio-Gel P-2 Gel was from Bio-Rad (Hercules, CA). All the siRNAs (DS scrambled negative control, RLuc-S1 DS positive control, Cy-3) and pDNA (psiCHECKTM-2, Promega, Madison, WI) were kindly provided by Integrated DNA Technologies (IDT, Coralville, IA).

Pegylation and mannosylation of chitosan

First of all, low molecular weight chitosan (50~190kDa) was hydrolyzed before any modification with sodium nitrite (NaN_3) to make 30kDa chitosan with a degree of deacetylation of 85%.

For mannosylation, chitosan was dissolved in NaHCO_3 buffer (8.516 mg/ml, pH 8.4) at 0.075 mg/ μl . An amount of 80 μl MPITC in DMSO at 0.125 mg/ μl was added into a solution containing 150 mg chitosan. The reaction mixture was stopped after overnight stirring by dialysis (MWCO 10,000, Pierce Biotechnology Inc., Rockford, IL)

for 3 days. Mannose-CS was recovered after lyophilization (Labconco FreeZone4.5, Kansas City, MO).

To conjugate PEG to chitosan, 500mg PEG was dissolved in 10ml toluene and heated up to 100°C. Maleic anhydride solution (33.1mg in 40ml toluene) was added into PEG in small increments. After the introduction of the maleic anhydride, the temperature was increased to 110°C and then the mixture was refluxed for 12 hours. Excess toluene was removed using rotary evaporation and the recovered product was dissolved in 2.5ml deionized water then purified with a P-2 column. The elution was lyophilized and redissolved in 10ml methanol. Then, 1ml maleic anhydride-PEG was slowly added into 50% w/v glutaraldehyde solution containing 50µl glutaraldehyde and 300µl methanol. The reaction was stopped by 2 hours and the mixture was loaded into a P-2 column. The elution was immediately added to a 2ml chitosan solution (150mg chitosan) for overnight reaction. CS-PEG was recovered after dialysis and lyophilized.

For Mannose-CS-PEG synthesis, 80µl of MPITC solution (dissolved at a concentration of 0.125mg/µl in DMSO) was added to pegylated chitosan for overnight mannosylation. The product was recovered after dialysis and lyophilized.

CS-PEG-Mannose was also constructed by adding 80µl MPITC solution to 2ml PEG solution (by NaHCO₃, 8.516mg/ml, pH 8.4) with 50mg PEG for overnight reaction, followed by the addition of 50µl of 50% w/v glutaraldehyde solution and 300µl methanol. The reaction was stopped in 2 hours and mannosylated PEG was recovered by dialysis. The collection was added to chitosan solution for overnight reaction. CS-PEG-mannose was recovered after dialysis and lyophilized.

Confirmation of pegylation and mannosylation

The presence of chitosan, PEG, and mannose in the modified polymers was verified using proton nuclear magnetic resonance (¹H NMR). The polymers were

dissolved in 1% w/v DCI/D₂O (Cambridge Isotope Lab, Andover, MA) at the concentration of 40mg/ml for characterization.

Quantification of mannose content

Resorcinol (Riedel-de Haen, Seelze, Germany) was dissolved in deionized water at the concentration of 6mg/ml. D-(+)-mannose pre-dried overnight at 100°C was used as standard. Mannose was dissolved in 1% w/v HAc at a concentration ranging from 9.0854 to 908.54µg/ml for standard curve. CS-PEG-mannose and mannose-CS-PEG samples were dissolved using 1% w/v HAc at appropriate concentrations. Each test mixture, consisted of 20µl mannose/sample solution, 20µl resorcinol, 50µl pristane (Acros, Fair Lawn, NJ), and 100µl 75% w/v sulfuric acid in a 96-well plate, was subjected to vortex for 30 seconds, heating at 93°C for 30 minutes and cooling down to room temperature for 30 minutes. The absorbance was recorded at 480nm absorbance (SpectraMax Plus384, Molecular Device). Content of mannose was calculated on standard curves.

Cell culture

Raw264.7 cells (ATCC, Manassas, VA) are murine macrophage cells that are known to overexpress mannose receptors and are typically hard to transfect. They were selected for *in vitro* experiments because macrophages were a potential target for this delivery system. The cells were cultured in Dulbecco's Modified Eagle's Medium (DMEM, Gibco) supplemented with 10% fetal bovine serum (FBS, Hyclone), and penicillin-streptomycin (100units penicillin; 100ug streptomycin/ml, Gibco). The cells were maintained at 37°C in a humidified, 5% carbon dioxide atmosphere.

Amplification and purification of pDNA

The psiCHECKTM-2 (Promega, Madison, WI) is a 6.3 kb pDNA designed to monitor a quantitative measurement of RNAi. It has genes encoding for firefly (hluc+)

luciferase and *Renilla* (hRluc) luciferase with each luciferase genes driven by a separate promoters. The firefly reporter gene has been constructed to serve as an intraplasmid standard so that the *Renilla* luciferase signal can be normalized to the firefly luciferase signal. The pDNA was transformed in *E.coli* DH5 α (invitrogen) and amplified in LB Broth media at 37 °C overnight on a plate shaker set at 250 rpm. The pDNA was extracted with Wizard® Plus Maxipreps DNA Purification System (Promega) followed by removal of bacterial endotoxin contamination with Endotoxin Removal Kit (MiraCLEAN®) according to the manufacturers' protocols. Purified pDNA was dissolved in Tris–EDTA buffer, and its purity and concentration were determined by UV absorbance at 260 and 280 nm.

Preparation of chitosan/siRNA nanoplexes

Polymer/siRNA nanoplexes were formed at desired N/P (nitrogen in cationic polymer per phosphate in nucleic acid) ratios with predetermined amounts of siRNA and polymer solutions. A mass per phosphate of 325 Da for RNA and mass per charge of 167 Da for chitosan were used to calculate the N/P ratio. A 0.01M modified chitosan solution in 1% acetic acid was dropped into a siRNA solution, then the mixture was vortexed for 20 seconds followed by 30 minutes of incubation at room temperature.

Size distribution and surface morphology analysis

SiRNA/polymer nanoplexes were formed as described above. Then the nanoplex solutions were sprayed using an All-Glass Nebulizer (PELCO, Redding, CA) onto silicon wafers. The silicon wafers were stained with 4% osmium tetroxide vapor under the hood overnight and mounted on aluminium stubs using liquid colloid silver adhesives followed by overnight drying at room temperature. The stubs were coated with approximately 5 nm of gold by ion beam evaporation before examination in the SEM that was operated at 1.5 kV accelerating voltage. The specimens were observed using scanning electron microscopy (SEM, Hitachi S-4800). Nanoplex size measurements were conducted using

the Zetasizer Nano ZS (Malvern, Southborough, MA). The size measurements were performed at 25°C at a 173° scattering angle. The mean hydrodynamic diameter was determined by cumulative analysis.

SiRNA retardation ability

SiRNA/polymer nanoplexes were loaded in a 2% agarose gel with 0.5µg/ml EtBr and run at 60V in TAE buffer for 45 minutes. The gels were visualized with a UV transilluminator (Spectroline, Westbury, NY).

Intracellular trafficking

RAW264.7 cells were plated on 0.01% (w/v) poly L-lysine coated 8-well chamber slides (Lab-Tak) at 1.2×10^4 cells/well concentration and incubated overnight. For lysosomal staining the cells were incubated with 75nM LysoTracker® Green DND-26 (Molecular Probes®) containing opti-MEM media (Gibco) for 30 minutes then transfected with polymer/Cy3-labeled siRNA nanoplexes in fresh opti-MEM. At pre-determined time points, the cells were washed with PBS and fixed with 4% paraformaldehyde and mounted using DAPI-containing Vectashield mounting medium for nuclear staining (VECTOR Laboratories, UK). Then the slides were covered with coverslip followed by 4 °C storage in dark before visualized under multiphoton/confocal microscope (Bio-Rad Radiance 2100MP and Zeiss LSM 710). The image was then analyzed using ImageJ software.

In vitro gene knockdown efficiency on protein expression

RAW264.7 cells were seeded on a T25 flask (6.8×10^6 cells) on day 0 and incubated overnight. PsiCHECK™-2 was transfected using Lipofectamine 2000 (invitrogen, Carlsbad, CA) in opti-MEM media on day 1 for 4 hours, then trypsinized to be replated onto 24-well plates (3×10^5 cells/well). Then RLuc-S1 DS positive control siRNA, which encodes a complementary sequence for *Renilla luciferase* gene in

psiCHECKTM-2 vector, was transfected using each different polymer in opti-MEM media on day 2. The cells were incubated for 4 hours with transfection media followed by overnight incubation in fresh complete media. On day 3, luciferase gene expression was analyzed using the Dual Luciferase Reporter System (Promega, Madison, WI) according to the product manual and using a Lumat LB 9507 (Berthold Technologies, Bad Wildbad, Germany). SiRNA/polymer nanoplexes were prepared as described above at precalculated N/P ratios. DS scrambled neg. siRNA, non-targeting sequences in the human, mouse, or rat transcriptome, served as a negative control. The *Renilla* luciferase gene expression was normalized to the firefly luciferase gene expression as internal control. Then the normalized *Renilla* luciferase gene expression was represented as relative gene expression setting the DS neg. scrambled siRNA transfected group as 1. The data was reported as mean \pm standard deviation for triplicate samples using Microsoft Excel and Prism[®] software (GraphPad Software, Inc). Experiments were repeated at least twice.

Cytotoxicity evaluation

Cytotoxicity was determined using the MTS assay (CellTiter 96[®] AQueous One Solution Cell Proliferation Assay, Promega, Madison, WI) using the protocol provided by the manufacturer. In brief, the Raw264.7 cells were seeded in 96-well plates (5×10^5 cells/well) and incubated overnight. The polymer containing DMEM media were prepared at different concentrations and added to cells for incubation. 20 μ l MTS solution per 100 μ l media was added to each well for a further 1 to 3 hours incubation at 37°C in a humidified, 5% CO₂ atmosphere. The plate was then measured at 490nm absorbance (SpectraMax Plus384, Molecular Device), and the relative cell viability was calculated on standard curves. Experiments were repeated at least three times.

Statistical analysis

Group data are reported as mean \pm standard deviation. Statistical analysis was carried out using one-way ANOVA followed by Tukey's multiple comparison test. Levels of significance were accepted at the $p < 0.05$. Prism software (GraphPad Software, San Diego, CA) was used to perform statistical analyses.

Results

Pegylation and mannosylation of chitosan are verified

Unmodified chitosan showed multiple peaks from 1.9ppm to 3.5ppm including δ 1.9 (acetyl) and δ 2.9 (C2 free). (Figure 3-1A) Chitosan-PEG showed peaks of glutaraldehyde (GA) linked to PEG at 1.8ppm in addition to peak at δ 3.5 (PEG-CH). (Figure 3-1B) CS-PEG-mannose and mannose-CS-PEG showed peaks at δ 7.0 (MPITC phenyl-H), δ 3.5 (PEG-CH), δ 1.8 (GA-PEG), and δ 1.9 (acetyl in chitosan) indicating successful conjugation of PEG and mannose to chitosan backbone. (Figure 3-1C and D) A relatively weak signal was found at 7ppm supporting the conjugation of mannose (data not shown).

The conjugation/substitution ratio was calculated based on the ratio of peak areas between 3.5ppm PEG and 1.9-3.5ppm Chitosan. (Table 3-2) The molar ratio of chitosan to PEG was 0.441 in pegylated chitosan. Mannose-CS-PEG had a chitosan/PEG ratio of 0.383 and CS-PEG-mannose had 0.378. All the modified polymers had similar conjugation/substitution ratio between 0.378-0.441. There was no significant difference between the ^1H NMR spectra of mannose-CS-PEG and CS-PEG-mannose.

Mannose quantity is determined

The resorcinol assay is a commonly used method to determine the content of monosaccharides in polymeric structures.¹²⁵ The mannose content in our products was determined using this technique. (Table 3-2) The mannose content of mannosylated

chitosan is 0.169 μ mol/mg. CS-PEG-mannose had 0.054 μ mol/mg and mannose-CS-PEG had 0.137 μ mol/mg of mannose, respectively.

Nanoplexes are spherical and coarse in appearance

SEM images were used to observe surface morphology and shape of the polymer/siRNA nanoplexes. Both unmodified and modified polymers/siRNA nanoplexes were spherically shaped with smooth surfaces. (Figure 3-2) Nanoplex sizes ranged from 80 to 300 nm diameter as determined by Zetasizer Nano ZS measurements, which suggested that some of the larger nanoplexes observed by SEM, represented clusters of nanoplexes formed during the drying process of SEM sample preparation.

Modified chitosan polymers complex and retard siRNA migration

To be capable of delivering siRNA, the mannosylated and pegylated chitosan products must be able to complex and condense siRNA. Cationic polymers form nanoplexes with anionic siRNAs and compact them by electrostatic interactions. This complexation capacity was analyzed using an EtBr gel electrophoresis assay. Increasing the polymer concentration decreased the migration of siRNA on the agarose gel. Unmodified chitosan, chitosan-mannose and chitosan-PEG were able to complex with siRNA efficiently from the N/P ratios of 50 to 300 so that they hindered siRNA migration in the gel retardation assays. (Figure 3-3A-C) Mannose-CS-PEG did not complex with siRNA as efficiently as others showing migration of siRNA at the highest N/P ratio of 300. (Figure 3-3D) However, CS-PEG-mannose did show effective exclusion of EtBr from N/P ratios 50 to 300 indicating a broad and strong complexation capacity with siRNA. (Figure 3-3E)

Modified chitosan/siRNA nanoplexes are endocytosed by RAW264.7 cells

To trace the endocytosis and intracellular localization of mannosylated pegylated chitosan/siRNA nanoplexes, siRNA and lysosomes were labeled with red and green fluorophores, respectively. At 2 hours post-transfection, most of the polymers/Cy3-siRNA nanoplexes (shown in red) were successfully internalized in the RAW264.7 cells. Chitosan/siRNA nanoplexes were taken up by cells and localized near lysosomes as observed by yellow coloration occurred with the overlap of the green lysosomal signal and red siRNA signal. (Figure 3-4A) Mannosylated CS and pegylated CS were able to deliver its complexed siRNA into cells with lower efficiency when compared to chitosan. (Figure 3-4B-C) Mannose-CS-PEG/siRNA nanoplexes were also found adjacent to the lysosomes. (Figure 3-4D) CS-PEG-mannose/siRNA nanoplexes showed efficient endocytosis found in most of the cells. (Figure 3-4E)

Modifications of chitosan do not reduce gene knockdown efficiency

Dual Luciferase Assay

To evaluate the siRNA delivery efficacy of mannosylated pegylated chitosan, *in vitro* gene expression analysis was performed using the dual-luciferase reporter system. Relative gene expression levels were analyzed after transfecting siRNA only targeting *Renilla* luciferase mRNA and leaving firefly gene expression as an internal control. (Figure 3-5) CS/siRNA nanoplexes suppressed *Renilla* gene expression to 80.3% at N/P ratio of 100 and 87.0% at N/P ratio of 200. CS-mannose/siRNA nanoplexes showed no inhibition of gene expression at N/P ratio of 100. However, CS-mannose/siRNA nanoplexes knocked down gene expression to 69.5% when N/P ratio was increased to 200. CS-PEG showed gene knockdown efficiency resulting in 93.2% and 85.0% remaining gene expression at N/P ratio 100 and 200, respectively. Gene expression of

cells transfected by mannose-CS-PEG/siRNA nanoplexes prepared at N/P ratio of 100 and 200 showed 73.1% and 87.3% gene expression, respectively. While cells treated with CS-PEG-mannose/siRNA nanoplexes exhibited gene knockdown efficiency of 62.6% when nanoplexes were prepared at N/P ratio of 100, this effect reduced when nanoplexes were prepared at N/P ratio of 200.

Modifications of chitosan reduce cytotoxicity

Raw264.7 cells were treated with various groups of nanoplexes to evaluate toxicity. At a concentration of 0.0078mg/ml, treating cells with chitosan showed the highest toxicity resulting in 49% cell viability. (Figure 3-6) Both CS-mannose and CS-PEG resulted in significantly higher cell viability of 72% and 77% when compared to unmodified chitosan at identical concentration. Cells treated with mannose-CS-PEG showed reduced toxicity of 70% viability relative to chitosan-treated cells. Cells treated with CS-PEG-mannose had 55% viability, which was better than the 49% cell viability displayed by the cells treated with chitosan alone. Cell viabilities were slightly decreased as cells treated with increasing concentrations of polymers. But all the polymers broadly displayed low toxicity at the highest concentration of 1mg/ml.

Discussion

A mannosylated pegylated chitosan carrier system was constructed and tested for potential delivery of siRNA. Mannose has been previously demonstrated to significantly increase binding of particles to cells that express the mannose receptor.^{124, 125, 128, 133, 135, 175, 176} Conjugation of PEG has been proven to extend the serum half-life of nanoparticles.^{115, 177, 178} To our knowledge, this is the first study to evaluate mannosylated pegylated chitosan for siRNA delivery, and to characterize the effect of the location of the mannose ligand in mannosylated pegylated chitosan constructs on gene delivery efficiency.

PEG and mannose were either both directly conjugated onto the chitosan backbone or mannose conjugated to the chitosan via a PEG spacer. ^1H NMR spectra confirmed that both constructs had chitosan, PEG, and mannose present. The peaks of the three components corresponded to the previously reported values.^{179, 180} Chitosan-mannose spectra looked very similar to the spectra of chitosan because both mannose and glucose are pyranose showing very few differences on spectra. The surface chain density of PEG is a critical factor in improving stealth shielding of polyplexes. The chitosan to PEG ratio of CS-PEG was 0.441, which suggested that every 30 kDa chitosan chain had 8.96 chains of 2 kDa PEG. CS-PEG-mannose had a 0.378 CS/PEG ratio indicating 10.5 PEG chains per chitosan. Mannose-CS-PEG displayed 0.383 CS/PEG ratio suggesting that there were 10.3 PEG chains for each chitosan. PEG chains have a larger range of motion at low surface coverage, that may cause gaps in the PEG protective layer.¹⁸¹ For PEG chains to fully cover the surface of CS/siRNA polyplexes, six short PEGs (5 kDa) or one long PEG (20 kDa) was needed.^{83, 177} Therefore, 8.96-10.5 chains of 2 kDa PEG was expected to provide a satisfactory level of pegylation for steric stabilization.

The mannose signal at 7 ppm in ^1H NMR spectra was relatively weak due to the low proportion of mannose in the overall construct composition. Therefore, the resorcinol assay was employed to quantify the amount of conjugated mannose in each construct. Mannose-CS-PEG and CS-PEG-mannose contained 0.14 $\mu\text{mol}/\text{mg}$ and 0.05 $\mu\text{mol}/\text{mg}$ of mannose indicating an average modification of 4.57 and 1.8 molecules of mannose existence per chitosan, respectively. The conjugation ratio of 1.8-4.57 mannose molecules per chitosan is expected to be sufficient to provide selective binding to mannose receptor-expressing cells. The ratio among the polymeric backbone, PEG, and mannose could be controlled by the use of various functionalized PEG and their feed ratio in the reaction.¹⁷³

Modified chitosan formed nanoplexes with siRNAs, and the nanoplexes ranged between 80 and 300 nm in size as determined by size measurements made on the

Zetasizer nano ZS. This particle size range is suitable for efficient endocytosis by cells.^{172, 182} Larger particles out of this range observed by SEM are likely to be clusters or aggregates of these smaller particles. Although Pegylation of CS marginally increase the average size of the particles, this increase was within the range of size that can still be efficiently endocytosed. The increase in size of nanoplexes of pegylated chitosan is likely to be due to the PEG chains interfering with the strength of the interaction between the chitosan and the siRNA.^{83, 113} The nanoplexes had a spherical shape with dense surface morphology.¹⁸³

Analysis with gel retardation showed that CS bound to and compacted siRNA in N/P ratio-dependent manner. The migration of siRNA when complexed with chitosan was similar to naked siRNA at low N/P ratios. However, the siRNA retardation ability of chitosan was increased in proportion to the presence of polymer.^{184,185} Complete binding of siRNA was achieved with all the various constructs at N/P ratios of 50 and higher. Condensation of siRNA with mannose-CS-PEG was reduced showing only partial retardation at high N/P ratio, while CS-PEG-mannose compacted siRNA with similar strength to unmodified chitosan. This could be explained by the structural difference between the two constructs because they both had similar degrees of conjugation of PEG as described above. The CS-PEG-mannose construct had PEG chain terminals conjugated with mannose moieties whereas PEG was exposed in mannose-CS-PEG. In the structure of mannose-CS-PEG/siRNA nanoplexes, it is unlikely that all mannose moieties were orientated towards the surface of the nanoplexes. It is possible that some of these moieties were placed in the interior of the nanoplexes and thereby hinder condensation. Charge aspects play a role but have less importance.¹⁸⁶

RAW264.7 cells, a murine macrophage cell line, were chosen for evaluation of *in vitro* properties because they are known to overexpress mannose receptors. Macrophages are a potential target for our pegylated and mannosylated chitosan delivery system.¹²⁸

The lysosomes were stained with LysoTracker GreenTM, and Cy-3 labeled siRNA was

used in the trafficking study. Two hours after transfection, lysosomes and red fluorescent-labeled (Cy3) siRNA were in close proximity. Co-localization of the green signals with red signals, shown in yellow, indicated that nanoplexes were internalized by endocytosis, which is consistent with previous reports on uptake by CS/nucleic acid polyplexes.¹⁸⁷ Large amounts of siRNA signal was found in lysosomal signal. This indicates that siRNA nanoplexes were uptaken by the cells but not released from the vesicles and still remained in the lysosomes. This could provide a reason for why modified chitosans were not as effectively improving gene knockdown. In order to achieve successful gene silencing, siRNA must interact with RISC to induce RNAi. If siRNA could not escape from lysosomal compartments, there would be less siRNA present in the cytosol to interact with RISC and hence, less RNAi induction. Perinuclear localization of siRNA enhances the potential to interact with RISC.^{40,188}

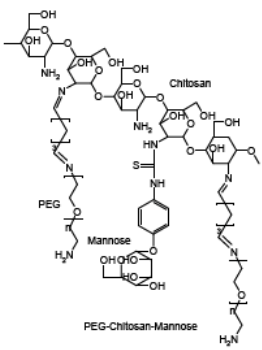
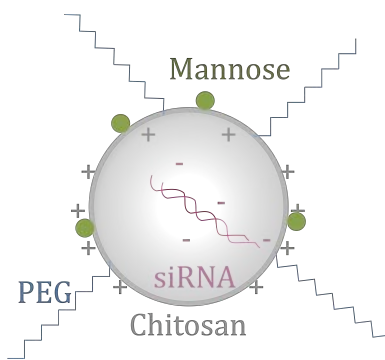
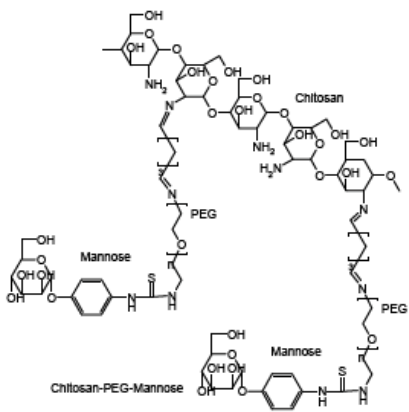
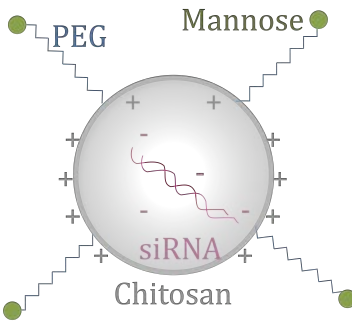
Mannosylation and pegylation of chitosan did not reduce gene knockdown efficiency relative to chitosan alone. However, the modifications did reduced toxicity. This reduction in toxicity was slightly offset by the mannosylation but not significantly so. In addition to observing the reduction in cellular toxicity, we anticipate that pegylation of the nanoplexes would also reduce toxicity at the systemic level by reducing aggregation of the nanoplexes.

One aspect of mannosylated pegylated chitosan delivery systems that has not been explored before is the importance of the location in which mannose is bound to the construct. In our studies, CS-PEG-mannose resulted in higher toxicity than mannose-CS-PEG. Furthermore, qualitatively we observed that CS-PEG-mannose/siRNA nanoplexes guided more stable uptake by RAW264.7 cells than mannose-CS-PEG/siRNA nanoplexes. This observation was not clearly understood but could be explained by the structural difference between the two constructs complexation of siRNA as observed in gel retardation assay. The CS-PEG-mannose construct has mannose moieties exposed at the tip of PEG chain whereas the mannose ligand in mannose-CS-PEG could be hindered

by the PEG chains. The mannose ligand-receptor interaction could be obstructed by the shielding effect of PEG chains. The use of a PEG chain can impair cell binding ability of CS and the ligand by shielding.¹⁸⁶ In our cell trafficking studies, we did observe that PEGylated chitosan had delayed cell uptake relative to chitosan alone, and this observation would support our hypothesis.

The advantages of pegylating polyplexes and incorporating cell-binding ligands for *in vivo* applications have been well established.^{108, 115, 122, 178, 180, 189, 190} Both mannose and PEG have contributed to *in vivo* delivery by selected cell binding, reduced systemic toxicity, and enhanced circulation.^{108, 135, 191} In particular, mannose ligands have shown significant potential for binding antigen presenting cells (APCs) such as mouse macrophages and dendritic cells.^{133, 175} Finally, the determination of the optimal location of cell binding ligands in the delivery construct is expected to have important implications in the design of several gene delivery systems currently in development that utilize alternative cell binding ligands, and alternative cationic backbones such as PEI.^{108, 128, 133, 135, 176, 186, 192}

Table 3-1: Molecular structures of two different constructs using chitosan, PEG, and mannose, and schematics of nanoplexes once complexed with siRNA.

	Structure	Nanoplexes
Construct #1 Man-CS-PEG	 <p>Chemical structure of Construct #1 (Man-CS-PEG) showing a chitosan backbone with mannose and PEG groups directly conjugated to it.</p>	 <p>Schematic of Construct #1 nanoplex showing a central siRNA molecule (pink) complexed with a chitosan core (grey) and mannose (green) and PEG (blue) groups extending outwards.</p>
Construct #2 CS-PEG-Man	 <p>Chemical structure of Construct #2 (CS-PEG-Man) showing a chitosan backbone with PEG groups directly conjugated to it, and mannose groups conjugated to the PEG spacers.</p>	 <p>Schematic of Construct #2 nanoplex showing a central siRNA molecule (pink) complexed with a chitosan core (grey) and PEG (blue) and mannose (green) groups extending outwards.</p>

Note: Chemical structures of modified chitosan constructs are shown in the left column and schematics of products after complexed with siRNA are shown in the right column. Mannose and PEG are directly conjugated to the chitosan backbone in construct #1, whilst mannose is conjugated to the chitosan via a PEG spacer in construct #2.

Table 3-2: Chitosan/PEG molar ratio and mannose content of the various modified chitosan (CS) polymers

Formulation	Polymer/PEG molar ratio	Mannose content ($\mu\text{mol}/\text{mg}$)
CS-Mannose	N/A	0.16865
CS-PEG	0.441	N/A
Mannose-CS-PEG	0.383	0.13715
CS-PEG-Mannose	0.378	0.05399

Note: The chitosan to PEG molar ratio was calculated based on the area of ^1H NMR peaks. Resorcinol measurements were used to determine the content of mannose (μmol mannose per 1mg polymer) in each construct.

Figure 3-1: ^1H NMR spectra of the modified chitosan polymers confirming the presence of chitosan, PEG, and mannose in each construct. Each component of the constructs is indicated with boxes. A, Chitosan showed multiple peaks including 1.9ppm (acetyl) and 2.9ppm (C2 free). B, Chitosan-PEG showed peaks of PEG at 3.5ppm and of GA at 1.8ppm. C, Mannose-Chitosan-PEG showed peaks of PEG at 3.5ppm (GA at 1.8), chitosan from 1.9ppm to 3.7ppm and mannose at 7ppm. D, Chitosan-PEG-mannose also showed each component at the same peaks.

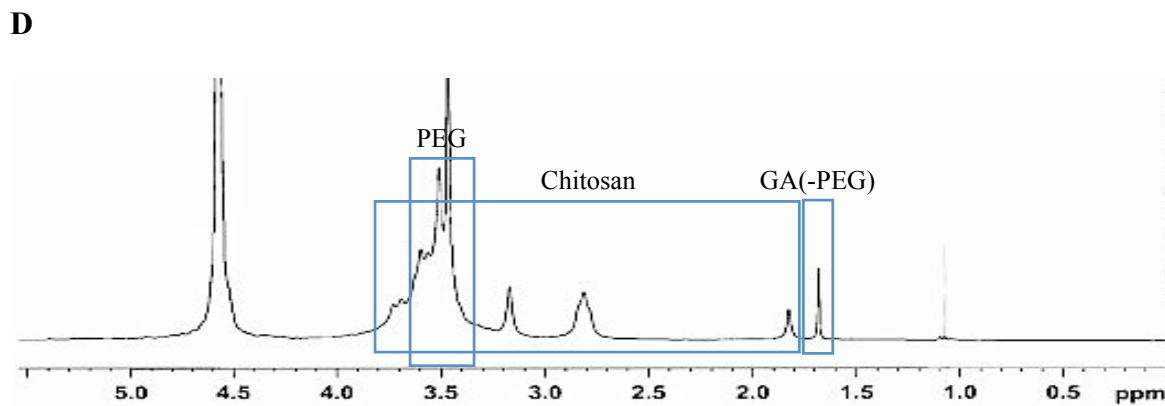
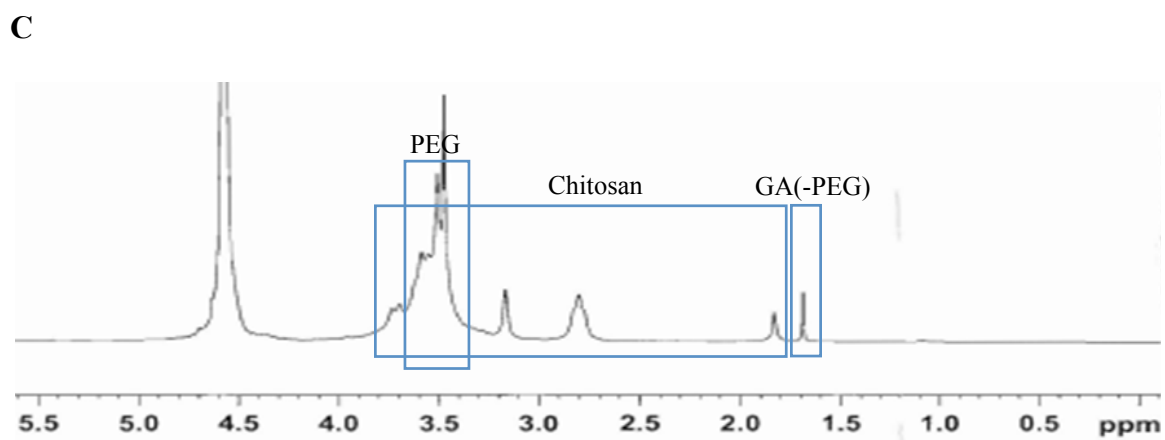
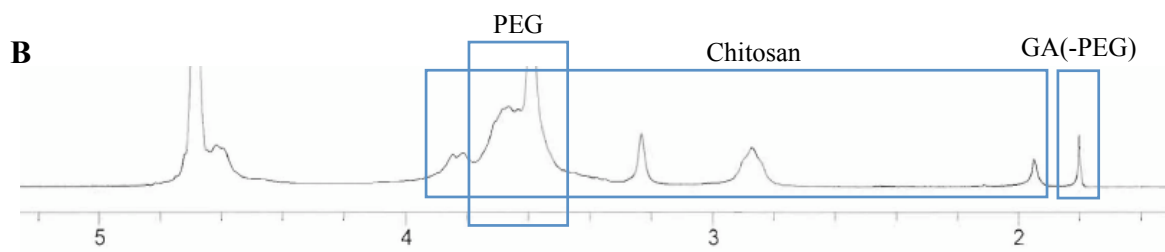
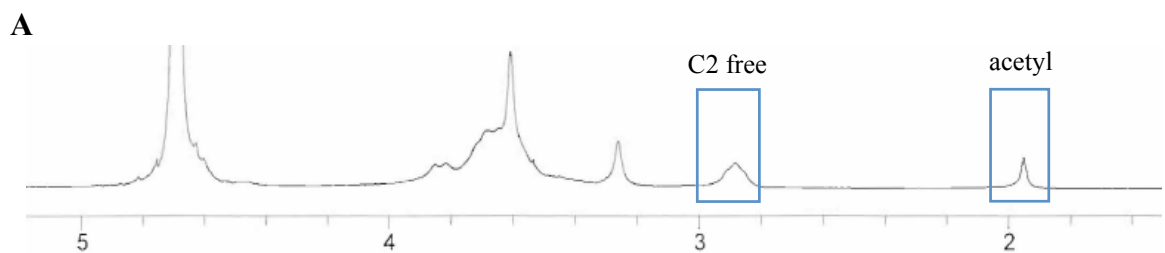
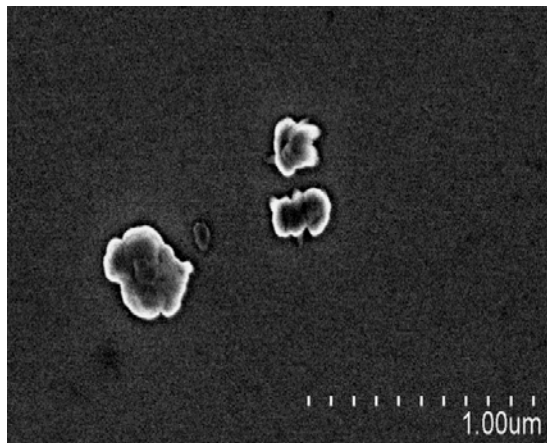
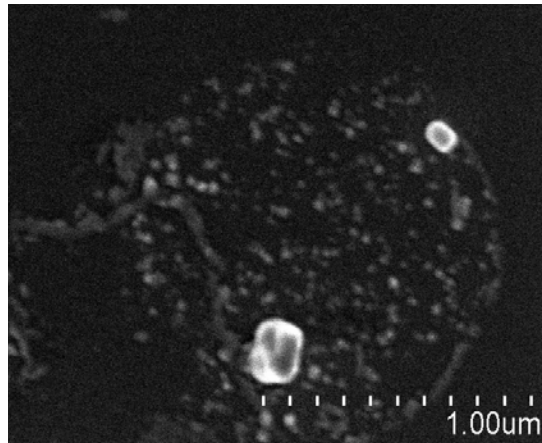


Figure 3-2: Scanning Electron Microscopy (SEM) images demonstrating the effect of pegylation and mannosylation on the size distribution and surface morphology of the modified chitosan/siRNA nanoplexes. A, CS/siRNA nanoplexes, B, CS-Mannose/siRNA nanoplexes, C, CS-PEG/siRNA nanoplexes, D, Mannose-CS-PEG/siRNA nanoplexes, E, CS-PEG-mannose/siRNA nanoplexes. All the nanoplexes were formed with 1 μ M siRNA at N/P ratio of 100. The experiments were repeated three times. The best representative images are shown.

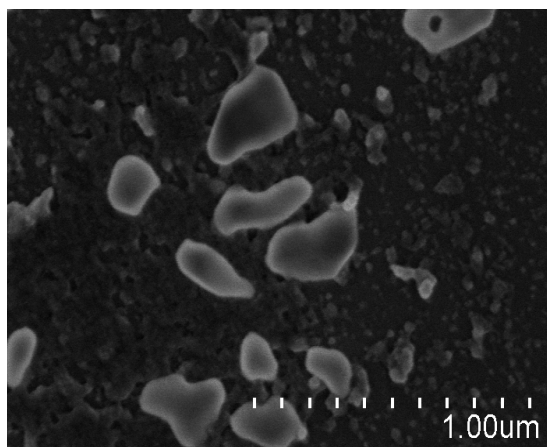
A



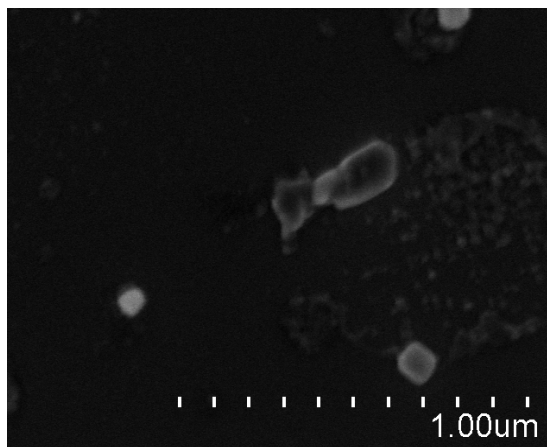
B



C



D



E

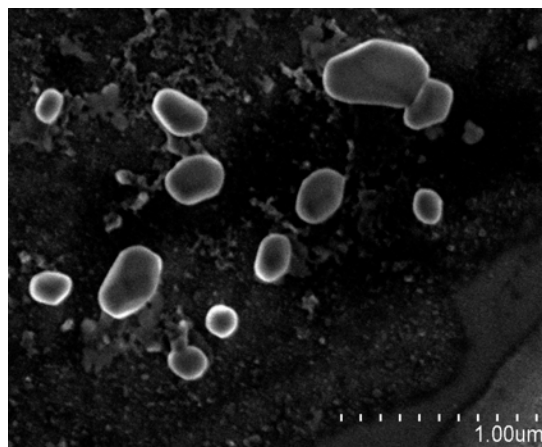


Figure 3-3: The effect of pegylation and mannosylation on siRNA retardation ability of the modified chitosan polymers using ethidium bromide agarose gel electrophoresis. A, CS/siRNA nanoplexes, B, CS-Mannose/siRNA nanoplexes, C, CS-PEG/siRNA nanoplexes, D, Mannose-CS-PEG/siRNA nanoplexes, E, CS-PEG-mannose/siRNA nanoplexes. All the nanoplexes were prepared with 1 μ M siRNA from N/P ratio 15 to 300. The experiments were repeated at least twice. The best representative images are shown.

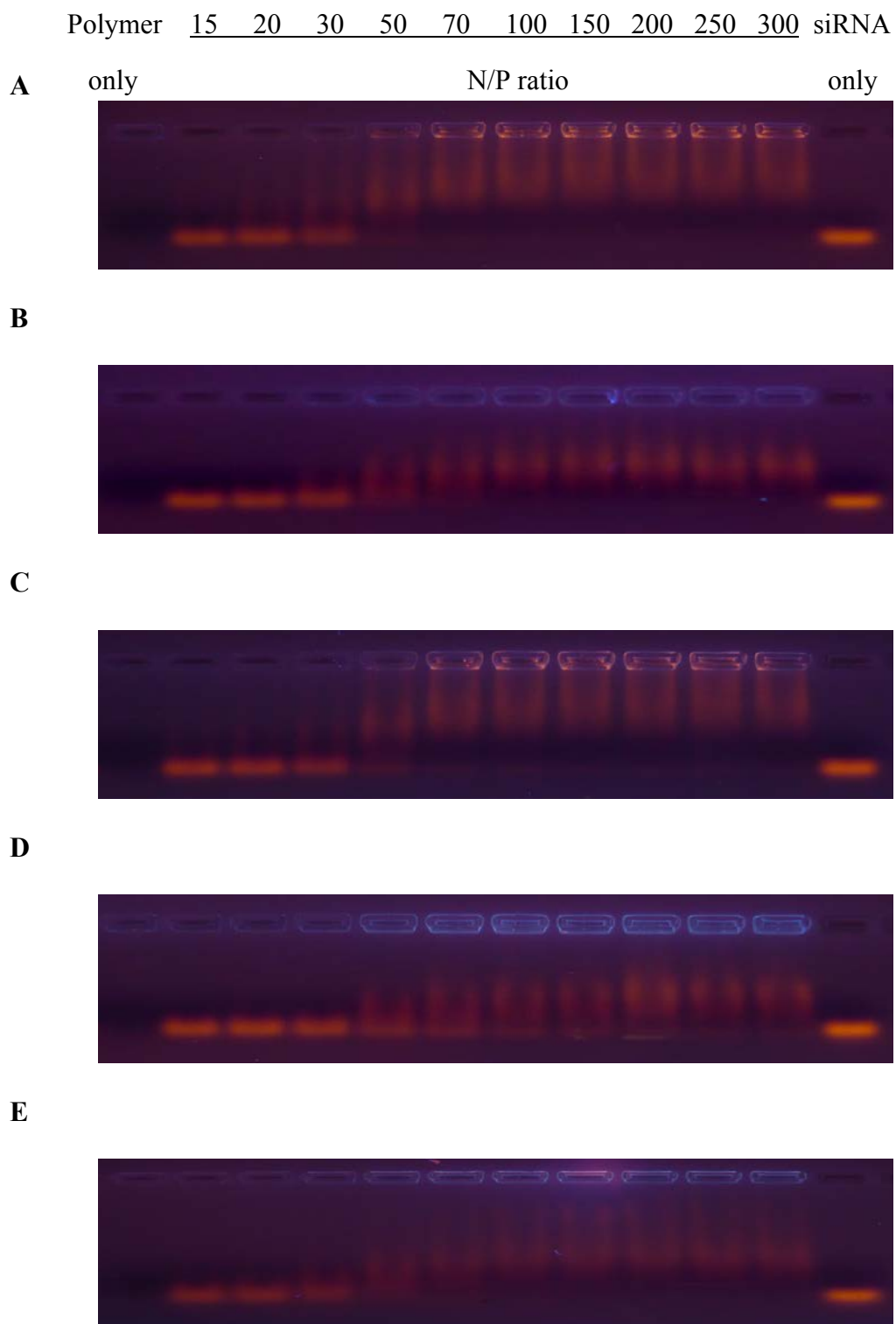


Figure 3-4: Confocal microscope images demonstrating the effect of pegylation and mannosylation on cellular uptake and intracellular localization of the modified chitosan/siRNA nanoplexes in RAW264.7 cells. The cells were stained with LysoTracker Green (green), incubated with nanoplexes formed using Cy-3 labeled siRNA (red), and then mounted with DAPI containing mounting solution after fixation. Co-localization of nanoplexes and lysosomes are shown as a yellow signal. A, CS/siRNA nanoplexes, B, CS-Mannose/siRNA nanoplexes, C, CS-PEG/siRNA nanoplexes, D, Mannose-CS-PEG/siRNA nanoplexes, E, CS-PEG-mannose/siRNA nanoplexes. The experiments were repeated at least twice. The best representative images are shown.

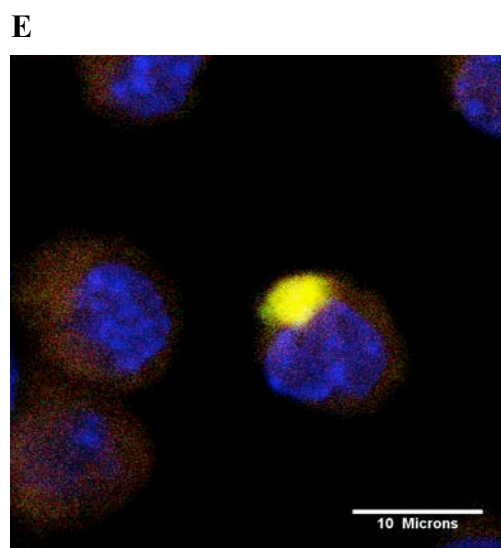
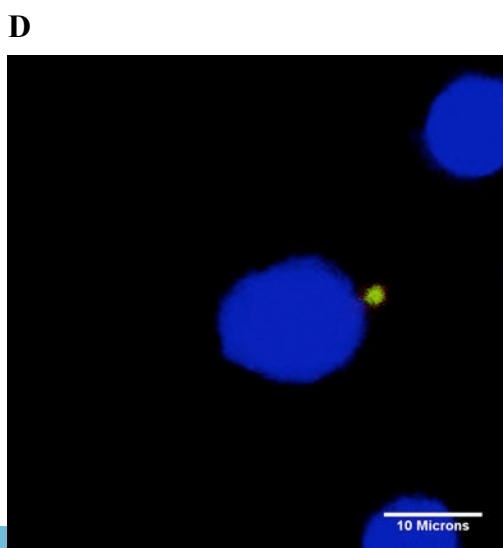
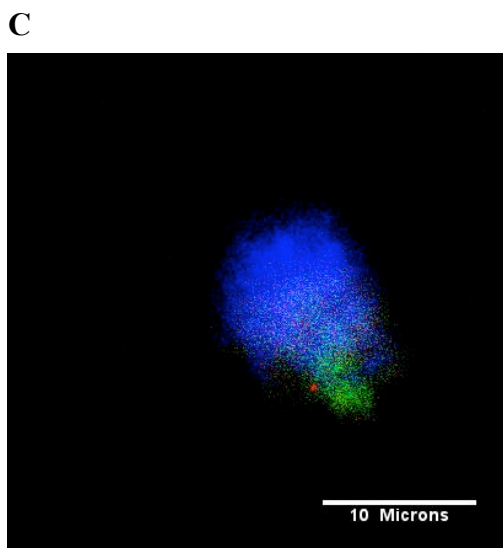
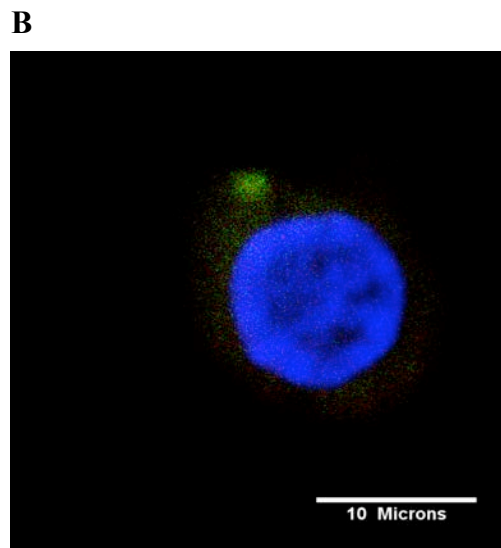
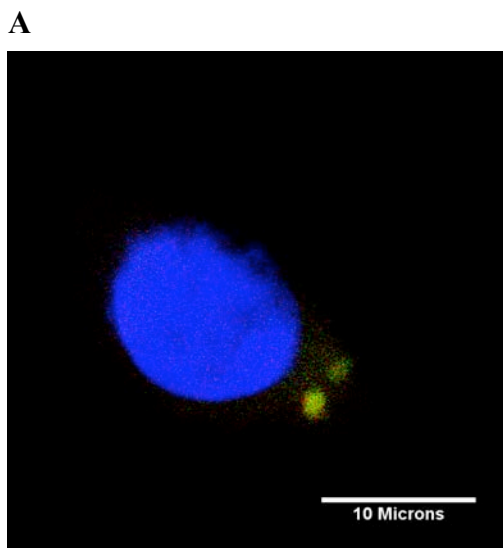


Figure 3-5: The effect of pegylation and mannosylation on luciferase gene knockdown efficiency of the modified chitosan/siRNA nanoplexes in RAW264.7 cells. Relative gene expression of *Renilla* luciferase is normalized to that of firefly luciferase, which served as an internal control. From the left, siLentFect/sihRluc, CS/sihRluc, CS-mannose/sihRluc, PEI-PEG/sihRluc, mannose-PEI-PEG/sihRluc, and PEI-PEG-mannose/sihRluc with N/P ratios at 100 and 200. The experiments were repeated at least twice. Data is represented as mean \pm standard deviation (n=3).

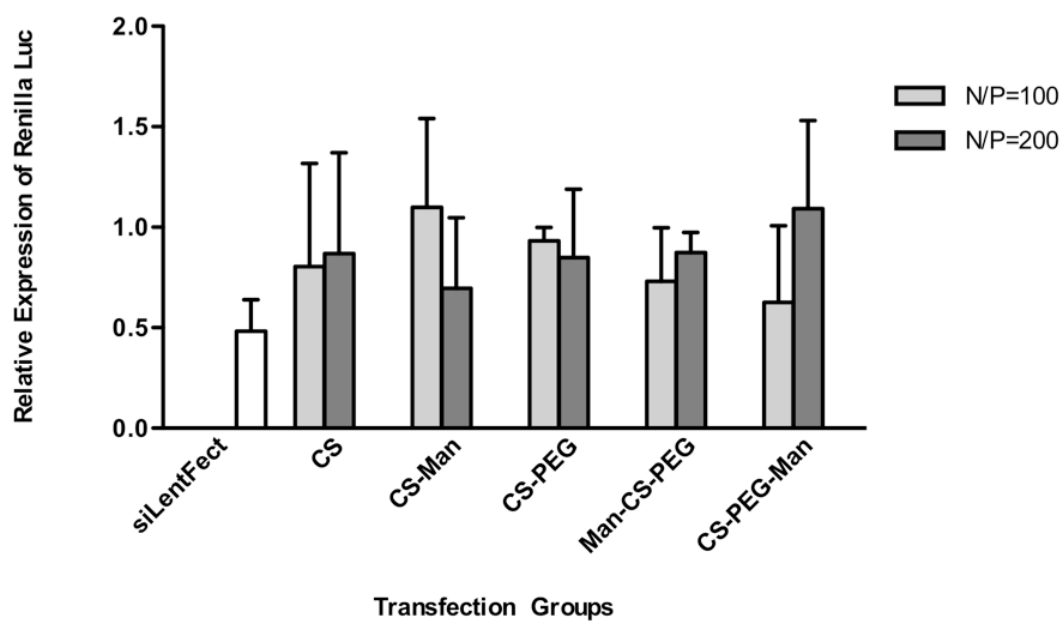
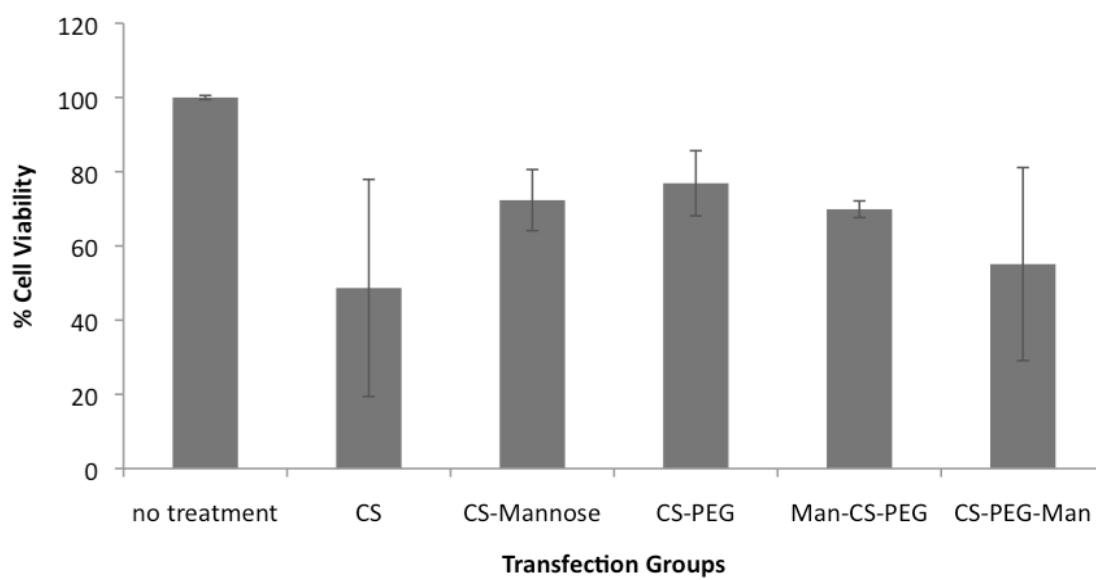


Figure 3-6: The effect of pegylation and mannosylation on cytotoxicity of the modified chitosan/siRNA nanoplexes in RAW264.7 cells. Cytotoxicity of various nanoplexes tested at the working concentration of 0.0078mg/ml. From the left; CS, CS-mannose, CS-PEG, mannose-CS-PEG, CS-PEG-mannose, and no treatment group. The relative cell viability was calculated by normalizing to the non-treatment group. The experiments were repeated at least twice. Data is represented as mean \pm standard deviation (n=3).



CHAPTER 4 : SIRNA DELIVERY SYSTEM COMPOSED OF POLYETHYLENIMINE, POLY(ETHYLENE GLYCOL) AND MANNOSE

Introduction

PEI is a synthetic cationic polymer that has been widely used to deliver oligonucleotides, siRNA and plasmid DNA *in vitro* and *in vivo*.^{44, 59, 79-85} Chitosan was modified in Chapter 3 to improve siRNA delivery efficiency of chitosan. However, the modified chitosan generated low gene knockdown efficiency. In this chapter, PEI is replacing chitosan to improve gene delivery efficiency. Similar to chitosan, PEI electrostatically condenses nucleic acids and forms stable polyplexes.⁸² Branched PEI with higher molecular weights is more efficient for *in vitro* transfection than linear PEI or PEIs of lower molecular weight because it condenses nucleic acids more effectively.⁹² Every third atom of PEI is a protonatable nitrogen atom, which enables the proton sponge effect at most pH. PEI buffers the acidification within the endosome after endocytosis. This process results in endosomal chloride accumulation, which leads to osmotic swelling and rupture. It allows endosomal escape of the PEI/siRNA polyplexes.⁸⁰ Although PEI has potential as a gene delivery vehicle, it is also associated with high toxicity compared to other non-viral vectors.^{44, 82, 94, 95} The toxicity can be reduced by modifying PEI such that its free amine groups served to conjugate cell binding ligands.^{83, 84, 106-108, 111, 112, 125, 189, 193-196}

Various modifications have been applied to PEI to reduce toxicity and increase target specificity.¹⁹⁷ For example, it is linked to other macromolecules like PEG, either alone or in combination with ligands for cell specific binding.^{81, 83, 108, 113, 114, 180, 193, 195, 198-200} Conjugation of PEG to a cationic polymer creates a hydrophilic layer around the nanoplexes. The hydrophilic layer provides steric hindrance and interferes with the adsorption of protein in serum. Therefore, PEG increases the circulatory half-life and

reduces immune response.^{115, 116} Ligands can be conjugated to PEI to improve target-specific delivery efficiency of siRNA.¹²⁴ Mannose induces ligand-receptor specific interaction and increases the delivery efficacy by a receptor-mediated endocytosis.¹²⁵ Its receptor is expressed on the surface of dendritic cell, macrophages, and liver endothelial cells, etc.¹²⁸

In this chapter, we synthesized a siRNA delivery system consists of PEI, PEG, and mannose. PEI is used to replace chitosan to improve delivery efficiency of siRNA. The delivery system was designed in two different structures as described in chapter 3 to study the effect of mannose location in the polymer formulation. In the first structure, both mannose and PEG were directly attached to the PEI backbone, whereas mannose was indirectly conjugated to PEI through PEG chain in the second structure. (Table 4-1) The pegylated and mannosylated PEIs were evaluated for its siRNA complexation capacity, size distribution and surface morphology, mRNA and protein knockdown efficiencies, and cytotoxicity.

Materials and Methods

Materials

Branched PEI 25kDa was purchased from Sigma-Aldrich (St. Louis, MO). NC1 (negative control 1) and HPRT (Hypoxanthine-Guanine Phosphoribosyl Transferase) siRNAs were kindly provided by Integrated DNA Technologies (Coralville, IA). The same materials described in Chapter 3 were used to synthesize mannosylated and pegylated PEI siRNA delivery system.

Pegylation and mannosylation of PEI

To synthesize pegylated and mannosylated PEI, the same process as described for the modified chitosan was carried out with the exception of PEI replacing chitosan (refer

to Materials and Methods, Chapter 3). The concentrations and amounts of polymers were maintained to keep the conjugation ratio consistent.

Confirmation of pegylation and mannosylation

The synthesis of pegylated and mannosylated PEI polymers was confirmed using proton nuclear magnetic resonance (^1H NMR). The polymers were prepared for the analysis following the same method as previously described in Chapter 3.

Quantification of mannose content

Resorcinol (Riedel-de Haen, Seelze, Germany) assay was used to evaluate the degree of mannosylation in the modified PEI polymers. The same preparation method was used as described in Chapter 3.

Cell culture

Raw264.7 cells (ATCC, Manassas, VA), a murine macrophage cell line that overexpresses mannose receptors were cultured in Dulbecco's Modified Eagle's Medium (DMEM, Gibco) supplemented with 10% fetal bovine serum (FBS, Hyclone), penicillin-streptomycin (100units penicillin; 100ug streptomycin/ml, Gibco). The cells were maintained at 37°C in a humidified, 5% carbon dioxide atmosphere.

Amplification and purification of pDNA

The psiCHECKTM-2 (Promega, Madison, WI) vector encoding firefly (hluc+) and *Renilla* (hRluc) luciferase was amplified and purified following the same method as described in Chapter 3.

Preparation of PEI/siRNA nanoplexes

PEI/siRNA nanoplexes were formed at predetermined N/P (nitrogen in cationic polymer per phosphate in nucleic acid) ratios with siRNA and polymer solutions. A mass per phosphate of 325Da for RNA and mass per charge of 43Da for PEI were used to

calculate N/P ratio. The nanoplexes were formed using the same method described in the previous chapter.

Size distribution and surface morphology analysis

The polymer/siRNA nanoplexes were analyzed for the size distribution and surface morphology using SEM and zeta sizer. The samples were prepared following the same process described in Chapter 3.

SiRNA retardation ability

The polymer/siRNA nanoplexes were analyzed for the degree of retardation in an EtBr agarose gel at the conditions described previously, with the exception of running time. The gels were run at 60V in TAE buffer for 40 minutes instead of 45 minutes.

Intracellular trafficking

Cellular uptake study with lysosomal staining was carried out following the same preparation process as described in Chapter 3. Trafficking with green fluorescent-labeled polymers (OregonGreen 488) was performed without lysosomal staining step. Briefly, RAW264.7 cells were plated onto 0.01% (w/v) poly L-lysine coated 8-well chamber slides (Lab-Tak) at 1.2×10^4 /well concentration and incubated overnight. The cells were transfected with OregonGreen polymer/Cy3-labeled siRNA nanoplexes in fresh opti-MEM. At pre-determined time points, the cells were preserved until observation using the same method described before.

In vitro gene knockdown efficiency on mRNA expression

Cells were seeded onto 48-well plate (8×10^4 cells/well) for endogenous gene knockdown on day 0. Then NC1 (negative control) and HPRT siRNAs were transfected using various polymers in opti-MEM media on day 1 and incubated for 24 hours. Total RNA was extracted (Promega, SV96 Total RNA Isolation System) on day 2 followed by cDNA synthesis and real-time PCR. 150ng of total RNA was used for reverse

transcription using Superscript II reverse transcriptase (Invitrogen, San Diego, CA). cDNA equivalent to 10 ng total RNA was analyzed by real-time PCR in triplicate using Immolase polymerase (Bioline, Randolph, MA) on AB7900HT (Applied Biosystems). The data was reported as mean \pm standard deviation from triplicate RT-PCR reactions of each triplicate sample using Microsoft Excel and Prism® software (GraphPad Software, Inc). Experiments were repeated at least twice.

In vitro gene knockdown efficiency on protein expression

RAW264.7 cells were transfected with psiCHECK™-2 using PEI instead of Lipofectamine 2000 in contrast to the modified chitosan transfection analysis. The following process was the same as described in Chapter 3. Experiments were repeated at least three times.

Cytotoxicity evaluation

Cytotoxicity was determined using the MTS assay (CellTiter 96® AQueous One Solution Cell Proliferation Assay, Promega, Madison, WI) following the manufacturer's protocol. Experiments were repeated at least three times.

Statistical analysis

Group data are reported as mean \pm standard deviation. Statistical analysis was carried out using one-way ANOVA followed by Tukey's multiple comparison test. Prism software (GraphPad Software, San Diego, CA) was used to perform statistical analyses. $P < 0.05$ was considered as statistically significant difference.

Results

Pegylation and mannosylation of PEI are verified

PEI-PEG-mannose and mannose-PEI-PEG showed peaks at δ 7.0 (MPITC phenyl-H), δ 3.5 (PEG-CH), and δ 2.6 (PEI-CH) indicating successful incorporation of

PEI, PEG and mannose in the final product. (Figure 4-1D, E) The signal at 7ppm was relatively weak but indicated the presence of mannose. When comparing these spectra to the control spectra of PEI, PEI-mannose, and PEI-PEG (Figure 4-1A-C), the 3.5ppm peak matched to PEG and the 2.6ppm corresponded to the PEI hydrocarbon chain. The conjugation/substitution ratio was calculated based on the peak area ratio between 3.5ppm PEG and 2.6ppm PEI. (Table 4-2) The molar ratios of PEI to PEG were 3.704 in PEI-PEG and 1.23 in PEI-PEG-mannose. There were two different products of mannose-PEI-PEG. One product had a PEI/PEG ratio of 3.491 and the other had a PEI/PEG ratio of 0.962. The product with the 0.962 PEI/PEG ratio was selected for subsequent experiments (batch #1) because its mannose content was similar to the PEI-PEG-mannose construct. There was no significant difference between the ^1H NMR spectra of mannose-PEG-PEI and PEG-PEI-mannose.

Mannose quantity is determined

The resorcinol assay is a commonly used method to determine the content of monosaccharides in polymeric structures.¹²⁵ The mannose content in our products was determined using this technique. (Table 4-2) Mannosylated PEI showed 0.14 $\mu\text{mol}/\text{mg}$ mannose existence. PEI-PEG-mannose had 0.12 $\mu\text{mol}/\text{mg}$ of mannose. The two different products of mannose-PEI-PEG had 0.19 and 0.81 $\mu\text{mol}/\text{mg}$ mannose, respectively (batch #1 and batch #2). As described above, the mannose-PEI-PEG with 0.19 $\mu\text{mol}/\text{mg}$ mannose was selected for subsequent experiments to closely match the mannose content of the PEI-PEG-mannose construct.

Nanoplexes are spherical and coarse in appearance

SEM images were used to observe surface morphology and shape of the polymer/siRNA nanoplexes. The polymer/siRNA nanoplexes without pegylation were spherically or semi-spherically shaped with some porosity but otherwise smooth surfaces. (Figure 4-2A and C) In contrast, the PEGylated nanoplexes had more coarse features on

the surface. (Figures 4-2B, D and E) The particle sizes of various PEI polymers/siRNA nanoplexes are shown in Table 4-3. PEI/siRNA polyplexes and PEI-PEG/siRNA nanoplexes had 214.57 nm and 201.80 nm average diameters respectively. PEI-mannose/siRNA nanoplexes showed 257.53 nm in average. Man-PEI-PEG formed nanoplexes with siRNA with an average size of 169.10 nm. PEI-PEG-mannose/siRNA nanoplexes had an average size of 357.33 nm. In addition, the formulations had positive zeta potentials that could aid in attraction to the negatively charged cell membrane. The pegylated PEI/siRNA nanoplexes and PEI-PEG-Man/siRNA nanoplexes displayed zeta potentials (24.37 mV and 21.63 mV respectively) that were similar to unmodified PEI (21.94 mV). PEI-mannose/siRNA nanoplexes also showed similar surface charge of 26.37 mV. The zeta potential of nanoplexes prepared using Man-PEI-PEG had a lower value of 10.46 mV.

Modified PEI polymers complex and retard siRNA migration

For the mannosylated and pegylated PEI products we generated to be capable of delivering siRNA, they must be able to complex and condense the siRNA as efficiently as PEI alone. Cationic polymers form nanoplexes with anionic siRNAs and compact them by ionic/electrostatic interactions. This complexation capacity was analyzed using a gel electrophoresis assay. The migration of siRNA on the agarose gel was retarded with the use of all the polymer constructs. All the constructs including PEI (Figure 4-3A) and PEI-PEG (Figure 4-3C) showed excellent complexation with siRNA even at low N/P ratios of 1 that prevented siRNA migration in the gel retardation assays. PEI-Mannose/siRNA nanoplex also showed effective complexation at N/P ratio 3 and above. (Figure 4-3B) Both mannose-PEI-PEG and PEI-PEG-mannose showed complete exclusion of EtBr from N/P ratios 1 to 15 indicating a broad and strong complexation

capacity with siRNA. (Figures 4-3D and E) Based on this result, the following studies were carried out using nanoplexes prepared within this range of N/P ratios.

Modified PEI/siRNA nanoplexes are endocytosed by

RAW264.7 cells

To track the cellular uptake and distribution of the mannosylated pegylated PEI/siRNA nanoplexes, siRNA and endosomes were labeled with red and green fluorophores, respectively. At 2 hours post-transfection, all the polymer/Cy3-siRNA nanoplexes (shown in red) were successfully internalized in the RAW264.7 cells. PEI/siRNA and PEI-PEG/siRNA nanoplexes were taken up by cells and localized in vesicular structures as seen by yellow fluorescence due to the green staining of lysosome and red siRNA signal in close proximity. (Figures 4-4A and C) PEI-Mannose/siRNA signal was weak but found close to lysosomal signal. (Figure 4-4B) Mannose-PEI-PEG/siRNA nanoplexes were also endocytosed and located near lysosomes. (Figure 4-4D) PEI-PEG-mannose/siRNA nanoplexes showed the most uniformed endocytosis evenly distributed in a large group of cells. (Figures 4-4E) Several images showed nanoplexes in the cytoplasm at the perinuclear region as observed by the separation of the green and red signal (nuclei stained with blue) suggesting release of the nanoplexes from the endosomes. This phenomenon was more prominently detected in the cells transfected with PEI-PEG-mannose/siRNA nanoplexes due to the increased uptake and broad distribution of the siRNA.

Modifications of PEI improve gene knockdown efficiency

Real-Time Polymerase Chain Reaction (Quantitative PCR/qPCR)

Endogenous gene knockdown was carried out using HPRT (Hypoxanthine-Guanine Phosphoribosyl Transferase) siRNA transfection. HPRT is a ubiquitously expressed enzyme that is commonly used as a positive control for endogenous gene knockdown experiments. PEI/siRNA and PEI-mannose/siRNA nanoplexes resulted in

68.31% and 95.48% gene expression at N/P ratio 10. (Figure 4-5A) PEI-PEG/siRNA resulted in a 65.80% remaining gene expression. The tricomponent polymers, mannose-PEI-PEG and PEI-PEG-mannose, further enhanced gene delivery showing 62.15% and 61.19%, respectively. Mannosylation alone did not improve the gene knockdown efficacy of PEI. Whilst pegylation and mannosylation jointly improved knockdown at the mRNA level, none of these differences were significant.

Dual Luciferase Assay

In vitro transfection was performed using the dual-luciferase reporter system to evaluate the siRNA delivery potential of mannosylated pegylated PEI delivery systems. Relative gene expression levels were analyzed after transfecting siRNA only targeting *Renilla* luciferase mRNA and leaving firefly gene expression as an internal control. All the polymers successfully delivered siRNA and reduced target gene expression. (Figure 4-5B) PEI/siRNA nanoparticles inhibited *Renilla* gene expression to 33.6% at an N/P ratio of 3 and 18.8% at an N/P ratio 10. PEI-Mannose/siRNA showed relatively less effective than the others showing 52.2% gene expression at both N/P ratios 3 and 10. At an N/P ratio of 3, PEI-PEG had the strongest knockdown efficiency resulting in 11.3% expression, which is significantly lower than the other transfection groups including a commercial transfection reagent, siLentFect (48.2%). However, increasing the N/P ratio of PEI-PEG to 10 reduced knockdown to 58.6%. There was no statistically significant difference in gene silencing efficiency of PEI-PEG between the N/P ratio of 3 and 10 ($P > 0.05$). Mannose-PEI-PEG/siRNA nanoplexes generated 34.2% and 42.0% gene expression when used at N/P ratios 3 and 10, respectively. PEI-PEG-mannose decreased gene expression down to 19.9% at N/P ratio 3 and 22.9% at N/P ratio 10. No significant difference was found between the N/P ratios of 3 and 10 in both modified polymers ($P > 0.05$). Furthermore, the modified polymers showed no significant difference in gene silencing efficiency in comparison to unmodified PEI ($P > 0.05$). The luciferase assay was also carried out with the nanoplexes prepared at the N/P ratios of 5 and 7 (data not

shown). The result did not show significant differences in gene silencing efficiency when compared to nanoplexes prepared at N/P ratios of 3 and 10.

Modifications of PEI significantly reduce toxicity

Raw264.7 cells were treated with various groups of nanoplexes to evaluate toxicity. At a concentration of 0.0078mg/ml, PEI showed the highest toxicity resulting in 37.5% cell viability. (Figure 4-6) PEI-Mannose was the least toxic with 85.4% cell survival. PEI-PEG resulted in higher cell viability (79.1%) when compared to PEI alone. Mannose-PEI-PEG (68.9%) and PEI-PEG-mannose (53.9%) also resulted in higher cell viabilities than PEI alone. The modified PEI polymers demonstrated lower cytotoxicity relative to unmodified PEI. Cell viabilities were decreased by increasing concentrations of polymers for all the groups tested. However, the reduction in cytotoxicity when using modified polymers in comparison to unmodified PEI increased dramatically at the highest concentrations of 1 mg/ml tested (data not shown).

Discussion

In this study, we synthesized, characterized, and tested a mannosylated pegylated PEI delivery system for siRNA. Pegylation has potential to interfere with serum protein binding and increase the circulation time of nanoparticles.^{115, 177, 178} Mannose can increase binding of particles to mannose receptor-expressing cells and enhance cellular uptake.^{124, 125, 128, 133, 135, 175, 176} To our knowledge, this is the first study to evaluate mannosylated pegylated PEI for siRNA delivery, and it is the first study to characterize the effect of the location of the mannose ligand in mannosylated pegylated PEI constructs on knockdown efficiency.

Pegylation and mannosylation was carried out in two ways. PEG and mannose were directly conjugated onto the PEI backbone in one structure and mannose was conjugated to the PEI via a PEG spacer in the other. ¹H NMR spectra confirmed the presence of PEI, PEG, and mannose in both structures, and the peaks were consistent to

the previously reported values.^{179, 180} The signal for mannose at 7 ppm was weak because the relative amount of mannose in the overall construct composition was small. For this reason, we used the resorcinol assay to quantify the amount of mannose present in each construct.

The surface chain density of PEG is a critical factor in improving stealth shielding of the nanoplexes. The PEI to PEG ratio of 3.704 in PEI-PEG suggested that every 25 kDa PEI chain had 3.45 chains of 2 kDa PEG. PEI-PEG-mannose had a 1.23 PEI/PEG ratio indicating 10.16 PEG chains per PEI. The PEI/PEG ratio of 0.962 in mannose-PEI-PEG suggested that there are 13.3 PEG chains for each PEI. PEG chains have a larger range of motion at low surface coverage, that can lead to gaps in the PEG protective layer.¹⁸¹ For PEG chains to fully cover the surface of PEI/siRNA polyplexes, six short PEGs (5 kDa) or one long PEG (10 kDa) are needed.^{83, 177} Therefore, 3.45-13.3 chains of 2 kDa PEG was expected to provide a sufficient steric stabilization. PEI-mannose had 0.14 $\mu\text{mol}/\text{mg}$ of mannose representing 3.4 mannose molecules per every one 25 kDa PEI. Mannose-PEI-PEG and PEI-PEG-mannose each had 0.19 $\mu\text{mol}/\text{mg}$ and 0.12 $\mu\text{mol}/\text{mg}$ of mannose, which represented an average mannosylation of 4.7 and 3.0 molecules of mannose existence per PEI, respectively. This amount of mannose was expected to be sufficient to achieve selective binding of mannose receptors on cells. The degree of mannosylation and pegylation could be optimized by their feed ratio in the reaction.¹⁷³

The nanoplexes displayed spherical shapes with 169.10nm to 357.33nm in size as determined in the size measurement using the Zetasizer nano ZS. This size of nanoplexes was suitable for efficient endocytosis by cells. Nanoplexes larger than this range observed in the SEM images were probably clusters of smaller ones. The zeta potentials of PEI-PEG-Man/siRNA nanoplexes showed positive values that were approximately 21.63mV and similar to unmodified PEI and pegylated PEI. This result suggested that PEI-PEG-Man could form stable nanoplexes with siRNA. The zeta potential of Man-

PEI-PEG/siRNA nanoplexes was relatively low compared to PEI-PEG-Man/siRNA nanoplexes. This could explain the lower cellular uptake of Man-PEI-PEG observed in our intracellular trafficking studies. The lower zeta potential could lead to weaker interactions with siRNA and the cell surface, which in turn could lead to decreased endocytosis of the nanoplexes. Pegylation of PEI did increase the average size of the particles but not to the extent of interfering with endocytosis. Similar to the modified chitosan/siRNA, the increased size of pegylated PEI nanoplexes can be explained by the reduced intensity of interaction between PEI and siRNA by PEG chains.^{83, 113} The selection of a higher molecular weight (25kDa) branched PEI ensured that pegylated PEIs are able to condense and complex siRNA efficiently, even at N/P ratios of 1. Branched PEI was selected as the backbone for our system because the complexation of branched PEI with siRNA has been reported to exceed that of linear PEI.¹⁹⁴ As a result, in gel retardation assays, no reduction in siRNA condensation properties was found with PEGylated PEIs. Overall, complete binding of siRNA was achieved with all the various constructs at N/P ratios of 3 and higher. Mannosylation of PEI reduced the retardation of siRNA at the N/P ratio of 1, however this reduction was recovered at the N/P ratio of 3.

A murine macrophage cell line that overexpresses mannose receptors was chosen because macrophages are a potential target for our modified PEI delivery system.¹²⁸ In confocal images, co-localization of the green and red signals indicated that nanoplexes were being internalized by endocytosis as previously reported.²⁰¹ Unlike the cells transfected with the modified chitosan in Chapter 3, separate siRNA signals were abundantly found in the cytosol when transfected with the modified PEI. It indicates that siRNA was released from the endosomal compartments. The same was observed when we used green fluorescent-labeled (Oregon Green 488) polymer to complex siRNA. Thirty minutes after incubation, the nanoplexes was internalized by cells and localized in cytoplasm. After 2h, green fluorescent-labeled polymers and red fluorescent-labeled (Cy3) siRNA were separated in cytoplasm (data not shown) indicating that siRNA

nanoplexes was released from the vesicles as well as from the polymers and were distributed in the cytosol. This release of siRNA can be attributed to the proton sponge effect, which causes rupture of the endosomes because of the PEIs strong buffering capacity.⁸⁰ Intracellular trafficking plays an important role in the fate of siRNA polyplexes because their spatial distribution does not correspond to simple diffusion.¹⁸⁸ Perinuclear localization of siRNA, as seen in some cells, is required for successful gene silencing by interaction with RISC to induce RNAi. Interactions with RISC dictate siRNA localization even when siRNA is conjugated to cell-binding ligands such as the TAT peptide.⁴⁰ It suggests that the mannosylated pegylated PEI polymers developed in this study successfully protected siRNA during endocytosis and lysosomal escape in order to integrate siRNA into the RISC for RNAi induction. Mannosylation did not increase cellular uptake. Cell binding ligands do not always improve transfection efficiency. High affinity interactions between ligands and receptors decreased transfection efficiency by the increased amount of ligand, which prevents both the specific receptor-mediated endocytosis and non-specific endocytosis of the complexes.⁸⁵ The charge shielding of mannose could be another reason for this observation.

Mannosylation and pegylation, when conjugated together, did not reduce knockdown efficiency relative to unmodified PEI. The advantages of pegylating polyplexes and incorporating cell binding ligands for *in vivo* applications have been well established.^{108, 115, 122, 178, 180, 189, 190} Pegylation had no adverse effect on knockdown efficiency and also it reduced toxicity. This reduction in toxicity was slightly offset by the mannosylation. The difference in cytotoxicity between cells treated with modified PEI and unmodified PEI increased as the concentration of the nanoplexes that cells were treated with increased. Pegylation of the nanoplexes was also expected reduce toxicity at the systemic level by reducing aggregation of the nanoplexes and therefore the capillary embolism that has been associated with the use of unmodified PEI.¹⁰⁸ Mannose-conjugated PEI did not enhance the transfection efficiency showing lower gene

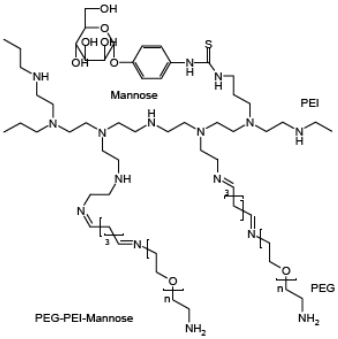
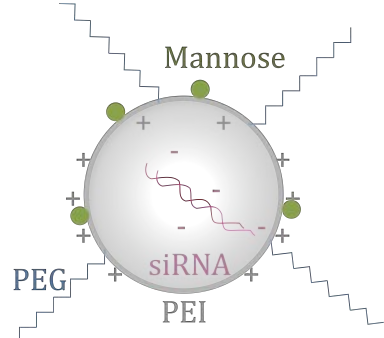
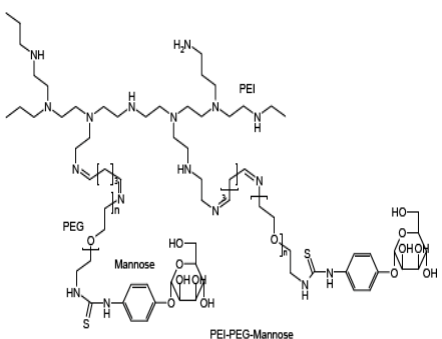
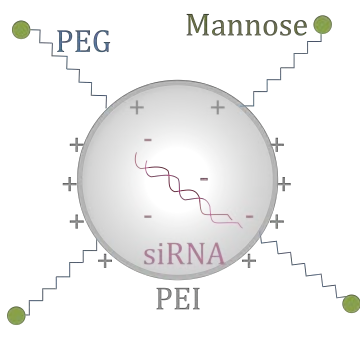
knockdown than unmodified PEI. It follows intracellular trafficking results in relation to the charge shielding of mannose.

The importance of the location in the construct has not yet studied in the mannosylated and pegylated PEI delivery system. PEI-PEG-mannose/siRNA nanoplexes resulted in higher toxicity and higher knockdown efficiency relative to mannose-PEI-PEG. Furthermore, PEI-PEG-mannose/siRNA nanoplexes had more stable uptake by RAW264.7 cells compared to mannose-PEI-PEG/siRNA nanoplexes. This observation could be explained by the structural difference between the two constructs. The PEI-PEG-mannose construct had mannose moieties exposed at the tip of PEG chain, whereas the PEG chains could hinder the mannose ligand in mannose-PEI-PEG. Thus the mannose ligand-receptor interaction could be physically hindered by the PEG chains. The PEG chain could interfere cell binding by shielding not only PEI but also the ligand.¹⁸⁶ We carried out cellular uptake time-lapse studies at various time points including 0.5, 1, 2, 4, 8, and 24 hours (data not shown). Throughout the course of experiment, we observe that PEGylated PEI had delayed cell uptake/endocytosis relative to PEI alone, and this observation would support our hypothesis. The reason that PEG-PEI without mannosylaton at an N:P ratio of 3 still has better luciferase knockdown than either the mannose-PEI-PEG or PEI-PEG-mannose constructs could be attributed to its better cytotoxicity profile.

The endogenous knockdown generated by the modified PEIs was significantly less effective than RNAiMax at targeted mRNA reduction. In addition, in our hands, TransIT-TKO can routinely provide 80-90% knockdown, which is significantly more effective than the modified PEIs (data not shown). Quantitative gene expression data such as qPCR results are normalized to the expression levels of housekeeping genes serving as control.²⁰² It is based on the assumption that the expression of housekeeping genes remain constant in the cells or tissues. In this study we used the expression level of HPRT house keeping gene as a target for endogenous mRNA knockdown.

The modified PEIs were more efficient at luciferase knockdown than that of another commercial transfection reagent, siLentFect. Moreover, both mannose and PEG had well established attributes for *in vivo* delivery such as selected cell binding, reduced systemic toxicity and enhanced circulation.^{108, 135, 191} In particular, mannose ligands have shown significant potential for binding antigen presenting cells (APCs) such as mouse macrophages and dendritic cells.^{133, 175} Furthermore, PEGylated PEI/siRNA nanoplexes decreased random uptake into non-specific organs including liver and spleen compared to unmodified PEI.^{107, 199} The location of cell binding ligands is expected to have important implications in the design of several plasmid DNA, oligonucleotide, and siRNA delivery systems currently in development that utilize alternative cell binding ligands.^{108, 128, 133, 135, 176, 186, 192} Additionally, we wanted to investigate the potential of this delivery system further for *in vivo* application PLGA microspheres.

Table 4-1: Molecular structures of two different constructs using PEI, PEG, and mannose, and schematics of nanoplexes once complexed with siRNA.

	Structure	Nanoplex
<p>Construct #1</p> <p>Man-PEI-PEG</p>	 <p>Chemical structure of Construct #1 (Man-PEI-PEG) showing the PEI backbone, mannose units, and PEG chains.</p>	 <p>Schematic of the nanoplex for Construct #1, showing the PEI backbone, siRNA, mannose units, and PEG chains.</p>
<p>Construct #2</p> <p>PEI-PEG-Man</p>	 <p>Chemical structure of Construct #2 (PEI-PEG-Man) showing the PEI backbone, PEG chains, and mannose units.</p>	 <p>Schematic of the nanoplex for Construct #2, showing the PEI backbone, siRNA, PEG chains, and mannose units.</p>

Note: Chemical structures of modified PEI constructs are shown in the left column and schematics of products after complexed with siRNA are shown in the right column. Mannose and PEG are directly conjugated to the PEI backbone in construct #1, whilst mannose is conjugated to the PEI via a PEG spacer in construct #2.

Table 4-2: PEI/PEG molar ratio and mannose content of the various modified PEI polymers

Formulation	Polymer/PEG molar ratio	Mannose content ($\mu\text{mol}/\text{mg}$)
PEI-Mannose	N/A	0.13671
PEI-PEG	3.704	N/A
Mannose-PEI-PEG (batch #1)	0.962	0.18679
Mannose-PEI-PEG (batch #2)	3.491	0.81315
PEI-PEG-Mannose	1.23	0.12122

Note: The PEI to PEG molar ratio was calculated based on the area of ^1H NMR peaks. Resorcinol measurements were used to determine the content of mannose (μmol mannose per 1mg polymer) in each construct.

Table 4-3: Hydrodynamic size and zeta potential of the modified PEI polymer/siRNA polyplexes

Formulation	Zeta Potential (mV)	Size (nm)
PEI	21.94 ± 0.50	214.57 ± 29.00
PEI-Mannose	26.37 ± 2.65	257.53 ± 8.77
PEI-PEG	24.37 ± 1.63	201.80 ± 4.95
Mannose-PEI-PEG	10.46 ± 0.91	169.10 ± 9.54
PEI-PEG-Mannose	21.63 ± 6.31	357.33 ± 92.90

Note: All the polyplexes were prepared with 1 μ M siRNA at N/P ratio 7. All data were represented as mean \pm SD (n = 3)

Figure 4-1: ^1H NMR spectra of the modified PEI polymers confirming the presence of PEI, PEG, and mannose in each construct. Each components of the constructs are indicated with boxes. A. unmodified PEI showed a peak at 2.6ppm. B. Mannosylated PEI showed peaks of PEI at 2.6ppm and mannose at 7ppm. C. Pegylated PEI showed peaks of PEI at 2.6ppm and PEG at 3.5ppm. D. Mannose-PEI-PEG showed peaks of PEG at 3.5ppm, PEI at 2.6ppm and mannose at 7ppm. E. PEI-PEG-mannose also showed each component at the same peaks as mannose-PEI-PEG.

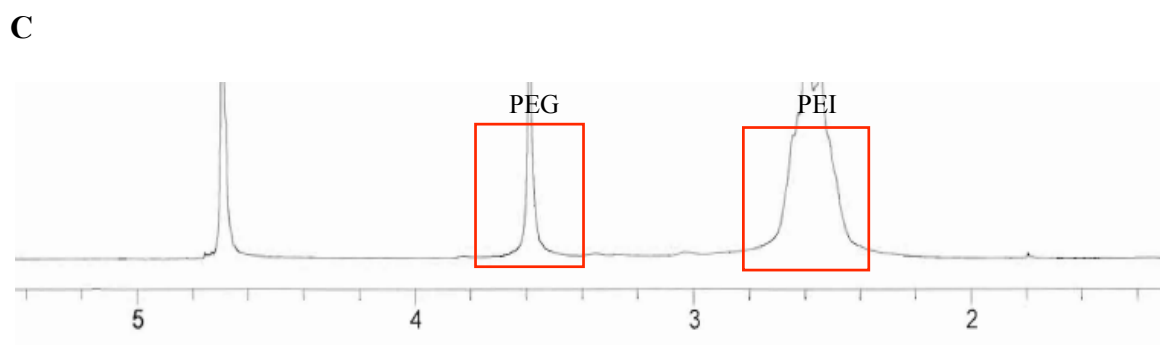
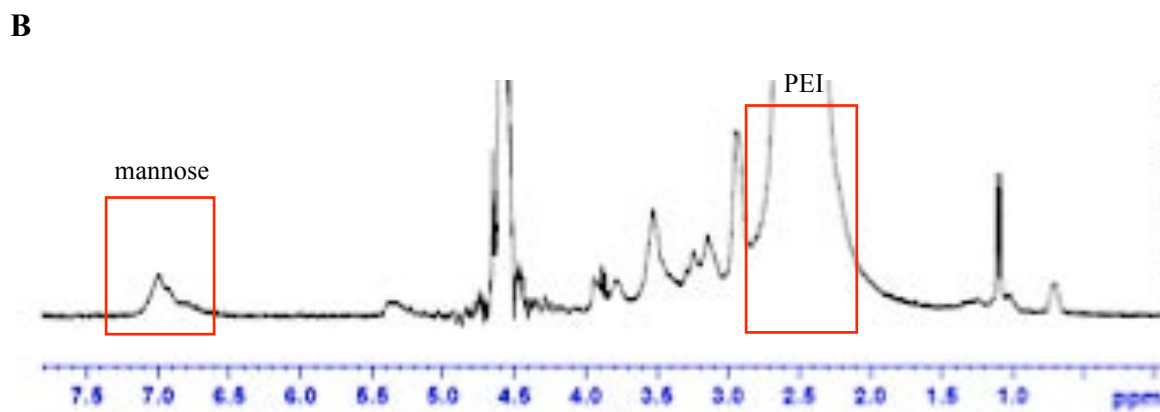
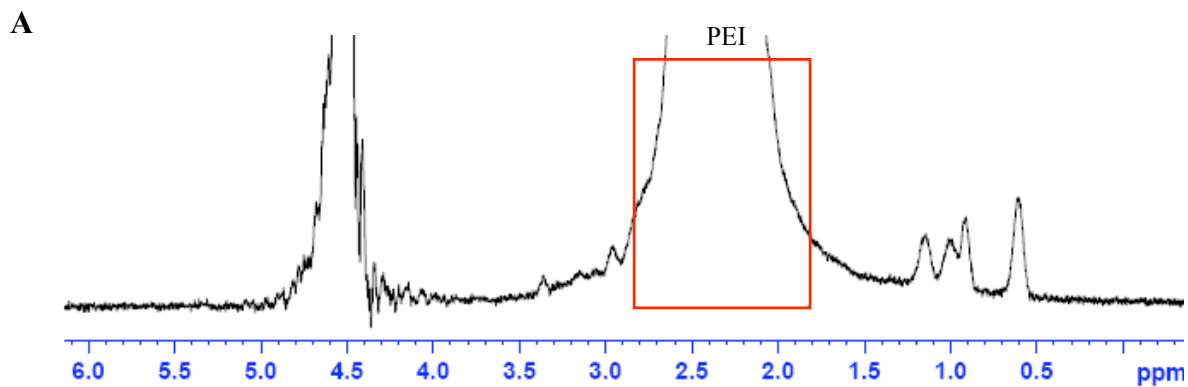
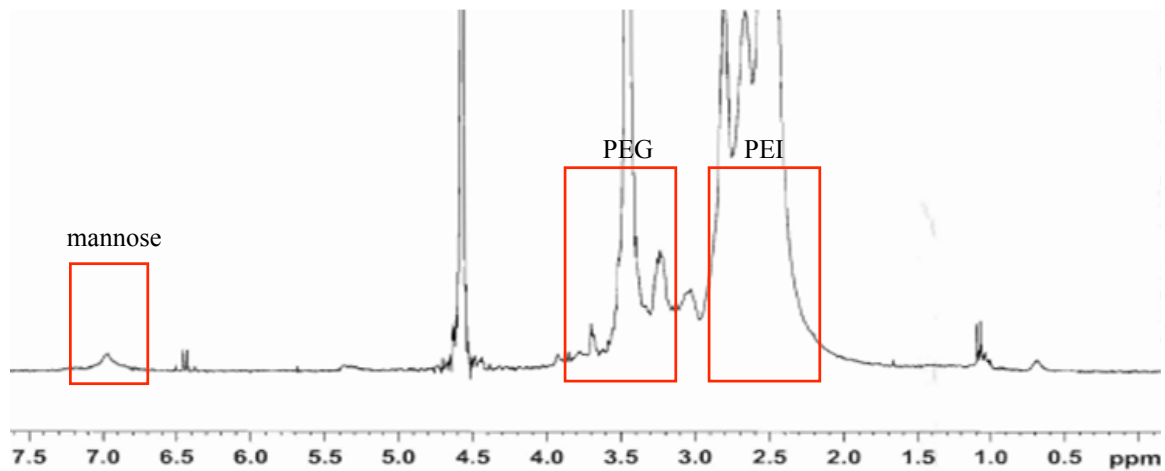


Figure 4-1 continued

D



E

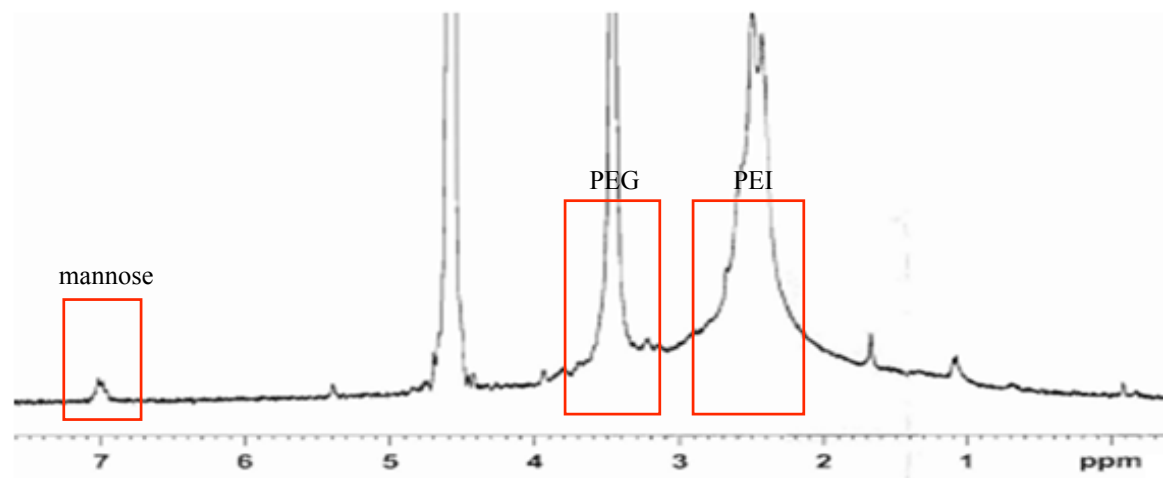
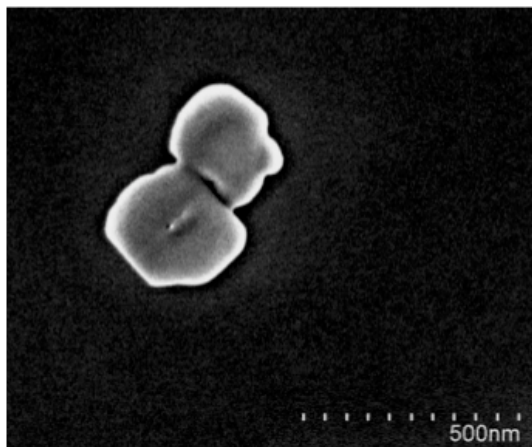
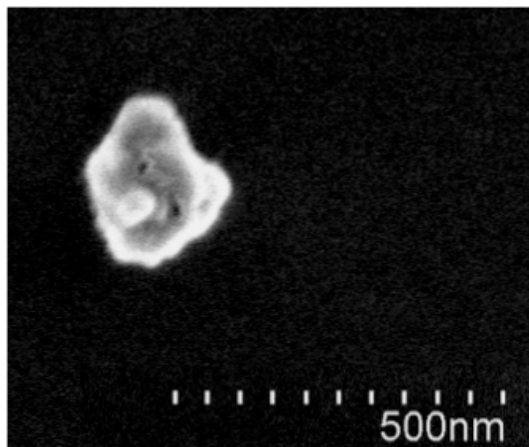


Figure 4-2: Scanning Electron Microscopy (SEM) images demonstrating the effect of pegylation and mannosylation on the size distribution and surface morphology of the modified PEI/siRNA nanoplexes. A, PEI/siRNA nanoplexes, B, PEI-Mannose/siRNA nanoplexes, C, PEI-PEG/siRNA nanoplexes, D, Mannose-PEI-PEG/siRNA nanoplexes, E, PEI-PEG-mannose/siRNA nanoplexes. All the nanoplexes were prepared with 1 μ M siRNA at N/P ratio 5. The experiments were repeated three times. The best representative images are shown.

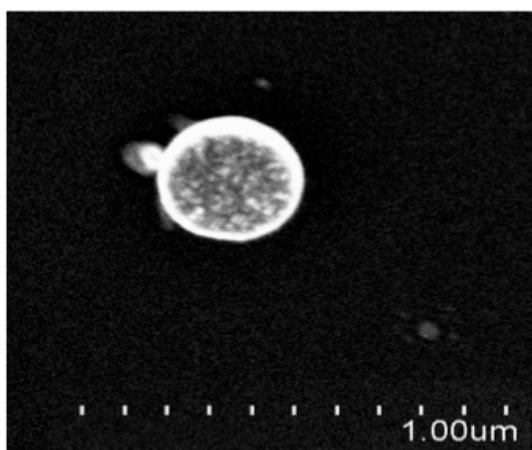
A



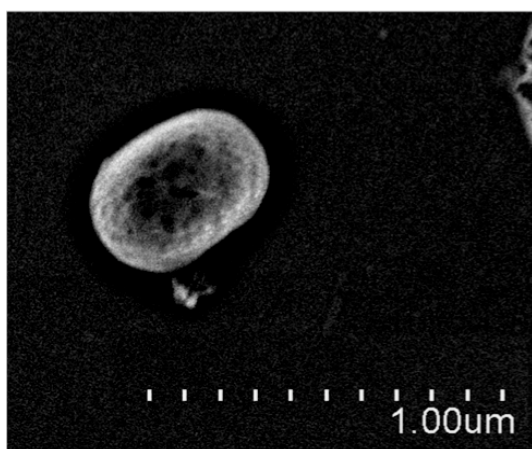
B



C



D



E

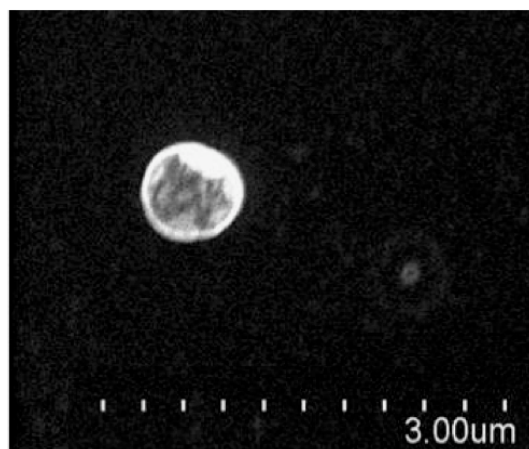


Figure 4-3: The effect of pegylation and mannosylation on siRNA retardation ability of the modified PEI polymers using ethidium bromide agarose gel electrophoresis. A, PEI/siRNA nanoplexes, B, PEI-mannose/siRNA nanoplexes, C, PEI-PEG/siRNA nanoplexes, D, Mannose-PEI-PEG/siRNA nanoplexes, E, PEI-PEG-mannose/siRNA nanoplexes. All the nanoplexes were prepared with 1 μ M siRNA from N/P ratio 1 to 15. The experiments were repeated at least twice. The best representative images are shown.

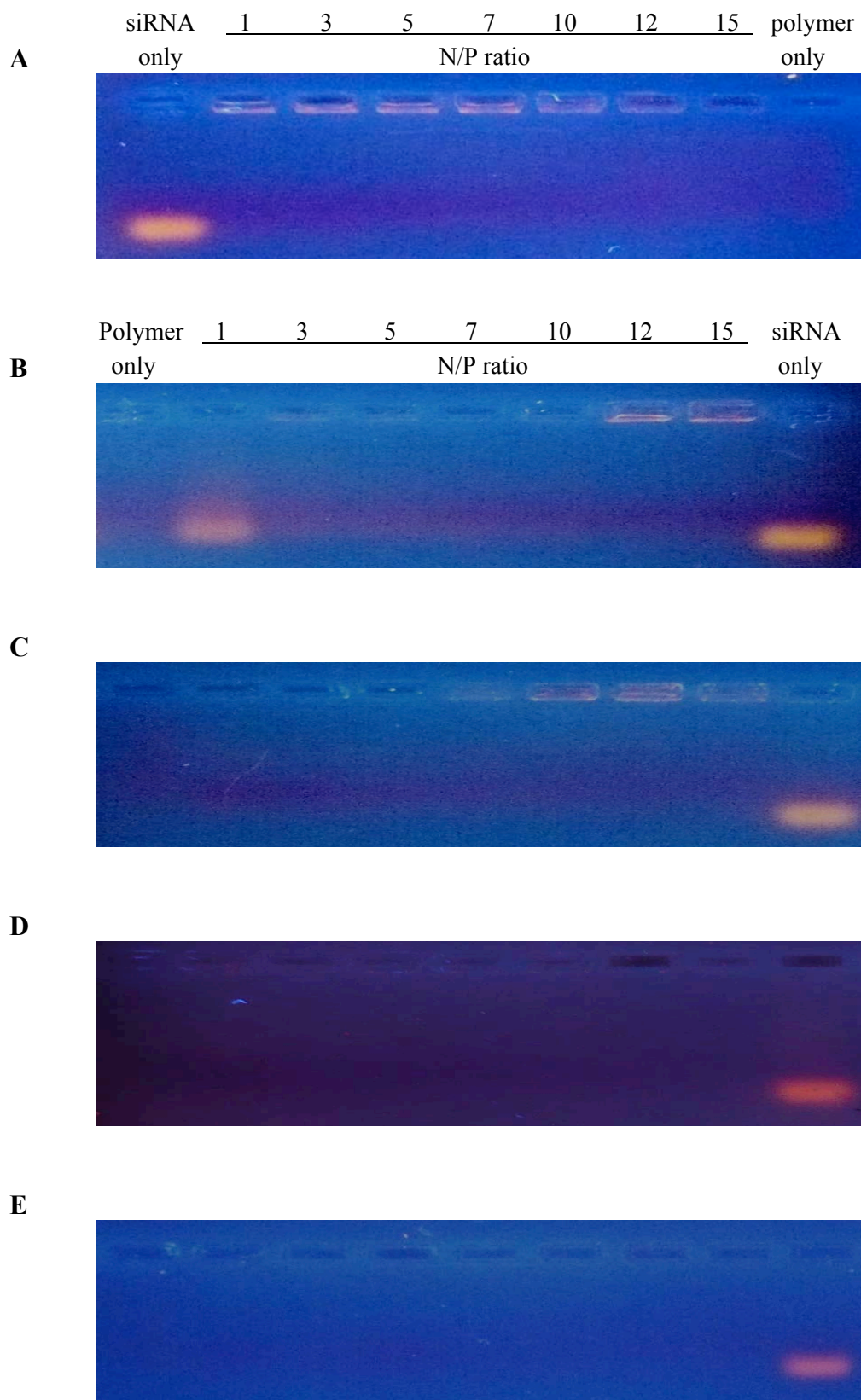


Figure 4-4: Confocal microscope images demonstrating the effect of pegylation and mannosylation on cellular uptake and intracellular localization of the modified PEI/siRNA nanoplexes in RAW264.7 cells. The cells were stained with LysoTracker Green (green), incubated with nanoplexes formed using Cy-3 labeled siRNA (red), and then mounted with DAPI containing mounting solution after fixation. Co-localization of nanoplexes and lysosomes are shown as a yellow signal. A, PEI/siRNA nanoplexes, B, PEI-mannose/siRNA nanoplexes, C, PEI-PEG/siRNA nanoplexes, D, Mannose-PEI-PEG/siRNA nanoplexes, E, PEI-PEG-mannose/siRNA nanoplexes. The experiments were repeated at least twice. The best representative images are shown.

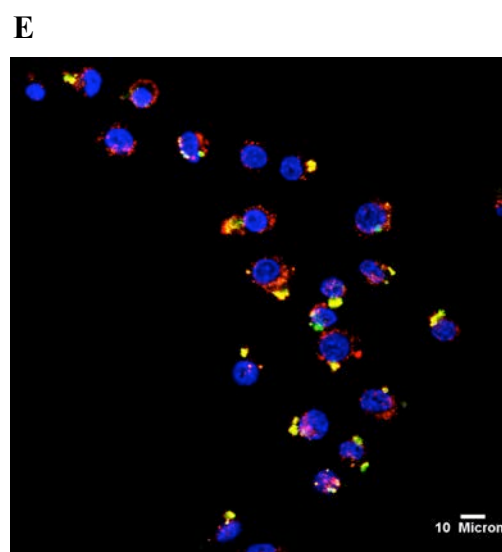
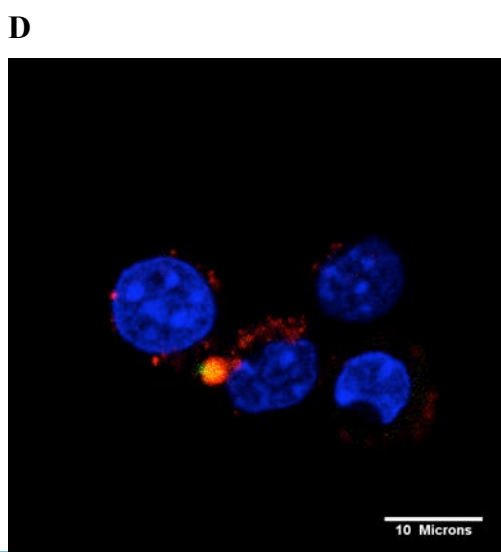
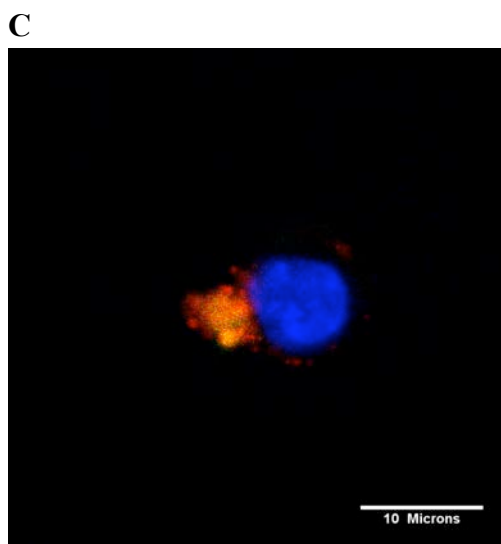
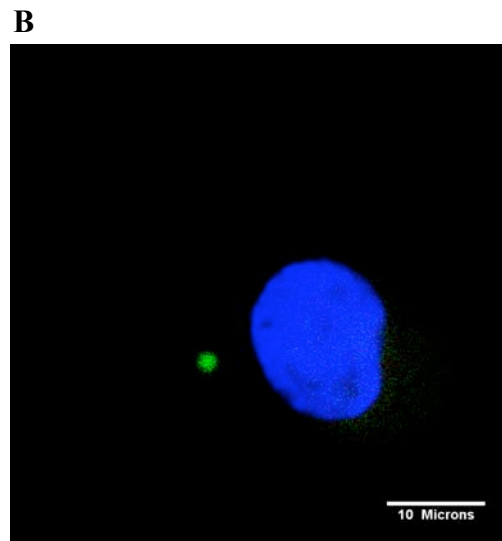
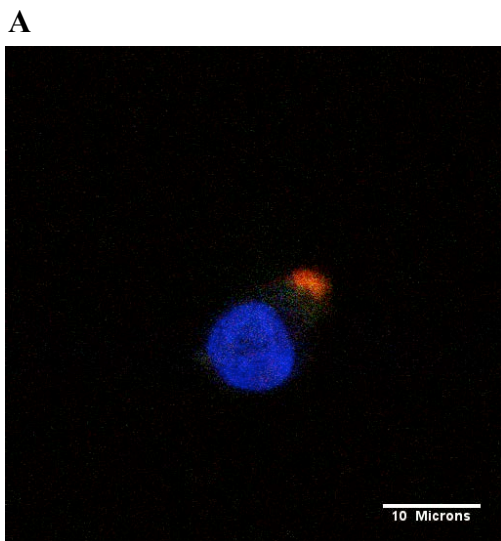
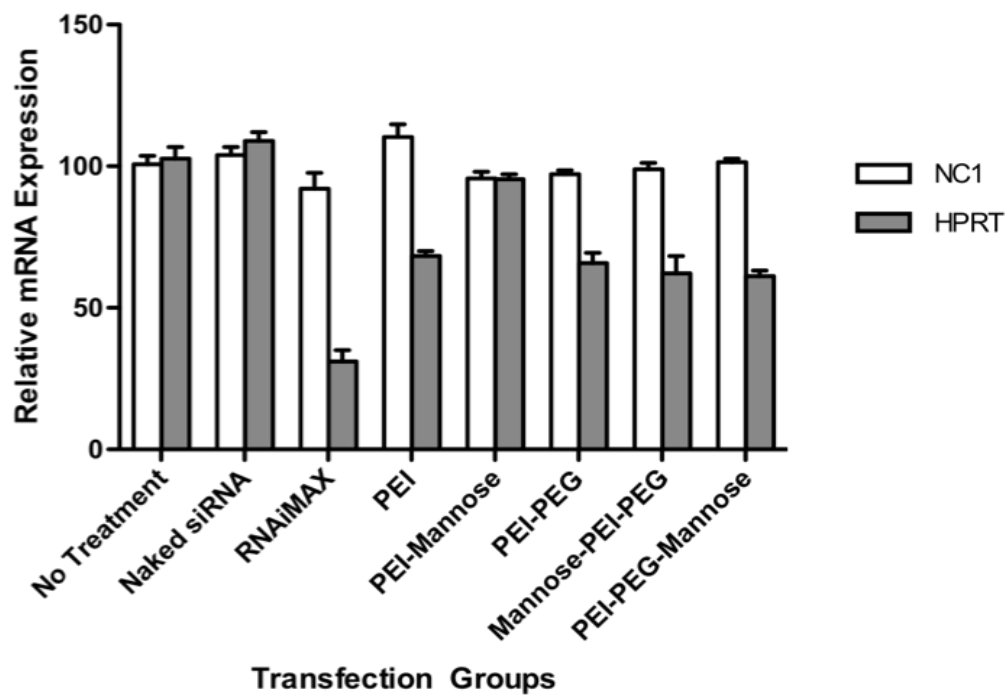


Figure 4-5: The effect of pegylation and mannosylation on gene knockdown efficiency of the modified PEI/siRNA nanoplexes demonstrated for luciferase protein and HPRT mRNA expression in RAW264.7 cells. A, Relative expression of HPRT mRNA levels normalized to that of NC1 mRNA. From the left, no treatment, naked siRNA, RNAiMax/siHPRT, PEI/siHPRT, PEI-mannose/siHPRT, PEI-PEG/siHPRT, mannose-PEI-PEG/siHPRT, PEI-PEG-mannose/siHPRT. The data was reported as mean \pm standard deviation from triplicate RT-PCR reactions of each triplicate sample. B, Relative gene expression of *Renilla* luciferase is normalized to that of firefly luciferase served as an internal control. From the left, PEI/DS neg. scrambled siRNA served as negative control, siLentFect/sihRluc served as positive control, PEI/sihRluc, PEI-mannose/sihRluc, PEI-PEG/sihRluc, mannose-PEI-PEG/sihRluc, and PEI-PEG-mannose/sihRluc with N/P ratios at 3 and 10. The experiments were repeated at least twice. Data is represented as mean \pm standard deviation (n=3).

A



B

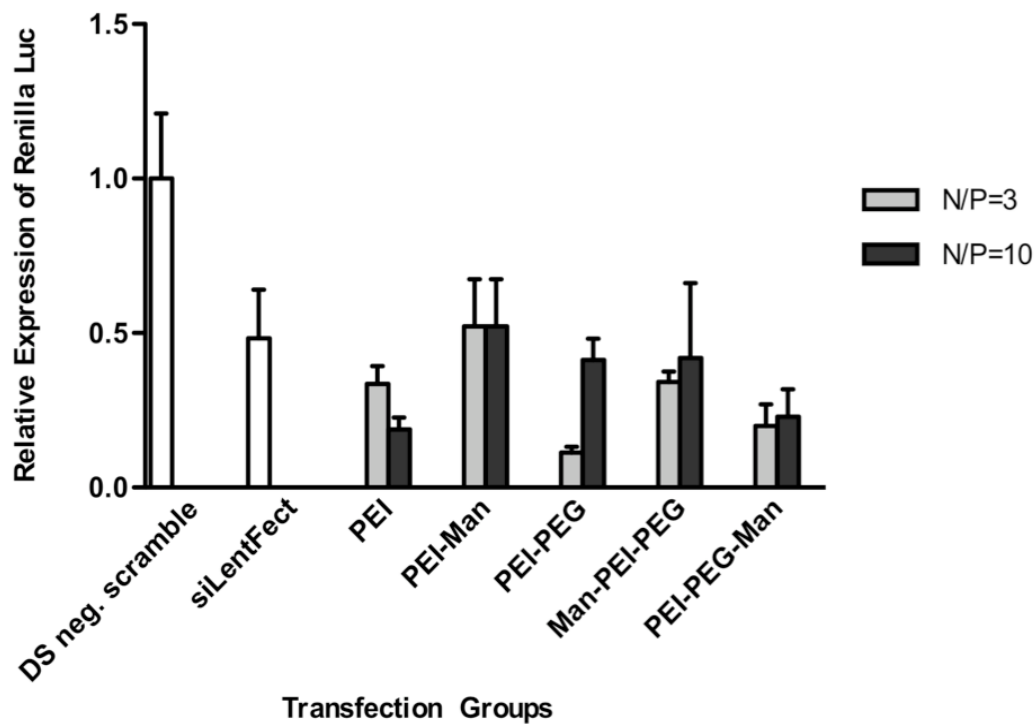
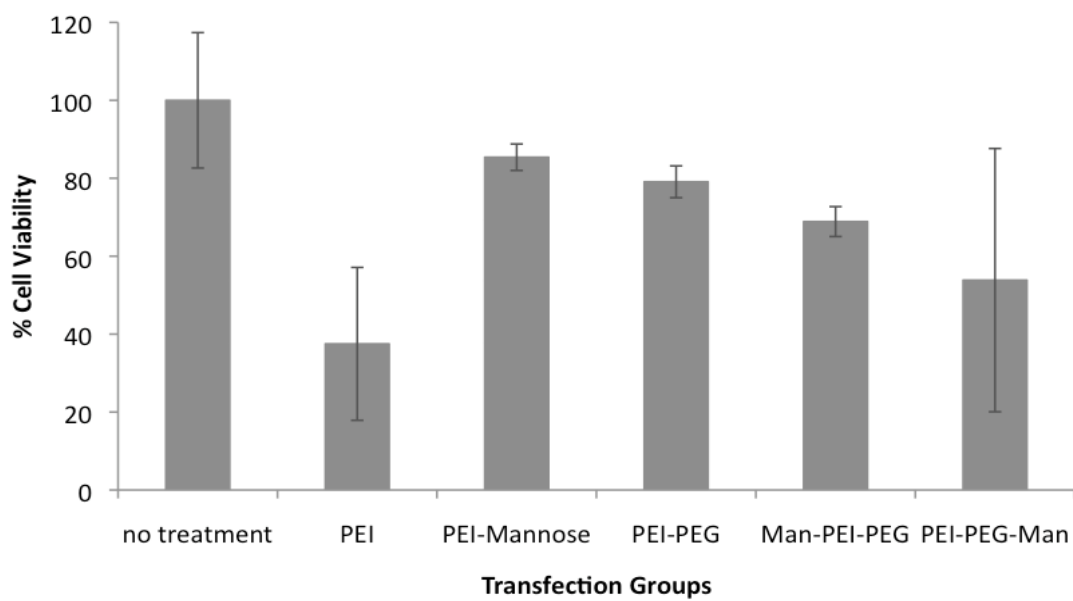


Figure 4-6: The effect of pegylation and mannosylation on cytotoxicity of the modified PEI/siRNA nanoplexes in RAW264.7 cells. Cytotoxicity of various nanoplexes tested at the working concentration of 0.0078 mg/ml. From the left; no treatment, PEI, PEI-mannose, PEI-PEG, mannose-PEI-PEG and PEI-PEG-mannose groups. The relative cell viability was calculated by normalizing to the no-treatment group. The experiments were repeated at least twice. Data is represented as mean \pm standard deviation (n=3).



CHAPTER 5: THERAPEUTIC PLGA MICROPARTICLES INCORPORATING THE MODIFIED PEI/SIRNA NANOPLEXES

Introduction

We have previously developed a siRNA delivery system that is composed of PEI, PEG, and mannose in two different constructions. Mannose and PEG, when conjugated in combination, reduced *in vitro* toxicity profile and did not impair siRNA knockdown efficiency of PEI. PEI-PEG-mannose produced stronger siRNA knockdown when compared to mannose-PEI-PEG. For this reason, the PEI-PEG-mannose construct was chosen to be investigated further for *in vivo* gene delivery efficiency. In this study, we incorporated the modified PEI/siRNA nanoplexes into PLGA microparticles in order to further protect siRNA, to improve *in vivo* delivery efficiency, and to create a long-acting delivery system. When encapsulated in biodegradable microparticles, the entrapped cargo can be protected from enzymatic degradation and released in a controlled manner.²⁰³ PLGA particles are efficiently phagocytosed by dendritic cells or macrophages *in vitro* and *in vivo*, and therefore capable of triggering robust immune responses.²⁰⁴⁻²⁰⁶ In terms of formulation, it is difficult to efficiently encapsulate high amounts of hydrophilic macromolecules such as siRNA into the PLGA particles due to the hydrophobic nature of PLGA.¹⁴⁸ One way to improve encapsulation of nucleic acids is to add a cationic polymer to the PLGA matrix.¹⁴⁹ Addition of PEI increased the loading efficiency of PLGA particles of nanoplexes. Modified PEI can be a good cationic excipient to PLGA microparticles and is expected to enhance encapsulation of siRNA.

The purpose of the overall research is to develop efficient siRNA delivery systems that can be ultimately applied to *in vivo* therapeutic model. In order to optimize the PLGA particle formulation with modified PEI/siRNA nanoplexes, the main goal of this chapter was to characterize and invest utility of unmodified PEI and the two different

modified PEIs as cationic excipients. The PLGA particles loaded with modified PEI/siRNA nanoplexes were characterized for encapsulation efficiency of siRNA, surface morphology, release and toxicity profiles. Adding the modified PEI to the PLGA particle matrix was expected to improve loading efficiency. We expected to modify surface features and size of the particles, which in turn will alter release profile. After the physicochemical characterizations, their delivery performance was evaluated *in vitro* and *in vivo* experiments. We also evaluated *in vivo* hepatotoxicity following the PLGA microparticles injection.

Materials and Methods

Materials

PLGA (75:25, inherent viscosity, 0.41 dL/g) were purchased from Lactel Absorbable Polymers (Cupertino, CA). Poly (vinyl alcohol) (PVA, 87 – 89 % hydrolyzed, MW 30- 67,000 Da) was from Sigma-Aldrich (St. Louis, MO). All other chemicals and solvents including dichloromethane (DCM) and acetonitrile used were of analytical grade. All the siRNAs (Cy-3, NC1, and GAPDH) was kindly provided by Integrated DNA Technologies (Coralville, IA).

Preparation of modified PEI/siRNA nanoplexes-loaded

PLGA microparticles

The modified PEIs were complexed with siRNA in 1% polyvinyl alcohol (PVA) solution as previously described in Chapter 3. Then PLGA microparticles were prepared using water-in-oil-in-water (W/O/W) double emulsion, solvent evaporation technique. (Figure 5-1) Polymer/siRNA nanoplexes in solution served as the internal aqueous phase. They were emulsified into an oil phase consisted of PLGA (75:25, 35kDa, inherent viscosity 0.41 dL/g) dissolved in dichloromethane (DCM) for 30 seconds using micro-tip sonicator at level 3 setting (10 Watts, Sonic Dismembrator Model 100, Fisher

Scientific, Pittsburgh, PA). The mixture, the primary water-in-oil emulsion, was immediately mixed into an external aqueous phase of 1% PVA solution and homogenized for 30 seconds at 9500rpm using IKA Ultra-Turrax T25 basic homogenizer (IKA, Wilmington, NC). Then the secondary water-in-oil-in-water emulsion was stirred in the hood for 2 hours to evaporate DCM. After the evaporation, the particles were washed with nuclease-free deionized water and recovered by centrifugation at 5000 x g for 10 minutes followed by lyophilization (Labconco FreeZone 4.5, Kansas City, MO) for storage.

Evaluating encapsulation efficiency (EE)

After the first centrifugation of the particles, the amount of free siRNA in the supernatant collected was measured using Nanodrop™ 2000 (Thermo Scientific, Wilmington, DE). Encapsulation efficiencies⁵⁷ of polymer/siRNA nanoplexes-loaded PLGA microparticles were calculated as follows:

$$EE (\%) = \frac{\text{Starting amount of siRNA} - \text{Free siRNA in supernatant}}{\text{Starting amount of siRNA}} \times 100$$

Alternatively, the encapsulation efficiencies of PLGA microparticles were calculated by measuring the amount of loaded siRNA using the Quant-IT™ PicoGreen® reagent (Invitrogen, Eugene, OR). The PLGA microparticles (50mg) were dissolved with 2ml DCM for 5-10 minutes to release siRNA and nuclease-free deionized water was added to dissolve siRNA out. The upper aqueous phase was removed to collect siRNA. Then the concentration of siRNA in the solution was determined according to the Quant-IT™ PicoGreen® reagent manufacturer's protocol.

Evaluating EE using fluorescent PLGA microparticles

Fluorescent-labeled Cy3 siRNA was utilized to visualize the incorporation of siRNA in the PLGA microparticles. The presence of siRNA was verified using confocal

microscopy and flow cytometry. The particles were dissolved in nuclease-free deionized water and immediately analyzed either using the confocal microscope (Zeiss LSM 710, Thornwood, NY) or using flow cytometry. The images from confocal microscopy were analyzed using ImageJ software and the data from flow cytometry was analyzed using FlowJo software (Tree Star, Stanford).

Size distribution and surface morphology analysis

The PLGA microparticles were suspended in nuclease-free deionized water and immediately dropped onto silicon wafers to be air-dried under the hood. Then the silicon wafers were mounted on aluminum stubs using liquid colloid silver adhesives followed by overnight drying at room temperature. The specimen stubs were coated with approximately 5nm of gold/palladium by ion beam evaporation before imaging. Size distribution and surface morphology were observed using Scanning Electron Microscopy (SEM, Hitachi S-4800) operated at 1.5kV accelerating voltage. The images were analyzed with Image J software. Size and zeta potential measurements were conducted using the Zetasizer Nano ZS (Malvern, Southborough, MA). The size measurements were performed at 25°C at a 173° scattering angle. The mean hydrodynamic diameter was determined by cumulative analysis.

In vitro release profile of siRNA from PLGA microparticles

The PLGA microparticles (50mg) were suspended in 1.2ml PBS and incubated at 37°C on a plate shaker. At various time points, the samples were centrifuged at 5000 rpm for 10 minutes and 1ml of supernatant was collected for evaluation. Fresh 1ml PBS was added in to resuspend the particles and resume incubation. The amount of released siRNA was calculated as a ratio (%) of the released siRNA to the total amount of encapsulated siRNA.

Intracellular tracking

HEK293 cells were plated on 0.01% (w/v) poly L-lysine coated 8-well chamber slides (Lab-Tak) at 1×10^4 cells/well concentration and incubated overnight. Lysosomal staining was carried out as described in Chapter 3. Then the cells were transfected with the Cy3 siRNA-loaded PLGA microparticles in fresh opti-MEM. After 24 hours incubation, the cells were washed with PBS and fixed with 4% paraformaldehyde. The following procedure was carried out as described in Chapter 3 before the samples were visualized under confocal microscope (Zeiss LSM 710). The image was then analyzed using ImageJ software.

Construction of EGFP-expressing HEK293 cell line

EGFP stably expressing HEK293 cell line was constructed to evaluate endogenous gene knockdown. This system could offer a more practical *in vitro* model for RNAi applications than a transient gene knockdown. HEK293 cells were transfected with pEGFP-C1 (Clontech, Figure 5-2). pEGFP-C1 (4.7kb) vector encodes an enhanced green fluorescent protein (EGFP) gene and neomycin resistance cassette. This vector expresses EGFP protein that can simplify detection of protein expression using fluorescent microscope or spectrophotometer. Neomycin resistance gene allows stably transfected eukaryotic cells to be selected using G-418 sulfate (Geneticin, Gibco), an analog of neomycin sulfate. The cells can be maintained in growth media containing G-418 sulfate. The following day of transfection, the transfection media was replaced with the growth media containing G-418 sulfate. The concentration of G-418 sulfate was gradually increased to 500 $\mu\text{g/ml}$. The cells were maintained for 2 weeks in G-418 sulfate media that was replaced every 2 days. Over time this process selected for cells that have stably incorporated the EGFP plasmid into their genomic DNA. After 2 weeks of selection, EGFP expressing fluorescent cells were sorted using fluorescence activated

cell sorting (FACS). The sorted population of EGFP-HEK293 cells was maintained and used for *in vitro* endogenous gene knockdown study. (Figure 5-3)

Evaluating *in vitro* gene knockdown efficiency

EGFP-HEK293 cells were seeded onto 96-well plate (1.5×10^4 cells/well) for endogenous gene knockdown on day 0. Then 0.1mg of the microparticles loaded with NC1 (negative control) and EGFP siRNAs were added in opti-MEM media on day 1. 0.1mg particles contain approximately 10ng of siRNA, which was equivalent to 100nM siRNA transfection with polymer nanoplexes used in previous chapters. Every 24 hours, EGFP expression was measured at excitation maximum of 488nm and emission maximum of 525nm with SpectraMax® M5 multi-mode microplate reader (Molecular Devices, CA). Experiments were repeated at least three times.

Cytotoxicity evaluation

Cytotoxicity was determined using the MTS assay (CellTiter 96® AQueous One Solution Cell Proliferation Assay, Promega, Madison, WI). In brief, the HEK293 cells were seeded in 96-well plates (5×10^5 cells/well) and incubated overnight. The microparticle containing DMEM media were prepared at 0.25mg/ml concentrations and added to cells for incubation. The following procedures were carried out as described in Chapter 3. Experiments were repeated at least three times.

Evaluating *in vivo* gene knockdown efficiency in mouse

model

To evaluate *in vivo* gene knockdown efficiency, the PLGA microparticles loaded with siNC1 (negative control) and siGAPDH (Glyceraldehyde-3-phosphate dehydrogenase) were prepared using double emulsion, solvent evaporation technique. One exception is that the second emulsion was formulated by sonication as opposed to homogenization to increase encapsulation efficiency and cumulative release profile.

C57/Black6 mice (6-8 weeks old) were purchased from the National Cancer Institute (Bethesda, MD) and were maintained in filtered cages before experiment. The PLGA microparticles containing a dose of 3mg siRNA/kg mouse and 2.78mg PEI/kg mouse were dissolved in PBS and injected via intraperitoneal route. After three days, the mice were sacrificed and five organs were removed: liver, lung, kidney, heart, and spleen. The organs were immediately submerged in RNAlater[®] (Ambion) solution and stored at 4°C for more than 24 hours to stabilize and protect RNA. The RNAlater solution was drained, and the organs were frozen for storage until processed. The injection groups are described in Table 5-2. Each experimental group consisted of 5 mice. All animal experiments were conducted in accordance with the procedures outlined in the University of Iowa's Guidelines for Care and Use of Experimental Animals.

Total RNA was extracted from tissues using Qiazol (Qiagen) according to the manufacturer's protocol. Then contaminating DNA was removed from the total RNA samples using Turbo DNase-free[™] kit (Ambion). The RNA samples were analyzed for the quality and quantity using Experion[™] electrophoresis system (Bio-Rad). To determine the concentration of the samples, a standard RNA of a known concentration was run in the electrophoresis along with the samples. From the DNased RNA, cDNA was synthesized and real-time PCR was carried out. Total RNA of 150ng was used for reverse transcription using Superscript II reverse transcriptase (Invitrogen, San Diego, CA). cDNA equivalent to 10ng total RNA was analyzed by real-time PCR in triplicate using Immolase polymerase (Bioline, Randolph, MA) on AB7900HT (Applied Biosystems). The data was reported as mean \pm standard deviation from triplicate RT-PCR reactions of each sample using Microsoft Excel and Prism software (GraphPad Software, San Diego, CA).

Liver toxicity evaluations by AST and ALT serum concentrations

To test hepatotoxicity of the PLGA microparticle formulations, liver function analysis for aspartate aminotransferase¹⁸ and alanine aminotransferase (ALT) was carried out. The mice were bled from submandibular area on the next day of the PLGA microparticles injection to harvest serum. The collected blood was incubated for 2 hours at room temperature then centrifuged at 4°C, 3000 x g for 10 minutes. The serum was harvested by transferring supernatant and stored at -80°C until analyzed. Liver toxicity markers, AST and ALT, were evaluated in plasma samples by Animal Fluid Analysis Core (AFAC) service at the University of Iowa Hospitals and Clinics.

Statistical analysis

Group data are reported as mean ± standard deviation. Statistical analysis was carried out using one-way ANOVA followed by Tukey's multiple comparison test. Prism software (GraphPad Software, San Diego, CA) was used to perform statistical analyses. P < 0.05 was considered as statistically significant difference.

Results

Incorporating modified PEIs enhances EE of siRNA into

PLGA microparticles

PLGA microparticles without PEI showed 63.24% encapsulation of naked siRNA and the ones loaded with unmodified PEI/siRNA nanoplexes showed 61.72% encapsulation efficiencies. (Table 5-1) On the other hand, incorporating modified PEIs significantly improved the encapsulation efficiencies of microparticles. PLGA(Man-PEI-PEG/siRNA) and PLGA(PEI-PEG-Man/siRNA) showed 87.48 and 84.32% of siRNA entrapment, respectively.

With the purpose of visualizing siRNA entrapment in the PLGA microparticles and of examining the siRNA loaded population, fluorescently labeled Cy3 siRNA was employed in confocal microscopy and flow cytometry analyses. (Figure 5-4) The same phenomenon was observed as reported above. The PLGA microparticles with the unmodified PEI/siRNA nanoplexes showed 65.41% encapsulation efficiency of Cy3-labeled siRNA (Figure 5-4B and E) compared to the PLGA microparticles without Cy3 siRNA (4%). (Figure 5-4A) The PLGA particles with the modified PEI showed significantly improved encapsulation efficiencies. The PLGA microparticles loaded with mannose-PEI-PEG/Cy3 siRNA nanoplexes displayed 78.98% (Figure 5-4C and F) and the PLGA particles loaded with PEI-PEG-Man/Cy3 siRNA nanoplexes showed 74.46% encapsulation efficiencies of siRNA. (Figure 5-4D and G)

PLGA microparticles have smooth surface and sufficient size for cellular uptake

Figure 5-5 shows the surface morphology and size of the PLGA microparticles taken from Scanning Electron Microscopy (SEM). Blank microparticles showed smooth surface features with no porosity. The PLGA microparticles with PEI or siRNA alone displayed a little porosity on the surface. Incorporating PEI/siRNA nanoplexes increased the porosity of the microparticles, however this increase was not significantly. Change in porosity can affect release profile of siRNA from the microparticles. Particle size is an important factor in regards to cellular uptake of the particle. All the formulations showed particles smaller than 6 μ m. Incorporating the various PEI polymers did not alter the particle size. This result corresponds to the zeta-sizer analysis of the particle size displaying an average hydrodynamic diameter from 1 μ m to 5 μ m. The particles had zeta potentials ranging from -26mV to -40mV.

Sustained release profile is improved by incorporating modified PEI

In vitro release profiles of the modified PEIs/siRNA nanoplexes-loaded PLGA microparticles is given in Figure 5-6. The microparticles exhibited an initial burst release from day 1 to 7 followed by a sustained release with secondary release from day 18 to 24. The PLGA particles loaded with siRNA alone showed relatively low initial burst of 28% at day 7 compared to the particles encapsulating PEI/siRNA nanoplexes. Then the particles loaded with naked siRNA released increasing amount of siRNA afterwards. The microparticles loaded with unmodified PEI/siRNA nanoplexes showed higher initial burst of siRNA when compared to the other microparticles exhibiting 33% cumulative release at day 7. Then the PEI/siRNA nanoplexes-loaded microparticles maintained the higher release for the duration of the experiment. The particles encapsulating mannose-PEI-PEG/siRNA nanoplexes displayed decreased initial burst of 30% followed by lower secondary release relative to the PLGA microparticles loaded with PEI/siRNA nanoplexes. PEI-PEG-mannose/siRNA nanoplexes significantly reduced the initial burst of the PLGA microparticles loaded with PEI/siRNA nanoplexes releasing 26% of encapsulated siRNA. They also reduced secondary release of siRNA. This low release profile of the PLGA particles loaded with PEI-PEG-mannose/siRNA nanoplexes was different from the PLGA particles loaded with naked siRNA or PEI/siRNA nanoplexes with statistical significance ($p < 0.05$).

PLGA microparticles are endocytosed at 24 hours post-transfection

In order to track the cellular uptake and intracellular distribution of the microparticles, fluorescence labeled Cy3 siRNA and staining of intracellular organelles were utilized. Nuclei and lysosomes were labeled with blue and green fluorophores, respectively. At 24 hours post-transfection, the PLGA particles loaded with

polymers/siRNA nanoplexes (shown in red) were successfully internalized in the HEK293 cells. (Figure 5-7) The particles were taken up by the cells and localized near vesicular structures as seen by yellow fluorescence due to the overlapping of the green staining of lysosome and the red siRNA signal in close proximity. The PEI/siRNA nanoplexes loaded PLGA particles were found in the cytosol and colocalized with lysosomal vesicles. (Figure 5-7A) The particles entrapping Mannose-PEI-PEG/siRNA nanoplexes were also endocytosed and located near lysosomes. (Figure 5-7B) The PLGA particles loaded with PEI-PEG-mannose/siRNA nanoplexes exhibited the highest cellular uptake capacity showing abundant yellow signals in a large group of cells. (Figures 5-7C) Particles were also found in the cytosol that were escaped from the lysosomes and located close to nucleus suggesting the potential of initiating RNAi.

Incorporating modified PEI do not enhance in vitro gene knockdown efficiency

The *in vitro* delivery efficacy of PLGA microparticles loaded with modified PEI/siRNA nanoplexes were evaluated using EGFP-HEK293 cells. Endogenous gene knockdown was carried out using EGFP siRNA transfection. The relative gene expression level of various particles transfected cells were normalized to that of blank PLGA transfected cells set as a 100%. The PLGA particles loaded with siEGFP reduced gene expression of EGFP to 84.14% on day 1, 80.89% on day 2 and 74.03% on day 3. (Figure 5-8) The PLGA microparticles entrapping PEI/siEGFP nanoplexes showed low gene knockdown efficiency showing 103.48%, 111.03% and 97.63% on day 1, 2 and 3, respectively. The PLGA particles loaded with mannose-PEI-PEG/siEGFP nanoplexes had minimal gene knockdown effect resulting in 111.21%, 105.88% and 98.05% relative EGFP expression. The PLGA microparticles loaded with PEI-PEG-Man/siRNA nanoplexes showed similar knockdown efficiency as the particles loaded with PEI/siEGFP nanoplexes showing 88.45%, 84.44% and 84.09% remaining gene

expression. While the PLGA particles loaded with PEI/siEGFP and PEI-PEG-Man/siEGFP nanoplexes showed some inhibition of EGFP gene expression, there was no significant differences. The overall gene knockdown efficiency was insufficient to evaluate gene delivery capacity of the polymer/siRNA nanoplexes-loaded PLGA microparticles.

PLGA microparticles display very low in vitro cytotoxicity

To assess the toxicity profile of the microparticles, the MTS cell proliferation assays were carried out. (Figure 5-9) All the microparticles showed minimal cytotoxicity compared to the no treatment group at the concentration of 0.25mg/ml. Cells treated with blank PLGA particles had 99.64% cell viability. The PLGA particles loaded with PEI and naked siRNA resulted in 102.57% and 97.49% cell viability, respectively. Cells treated with the PLGA microparticles loaded with Man-PEI-PEG/siRNA nanoplexes showed reduced toxicity of 99.86% cell proliferation. The PEI-PEG-Man/siRNA nanoplexes loaded PLGA microparticles were more toxic than other particles resulting in 89.68% relative cell survival. No significant cytotoxicities were found in any of the treating groups.

Incorporating modified PEI do not improve in vivo gene knockdown efficiency in mouse model

The total RNA samples were evaluated for integrity and quantity using gel electrophoresis. (Figure 5-10) The ratios of 28S to 18S ribosomal RNA (rRNA) peaks were in the range of 1 to 2. After the integrity and quantity of the RNA samples were analyzed, the *in vivo* gene knockdown efficiency generated by the PLGA particles encapsulating the modified PEI/siRNA nanoplexes were assessed in the mouse model. Selective gene knockdown of GAPDH was carried out using the PLGA microparticles formulated with the PEI polymers and GAPDH siRNA. GAPDH gene expression levels in siGAPDH-treated mouse organs were normalized to that in siNC1-treated mouse

organs. (Figure 5-11) Naked siGAPDH injected mouse organs resulted in 85%, 100.2%, 92%, 100.6%, and 93.8% relative gene expression in spleen, kidney, liver, lung, and heart, respectively. PEI/siGAPDH nanoplexes resulted in no significant gene knockdown efficiency in mice organs, showing 96.4%, 142.6%, 131.6%, 108%, and 144.4% of GAPDH mRNA expression in spleen, kidney, liver, lung, and heart, respectively. PEI-PEG-mannose improved siRNA delivery relative to PEI with 84.6%, 89.4%, 87.4%, 93.2% and 92.8% of relative gene expression in spleen, kidney, liver, lung, and heart, respectively. The PLGA microparticles loaded with siGAPDH decreased gene activity in the spleen to 67.8% but did not have significant effect in kidney, liver, lung, and heart showing 111.4%, 100.2%, 90.4%, and 123%, respectively. The PLGA particles encapsulating PEI/siGAPDH significantly reduced the gene expression of GAPDH on heart to 65.4%. GAPDH mRNA expression of other organs were not significantly affected by the treatment of the PLGA particles loaded with PEI/siGAPDH nanoplexes displaying 129.6%, 97.8%, 87.6%, and 93.6% in spleen, kidney, liver, and lung, respectively. The PLGA microparticles encapsulating PEI-PEG-mannose/siGAPDH nanoplexes showed 96.8%, 108%, 121%, 131.6%, and 141.33% of GAPDH gene expression in spleen, kidney, liver, lung, and heart, respectively.

PLGA microparticles display no significant hepatotoxicities

To test the hepatotoxicity of the PLGA microparticles in mouse model, serum aspartate aminotransferase¹⁸ and alanine aminotransferase (ALT) levels were analyzed. (Figure 5-12) No significant increase of AST and ALT levels were observed after the injection of the nanoplexes or the PLGA microparticles. AST levels of the PBS and naked siGAPDH injected mouse group were 64.2 and 50.8 U/L, respectively. (Figure 5-12A) Mice injected with PEI/siGAPDH and PEI-PEG-mannose/siGAPDH nanoplexes produced 71.2 and 70.6 U/L of AST levels. Mice treated with the PLGA microparticles loaded with siGAPDH alone showed 50.6 U/L of average AST level. Serum AST levels

in mice injected with the PLGA microparticles encapsulating PEI/siGAPDH and PEI-PEG-mannose/siGAPDH nanoplexes were 57.4 and 59.8 U/L, respectively. Mouse groups treated with PBS and naked siGAPDH, plasma ALT levels were 57.8 and 48.2 U/L, respectively. (Figure 5-12B) Mice injected with PEI/siGAPDH and PEI-PEG-mannose/siGAPDH nanoplexes resulted in 63 and 54.4 U/L of serum ALT levels. Mice treated with the PLGA microparticles encapsulating naked siGAPDH produced 31 U/L of average serum ALT level. Plasma ALT levels in mouse groups injected with the PLGA microparticles loaded with PEI/siGAPDH and PEI-PEG-mannose/siGAPDH nanoplexes were 41 and 28.6 U/L, respectively.

Discussion

In the previous chapters, we have developed pegylated mannosylated chitosan and PEI to improve delivery efficacy of siRNA. The modified cationic polymers, especially the modified PEIs, demonstrated potential as an efficient siRNA delivery system. Pegylation and mannosylation used in combination increased cellular uptake and reduced toxicity of PEI. In regards to the location of mannose ligand in the construct, PEI-PEG-mannose displayed higher cellular uptake and gene silencing efficiency than mannose-PEI-PEG. However, the toxicity of PEI limits clinical application of this system. PLGA was utilized to further reduce the toxicity and provide sustained release of the PEI/siRNA nanoplexes for *in vivo* and clinical applications. Previous studies have shown the potential of PLGA particles for *in vivo* gene delivery applications.²⁰⁷⁻²⁰⁹ PLGA nanoparticles escape the lysosomes by selective reversal of the surface charge of the particles, from anionic to cationic, in the acidic lysosomal compartment. This process allows the particles to interact with the endo-lysosomal membrane and escape into the cytosol. PLGA nanoparticles deliver macromolecules such as DNA and low molecular weight drugs intracellularly at a slow rate resulting in a sustained therapeutic effect.²¹⁰

The modified PEI significantly improved siRNA encapsulation efficiencies in the PLGA microparticles relative to unmodified PEI and siRNA alone. It is the result of modified PEI compacting siRNA tightly by electrostatic interaction and enhancing siRNA loading into the PLGA particles.²¹¹ The improved encapsulation efficiencies of the PLGA microparticles loaded with modified PEI/siRNA nanoplexes were confirmed using confocal microscopy and flow cytometry analysis. The number of the fluorescent siRNA loaded particles was significantly higher in the PLGA particles loaded with the modified PEI/siRNA nanoplexes relative to the PEI/siRNA nanoplexes and siRNA only.

The particles encapsulating modified PEI/siRNA nanoplexes showed surface porosity in SEM images. Smooth surface features and spherical shape as observed with blank PLGA particles are common characteristics of PLGA particles.^{140,212} PLGA formed porous particles when PEI/oligonucleotide complexes were encapsulated.²¹³ It has been reported that a high osmotic pressure inside microparticles could increase particle size and surface porosity.^{214,215} In the double emulsion-solvent evaporation method, the inclusion of cationic polymer such as PEI causes high osmotic pressure within the internal aqueous phase increasing an influx of water.^{216,217} Increased water evaporates during lyophilization, which leaves an increased surface porosity.

Release of encapsulated hydrophilic molecules from PLGA microparticles generally shows a biphasic profile: an initial burst release followed by a sustained release due to the gradual degradation of polymer.²¹⁸ The modified PEI/siRNA nanoplexes were release from the PLGA microparticles exhibiting lower initial burst and lower subsequent controlled release relative to the PEI/siRNA nanoplexes and siRNA alone. This secondary sustained release lasted for over one month. The PLGA microparticles encapsulating PEI-PEG-mannose/siRNA nanoplexes showed the lowest initial burst and the lowest secondary release when compared to the PLGA microparticles loaded with siRNA alone, PEI/siRNA nanoplexes, and mannose-PEI-PEG/siRNA nanoplexes. Since the PLGA microparticles loaded with the modified PEI/siRNA nanoplexes had more

surface porosity than the PLGA microparticles loaded with naked siRNA, we expected it to have higher initial burst and increased overall release. However, the lower initial burst can be attributed to higher encapsulation efficiency of the modified PEI/siRNA nanoplexes-loaded PLGA microparticles. The PLGA microparticles loaded with PEI/siRNA nanoplexes exhibited similar release profile to the PLGA microparticles encapsulating siRNA only.

In our cellular uptake studies, the PLGA microparticles with the incorporation of the modified PEI/siRNA nanoplexes had higher cellular uptake of siRNA into the cells. The higher cellular uptake could be a result of the mild net cationic charge of the PLGA-PEI microparticles.^{219, 220} The net positive charge could facilitate stronger interaction with cell membrane and more nanoparticles to escape from lysosomes. Cy3 labeled siRNA signals were found in the cytosol separated from the lysotracker stained lysosomes, suggesting the siRNAs were released from the lysosomes. The PLGA microparticles loaded with PEI-PEG-Man/siRNA nanoplexes significantly increased cellular uptake relative to the PLGA microparticles loaded with PEI/siRNA and Man-PEI-PEG/siRNA nanoplexes. This was observed as abundant yellow signals distributed in a large group of cells. Similar result has been observed with cellular uptake of PEI-PEG-mannose/siRNA nanoplexes in Chapter 4. Mannose ligands when conjugated at the tip of PEG chains displayed significantly higher cellular uptake when compared to mannose and PEG conjugated directly to the backbone. Mannose ligand exposed at the surface of nanoplexes could readily cause the specific ligand-receptor interaction improving transfection efficiency. Even though mannose receptor is not as abundantly expressed on the extracellular surface of HEK293 cells as that of RAW264.7 cells, they still provide sufficient ligand-receptor interactions to improve the particle uptake. The PLGA particles loaded with the modified PEI/siRNA nanoplexes successfully protected siRNA during cellular uptake and found in the lysosomes.

Endogenous mRNA knockdown efficiency was analyzed using EGFP-HEK293 cells. It is significant to silencing endogenous gene expression in RNAi applications relative to silencing a transiently transfected gene expression. It provides us with potential for clinical applications such as genetic disorders. The PLGA microparticles did not have significant impact on gene knockdown efficacy from day 1 to day 3. The PLGA microparticles loaded with siEGFP alone and PEI-PEG-Man/siRNA nanoplexes reduced gene expression with no significant differences. Because the PLGA microparticles have sustained release profile, it could take longer than a few days for the particles to release siRNA for target gene silencing. Moreover, it is difficult to control cell proliferation for more than 4 days. The cells exhibited uncontrollable growth after day 4 and died from overpopulation. We tried to maintain the cell population using serum-deprived media (2% serum containing growth media) instead of normal 10% growth media. The challenges with evaluating long-term response of the PLGA microparticles are beyond 3 to 4 days when cell proliferation reaches the maximum capacity. Therefore, the gene knockdown efficiencies of PLGA microparticles are best evaluated *in vivo*.

PEI is known for its inherent toxicity.²²¹ MTS cell proliferation assay showed minimal toxicity of all the formulations at the concentration of 0.25mg/ml. The cytotoxicity of blank PLGA particles marginally increased proportional to the concentrations with no significance. The PLGA microparticles loaded with PEI alone, siRNA alone, and modified PEI/siRNA nanoplexes showed similar toxicities. In addition, encapsulating the modified PEIs into the PLGA particles significantly reduced the cytotoxicity profile of PEI. When tested at equivalent concentration, PEI displayed 37.5% cell viability in Chapter 4, whereas PEI/siRNA nanoplexes encapsulated into the PLGA microparticles resulted in 102.57% cell viability. PEI-PEG-mannose and mannose-PEI-PEG showed 53.9 % and 68.9% cell survival in Chapter 4. Incorporating the PLGA microparticles reduced the toxicity of the corresponding modified PEIs

displaying 99.86% and 89.68% cell viability, respectively. From this comparison, we can conclude that incorporation of the PLGA microparticles to PEI significantly reduced the cytotoxicity of PEI.

Assessing the integrity of an RNA sample is an important aspect of gene expression analysis. When comparing two or more samples, it is important that the samples are of similar integrity. Varying degrees of degradation could introduce inconsistencies in downstream results. RNA samples of good integrity shows two distinct peaks of 28S and 18S rRNA, which have a ratio of 2:1. Degradation of RNA can be identified by several characteristics. These include smeared rRNA bands on the gel, less pronounced peaks of rRNAs, and significantly smaller ratio of 28S to 18S peaks than 2. The total RNA samples from the mouse organs showed good quality and quantity. The ratios of 28S to 18S were in between 1-2, which is sufficient to run subsequent experiments.

To study further the effect of encapsulating the modified PEI/siRNA nanoplexes into the PLGA microparticles, we carried out an *in vivo* gene knockdown experiment in mouse model. First, GAPDH (Glyceraldehyde-3-phosphate dehydrogenase) was selected as a target mRNA to knockdown expression. GAPDH is one of the most commonly used housekeeping genes in gene expression studies. Quantitative gene expression data such as qPCR are normalized to the expression levels of housekeeping genes serving as a control.²⁰² It is based on the assumption that the expression of housekeeping genes remain constant in the cells or tissues. In this study we used the expression level of the GAPDH housekeeping gene as a target for endogenous knockdown. PEI-PEG-mannose improved the gene silencing efficiency of PEI in all the five organs particularly in kidney, liver, and heart. This result was consistent with *in vitro* gene knockdown study in Chapter 4, where PEI-PEG-mannose enhanced the luciferase gene silencing activity of PEI. The PLGA microparticles loaded with PEI/siGAPDH nanoplexes exhibited significant knockdown efficiency in the heart. The PLGA particles loaded with

siGAPDH alone showed efficient gene knockdown in spleen. The microparticles did not display significant gene silencing efficiency with the exception of the PLGA particles loaded with PEI/siGAPDH nanoplexes in heart. There could be two possible explanations for this observation. The first potential explanation is that the amount of siRNA might be too small for intraperitoneal route of administration. The second potential explanation is that the time point of the organ harvest might be too early for the PLGA microparticles. An intratumoral injection of 14 μ g siVEGF encapsulated within PLGA microspheres suppressed mouse tumor growth. Relative VEGF mRNA level in tumor tissue was significantly reduced compared to that of the blank microspheres and mock siRNA/PEI-microspheres.²²² In a study by Murata et al., intratumoral injection of 14 μ g siRNA had tumor suppression on day 6. Intraperitoneal injection of 3mg/kg siRNA might have been insufficient amount to detect notable RNA inhibition. We chose the intraperitoneal route of administration instead of intravenous administration due to the size of the PLGA microparticle. As discussed in the *in vivo* gene knockdown experiment section of Chapter 2, the particles with the size of 10 to 1000nm are injectable for intravenous injection. However, if the size of the particles is over 1 μ m, the particles can readily block capillaries and cause embolisms. Since the PLGA microparticle formulations were 2-4 μ m in size, the intraperitoneal injection was appropriate to avoid adverse side effects such as potential capillary embolisms. To verify the feasibility of intravenous injection with our PLGA microparticles, we injected the particles via lateral tail vein. It was not feasible for the size of the needle gauge and for the viscosity of the microparticle solution. The solutions containing the PLGA microparticles loaded with siGAPDH alone and PEI-PEG-mannose/siNC1 nanoplexes were not easily plunging through the 28 gauge needles, which is required for the intravenous route of administration. The solutions containing the blank PLGA microparticles, PLGA particles with PEI/siNC1, and PEI-PEG-mannose/siGAPDH were plunging through the 28 gauge needles. However, injecting these solutions was not feasible. It can be attributed to the

viscosity of the microparticle solutions. From this result, we chose to inject the microparticles through intravenous route of administration instead of intraperitoneal route.

Since there was minimal siRNA silencing effect in these five organs, future study could investigate to track the PLGA microparticles loaded with the modified PEI/siRNA nanoplexes. Using fluorescently labeled siRNA would allow us to visualize the location of siRNA with live animal imaging system. Focal site of inflammation would recruit inflammatory immune cells including monocytes and dendritic cells, therefore it would be potential focal site of siRNA endocytosed by macrophages. In addition, uptake of the PLGA particles by intraperitoneal macrophages could be examined. Analyzing cell population that engulfed the PLGA microparticles encapsulating the modified PEI/siRNA nanoplexes could provide estimation of *in vivo* delivery and gene silencing efficiency.

PLGA particles have shown gene delivery efficiency as early as one day after injection. PLGA microspheres encapsulating oligonucleotide (ODN) injected subcutaneously in mice were eliminated within 24 hours and released ODN. Both polymer and released free ODNs were found in the proximal convoluted tubules of the kidney and in the Kupffer cell of the liver. It has been suggested that PLGA microspheres could provide improved *in vivo* sustained delivery of gene silencing nucleic acids.²²³ Our PLGA microparticles have strong initial burst that is characteristics of the particles prepared with double-sonication method. Using sonication to form the secondary emulsion efficiently broke the oil phase into small droplets allowing them to disperse in the external aqueous phase. When the small droplets were added into an external aqueous phase, it results in instant diffusion of the secondary emulsion and rapid evaporation at the oil-water interface as a result of the larger surface area. The larger surface area associated with the smaller particles leads to a higher release rate. Nevertheless, the PLGA microparticles loaded with modified PEI/siRNA nanoplexes

exhibited more sustained release than particles loaded with naked siRNA. Therefore, three days might be too early to release sufficient amounts of siRNA to detect RNAi.

Since we included modified PEI, there is an issue of potential *in vivo* toxicity. Toxic profile of PEI when used as an *in vivo* delivery vehicle for siRNA was also investigated. In a study by Hobel et al., subcutaneous injection of PEI/siRNA complexes at the dose of 4mg of PEI/kg mouse and 0.4mg siRNA/kg mouse caused sedation/visible behavioral impairment (10%), weight loss (100%), and scurf formation (80%). But all of the side effects were reversed after a few hours to a few days. When injected intravenously at the same dose, there were no signs of toxicity. With the increased dose of 12mg PEI/kg mouse and 1.2 mg siRNA/kg mouse, it led to reversible weight loss (100%) and sedation (33%). There was no toxicity at the doses forementioned with intraperitoneal injection, and only at the dose of 40mg PEI/kg mouse and 4mg siRNA/kg mouse injection resulted in 50% acute side effect and 50% lethality.¹⁶⁷ Intravenous injection of linear PEI 50 μ g complexed with DNA caused 23% lethality within 24 hours of injection. Interestingly, the same dose of injection had worse effect on BalbC mice resulting in 50% lethality. Swiss nude mice were the most resilient to PEI toxicity showing only 4.76% lethality. All the mouse strains showed instant lethality when 85 μ g of L-PEI/DNA complexes were injected.²²⁴ For these reasons, preliminary tests were carried out with 3 mice prior to the *in vivo* knockdown experiment to assess toxicity of PEI in our experimental setting. Each of the mice was injected PEI/siRNA nanoplexes containing 1mg/kg, 5mg/kg, or 10mg/kg of PEI, respectively. They were monitored for 48 hours after injection to observe toxic side effects. The mouse that were given 10mg/kg of PEI/siRNA nanoplexes showed low motility as a sign of acute toxicity, but they recovered to normal in 90 minutes. No other side effects were detected such as weight loss, sedation, wound or scurf formation. Based on this preliminary result, we decided that it was safe to inject 2.78mg/kg of PEI for the *in vivo* gene knockdown study.

The PLGA microparticles did not increase the level of hepatotoxicity markers such as AST and ALT relative to PBS, regardless of polymer/siRNA nanoplexes encapsulation. No significant differences ($p < 0.05$) were found among the injection groups. PLGA encapsulation of a drug, tamoxifen, significantly decreased the hepatotoxicity of the drug in a murine breast cancer model.²²⁵ ALT and AST are specific biomarkers of hepatotoxicity.²²⁶ Their serum activity reflects damage to hepatocytes, and they are considered to be highly sensitive. Damaged hepatocytes produces elevated levels of ALT and AST into the circulation, therefore their levels in plasma are increased. ALT is primarily localized in the liver tissue. Serum ALT level is the most common indicator of hepatotoxic effects. Additional markers such as AST are analyzed in conjunction with ALT to confirm toxicity. AST is localized in the heart, brain, skeletal muscle and liver tissue. Damaged myocytes and hepatocytes release AST, which raises the level of AST in plasma. The ratio of AST to ALT in serum distinguishes liver damage from other organ damage. ALT levels are bigger than AST level in certain types of chronic liver disease such as hepatitis, whereas AST level increases in muscle necrosis. The AST to ALT ratio above 3:1 indicates muscle necrosis.²²⁷ All of the serum samples displayed the AST to ALT ratios of 1 to 2 suggesting no significant toxicity to either liver or muscle.

These findings can provide useful information in the future development of siRNA delivery. Incorporating the PEI-PEG-mannose/siRNA nanoplexes significantly improved encapsulation efficiencies of the PLGA microparticles and cellular uptake. Encapsulating the PEI-PEG-mannose/siRNA nanoplexes with the PLGA microparticles significantly reduced toxicity of PEI and provided sustained release profile of the siRNA. The PLGA microparticles loaded with PEI-PEG-mannose/siRNA nanoplexes have promising potential as a long-acting delivery system for siRNA.

Table 5-1: The effect of modified PEI incorporation on the encapsulation efficiency of the PLGA microparticles

PLGA Microparticles	Encapsulation Efficiency %
PLGA(Cy3)	63.24 ± 3.11
PLGA(PEI/Cy3)	61.72 ± 0.95
PLGA(Man-PEI-PEG/Cy3)	87.48 ± 0.82 *
PLGA(PEI-PEG-Man/Cy3)	84.32 ± 0.68 *

Note: * indicates statistical difference with significance of $p < 0.05$ when compared to PLGA(Cy3) and PLGA(PEI/Cy3).

Table 5-2: The mouse injection groups used to evaluate *in vivo* gene delivery efficiency of the various PLGA microparticle formulations in comparison to polymer/siRNA nanoplexes

Carrier	siNC1	siGAPDH
1. PBS	No siRNA	
No polymer	2. Naked siNC1	3. Naked siGAPDH
PEI	4. PEI/siNC1	5. PEI/siGAPDH
PEI-PEG-Man	6. PEI-PEG-Man/siNC1	7. PEI-PEG-Man/siGAPDH
PLGA	8. PLGA(siNC1)	9. PLGA(siGAPDH)
PLGA(PEI)	10. PLGA(PEI/siNC1)	11. PLGA(PEI/siGAPDH)
PLGA(PEI-PEG-Man)	12. PLGA(PEI-PEG-Man/siNC1)	13. PLGA(PEI-PEG-Man/siGAPDH)

Figure 5-1: Microparticle formulation technique using double emulsion, solvent evaporation method (Adapted from ²²⁸)

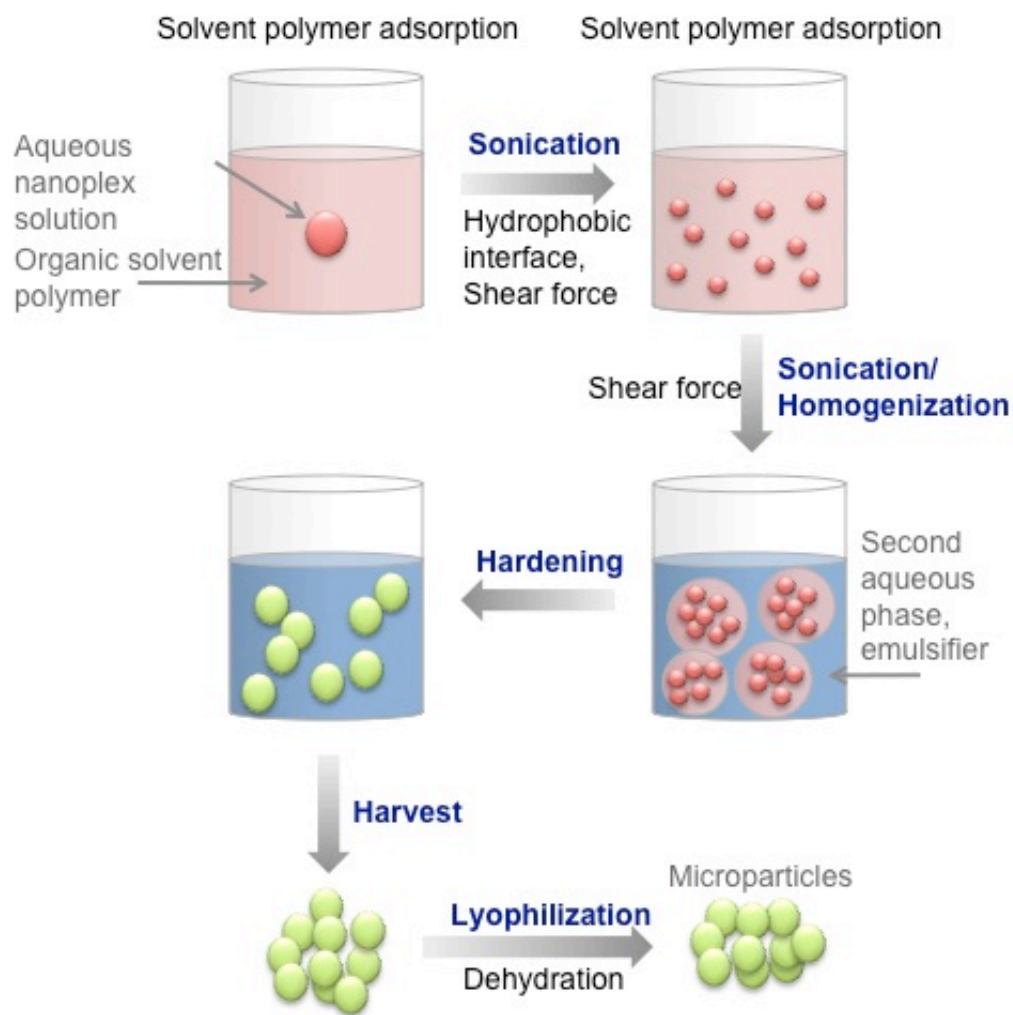


Figure 5-2: Map of pEGFP-C1 vector encoding enhanced green fluorescence protein (EGFP) utilized for *in vitro* gene knockdown study. It is a 4.7kb plasmid DNA encoding a green fluorescence protein (EGFP) gene and neomycin resistance cassette (Neor). EGFP sequence facilitates easy detection of protein using fluorescent microscope when expressed. Neomycin resistance gene allows stably transfected eukaryotic cells to be selected using G-418 sulfate, an analog of neomycin sulfate.²²⁹

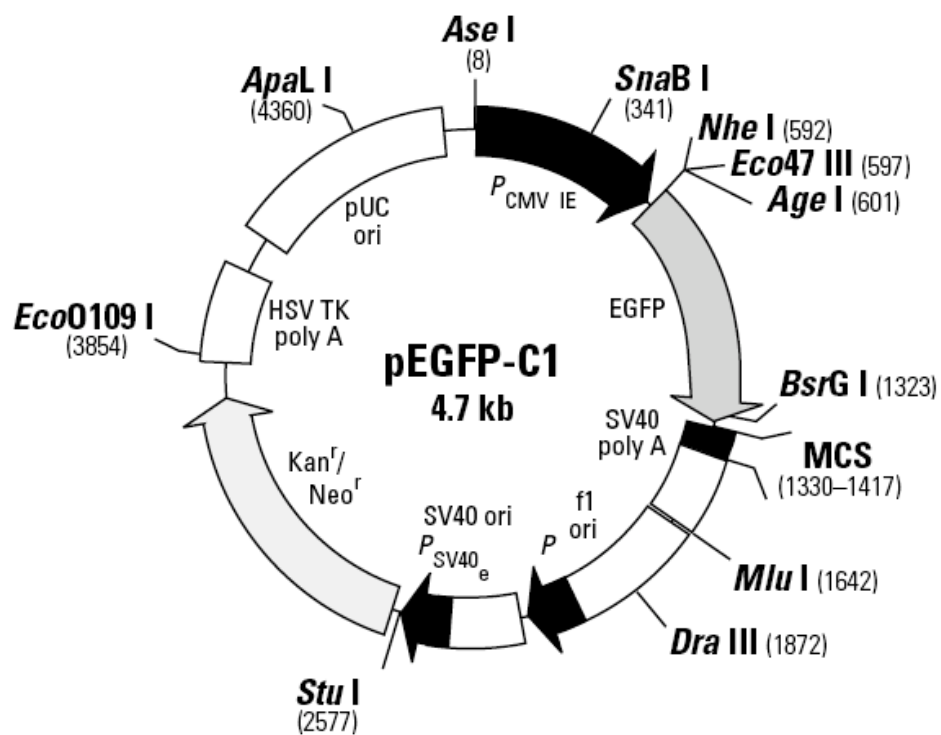
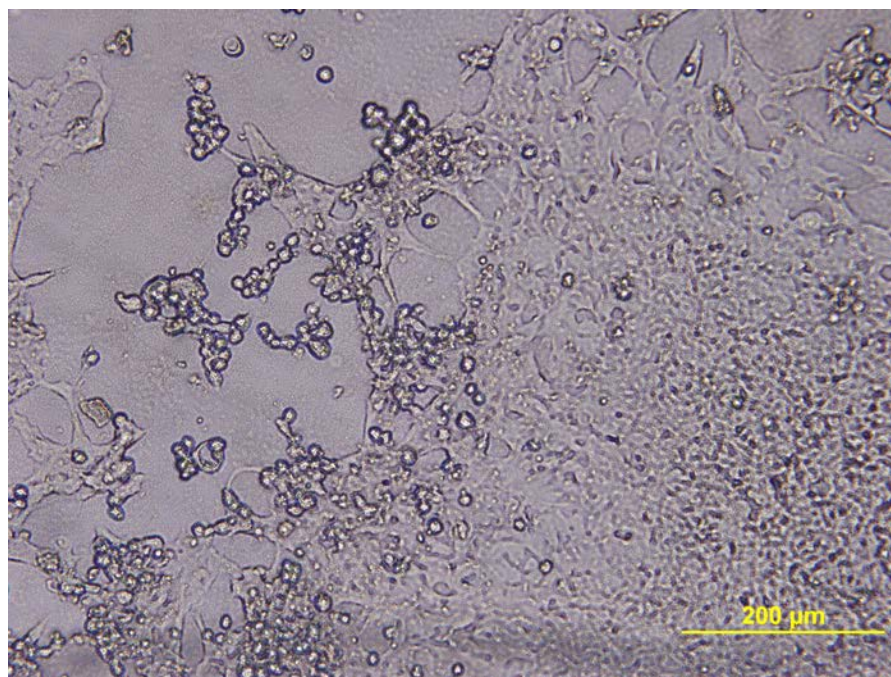


Figure 5-3: EGFP stably expressing HEK293 cells constructed for *in vitro* gene knockdown study. EGFP-HEK293 cells were visualized using fluorescent microscope (Olympus CKX41). After sorted by flow cytometry, the EGFP-HEK293 cells were maintained with normal growth media with G-418 sulfate. A. Bright field image, B. GFP fluorescence field image.

A



B

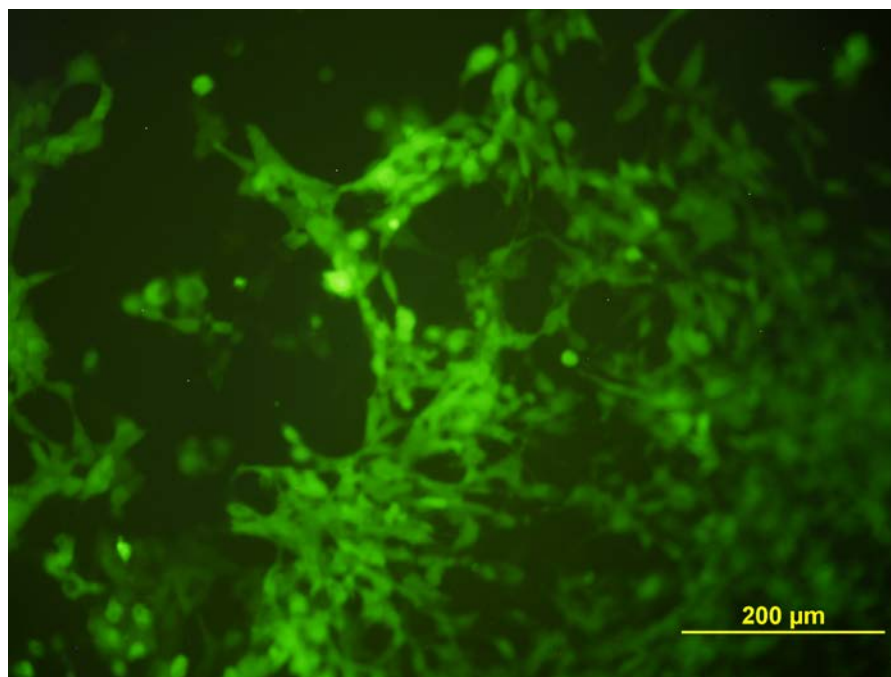


Figure 5-4: Confocal microscope images and flow cytometry analyses demonstrating the effect of the modified PEI incorporation into the PLGA microparticles on encapsulation efficiency of Cy3-labeled fluorescent RNA. A. PLGA(Cy3 siRNA), B. PLGA(PEI/Cy3 siRNA), C. PLGA(Man-PEI-PEG/Cy3 siRNA), D. PLGA(PEI-PEG-Man/Cy3 siRNA). Flow cytometry analyses of the microparticles. PLGA(PEI) was shadowed and used as standard in each diagram, E. PLGA(PEI/Cy3 siRNA), F. PLGA(Man-PEI-PEG/Cy3 siRNA), G. PLGA(PEI-PEG-Man/Cy3 siRNA). The experiments were repeated at least twice. The best representative images are shown.

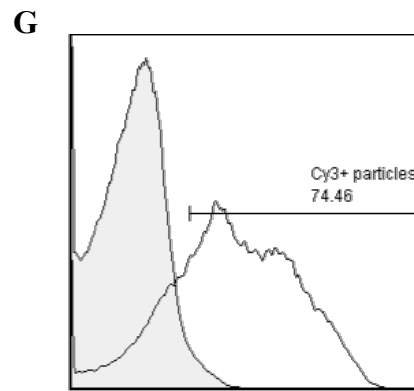
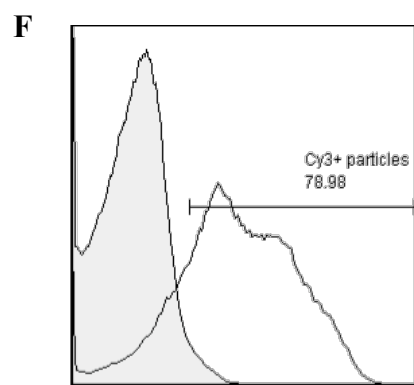
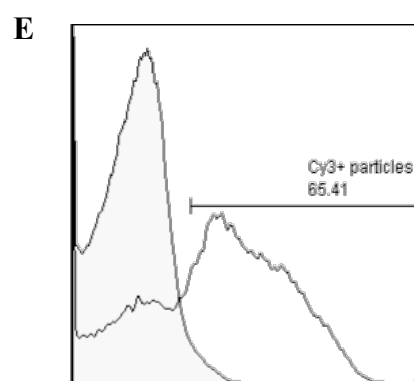
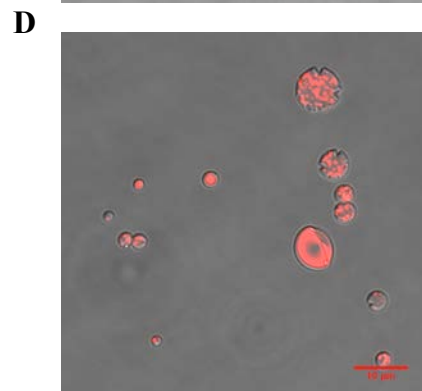
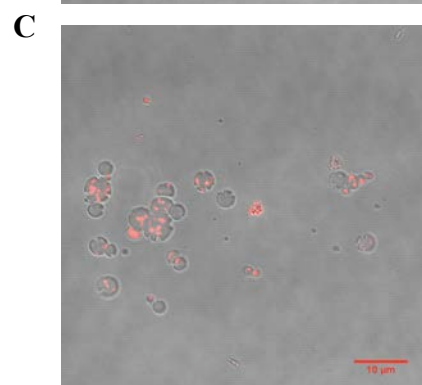
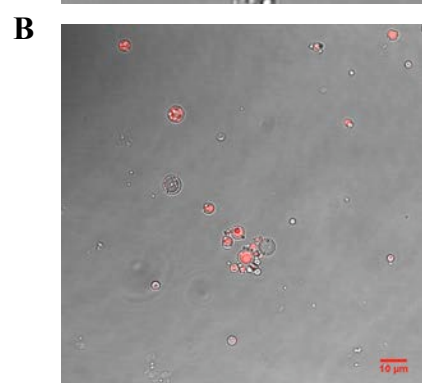
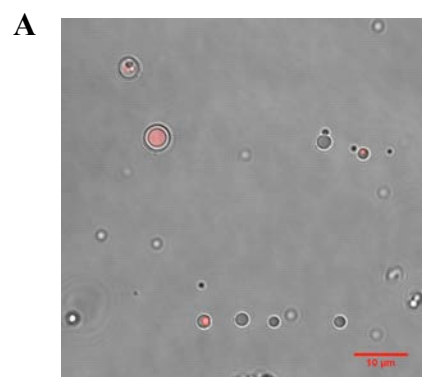


Figure 5-5: Scanning Electron Microscopy (SEM) images demonstrating the effect of the modified PEI incorporation on the size distribution and surface morphology of the various PLGA microparticles. A. Blank PLGA microparticles, B. PLGA(PEI) microparticles, C. PLGA(siRNA) microparticles, D. PLGA(PEI/siRNA) microparticles, E. PLGA(Man-PEI-PEG/siRNA) microparticles, F. PLGA(PEI-PEG-Man/siRNA) microparticles. The experiments were repeated three times. The best representative images are shown.

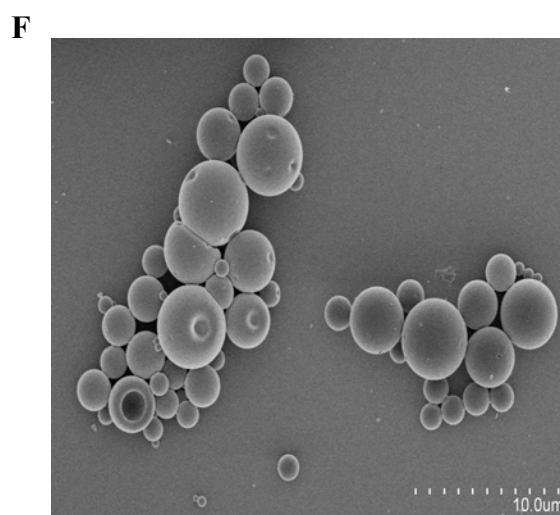
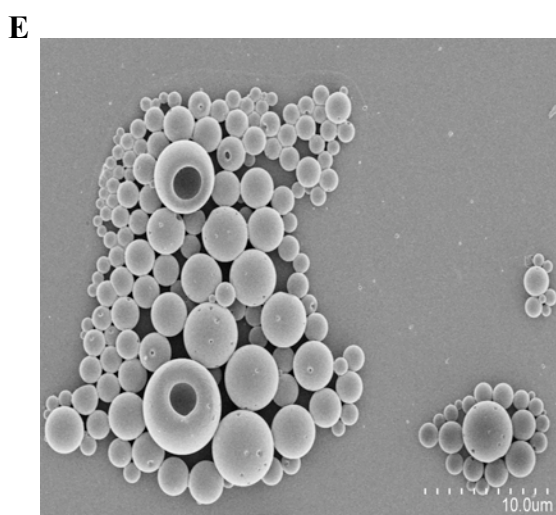
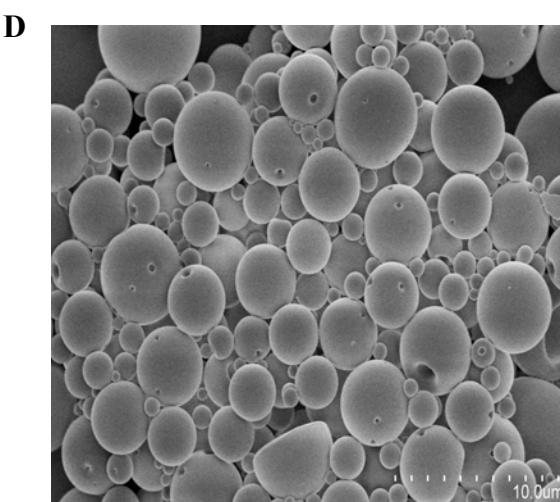
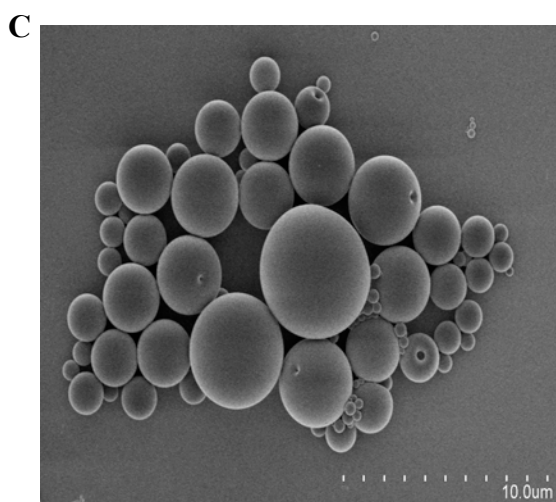
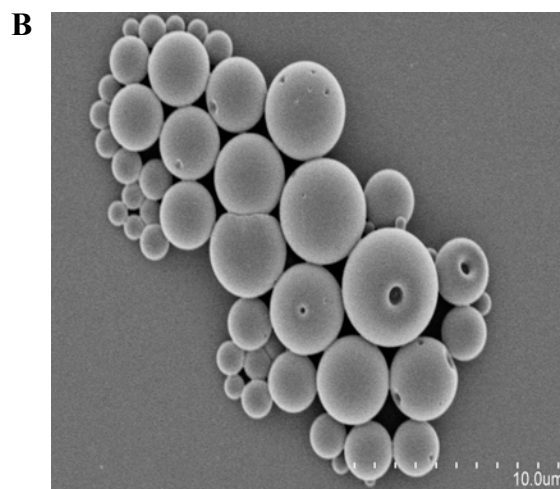
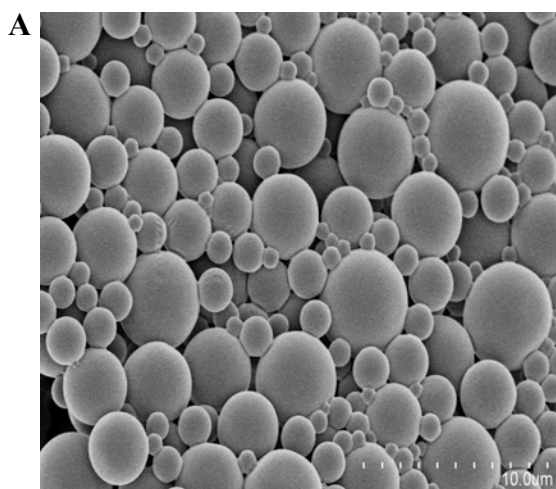


Figure 5-6: The effect of the modified PEI incorporation on *in vitro* release profile of siRNA from the polymer/siRNA nanoplexes-loaded PLGA microparticles in PBS, pH 7.4. Data is represented as mean \pm standard deviation (n=3). (*; p<0.05)

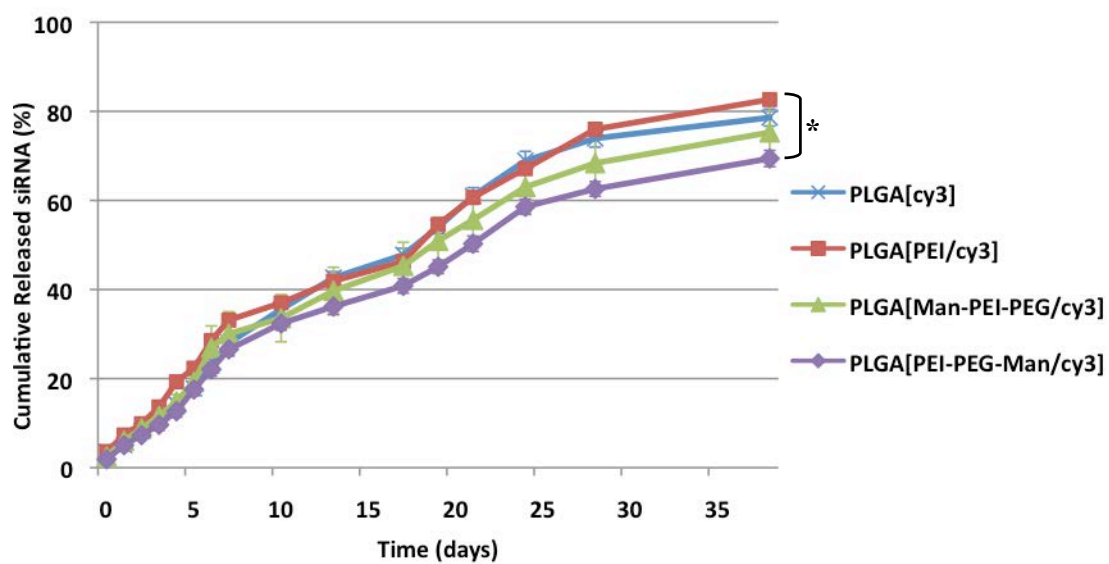


Figure 5-7: Confocal microscope images demonstrating the effect of the modified PEI incorporation on cellular uptake and intracellular localization of the PLGA microparticles. HEK293 cells were stained with Lysotracker Green (green), incubated with the microparticles loaded with Cy-3 labeled siRNA (red), and then mounted with DAPI containing mounting solution after fixation. Co-localization of nanoplexes and lysosomes are shown as a yellow signal. A. PLGA(PEI/Cy3 siRNA), B. PLGA(Man-PEI-PEG/Cy3 siRNA), C. PLGA(PEI-PEG-Man/Cy3 siRNA). The experiments were repeated at least twice. The best representative images are shown.

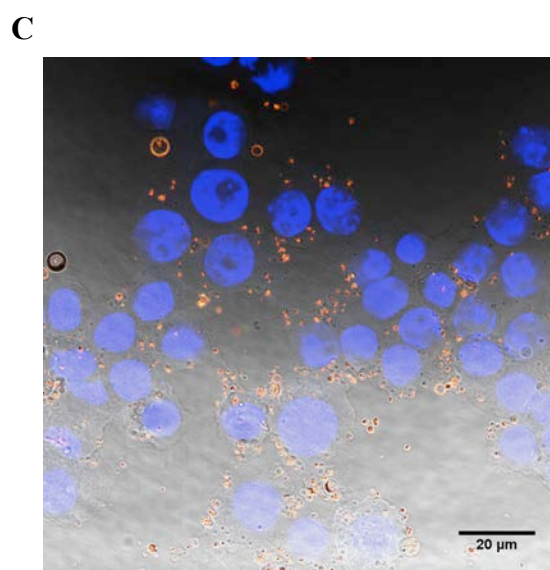
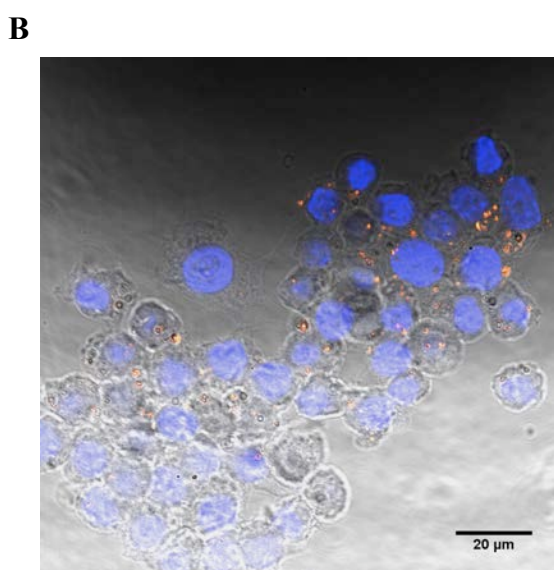
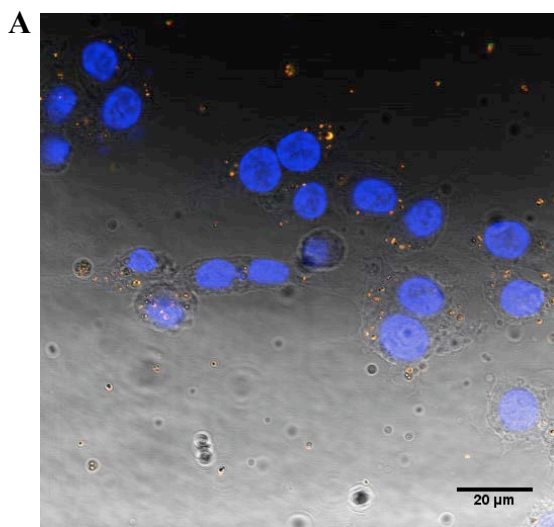


Figure 5-8: The effect of the modified PEI incorporation on *in vitro* gene knockdown efficiency of the PLGA microparticles in EGFP-HEK293 cells. The cells were transfected with the various PLGA formulations. EGFP gene expression levels of the PLGA microparticles were normalized to that of blank PLGA microparticles and represented as relative expression (%). The experiments were repeated at least twice. Data is represented as mean \pm standard deviation (n=3).

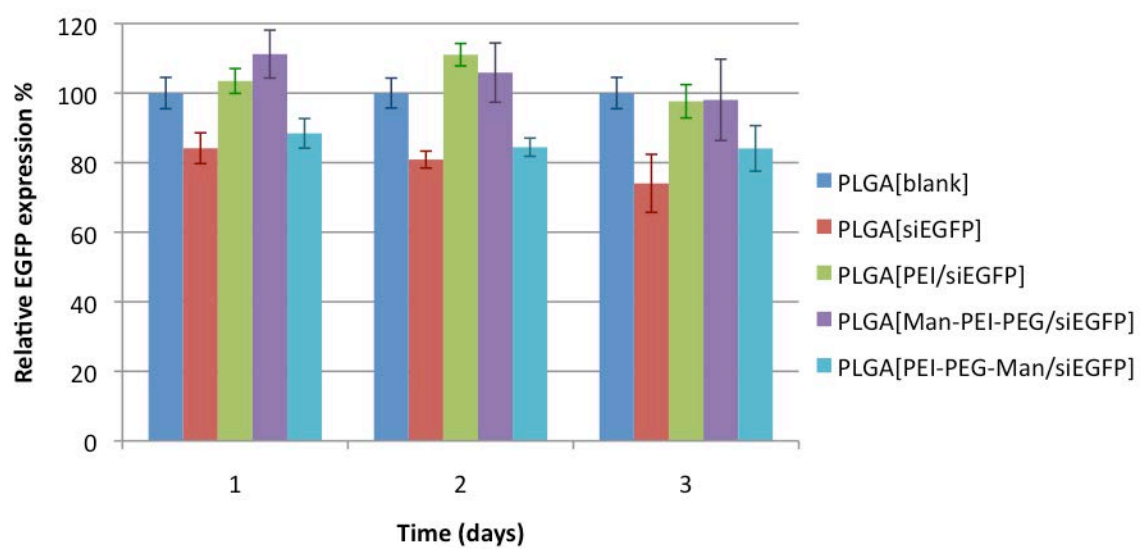


Figure 5-9: The effect of the modified PEI incorporation on cytotoxicity of the PLGA microparticles in HEK293 cells. Cytotoxicity of various PLGA microparticles were tested at the concentration of 0.25mg/ml. From the left; Bank PLGA, PLGA(PEI), PLGA(siRNA), PLGA(PEI/siRNA), PLGA(Man-PEI-PEG/siRNA), PLGA(PEI-PEG-Man/siRNA), no treatment. The relative cell viability was calculated by normalizing to the no-treatment group. The experiments were repeated at least twice. Data is represented as mean \pm standard deviation (n=3).

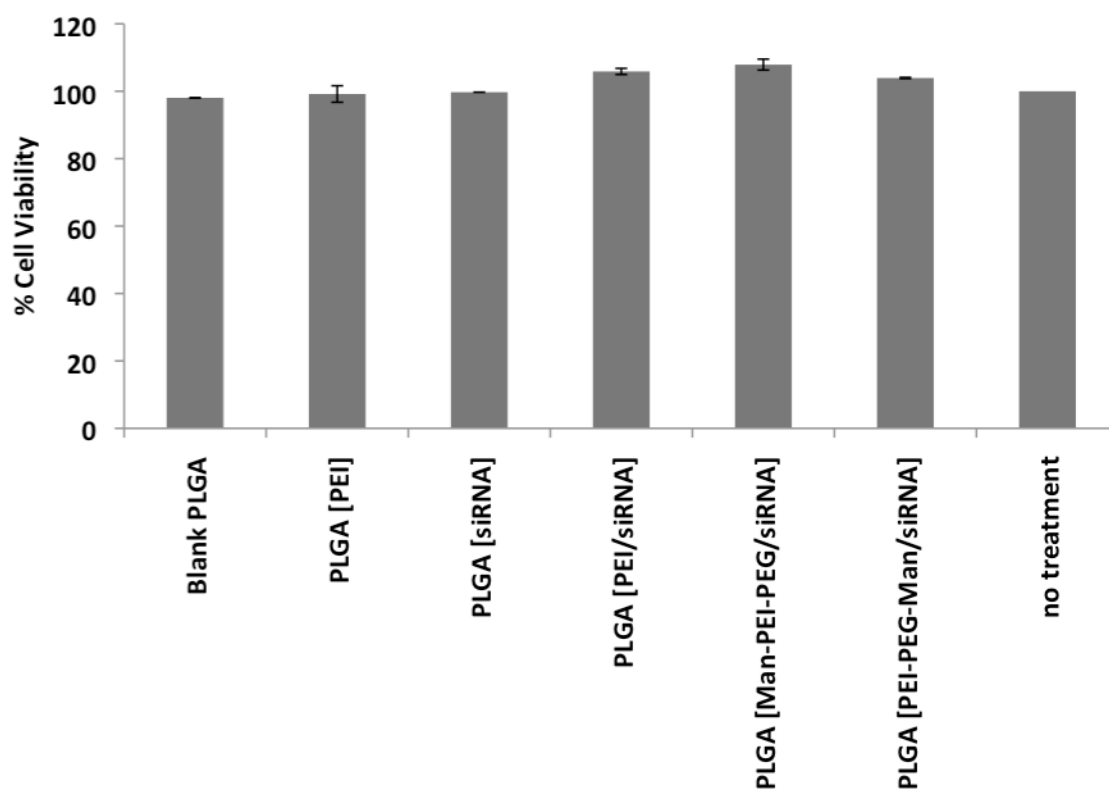
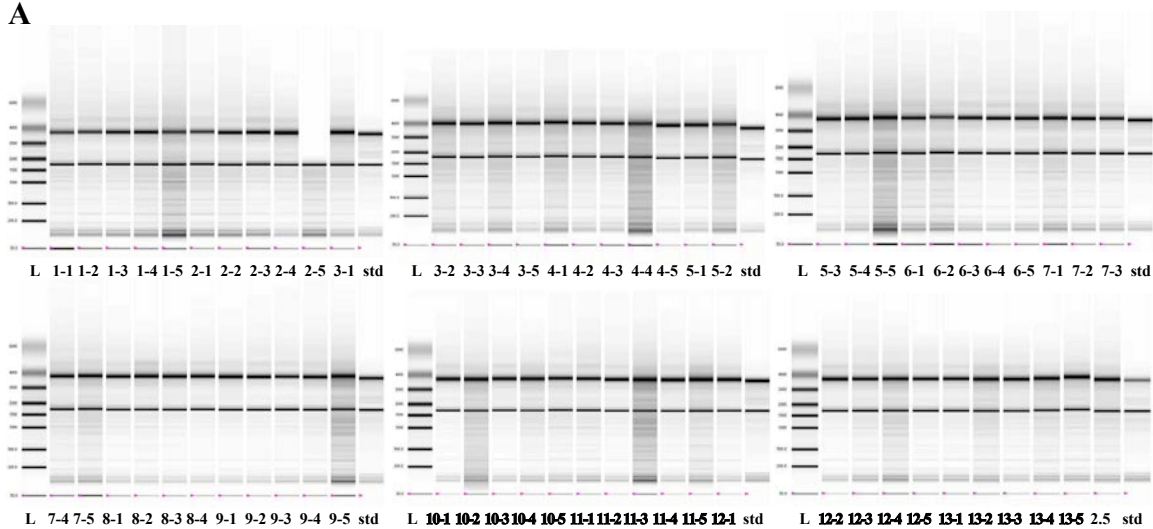
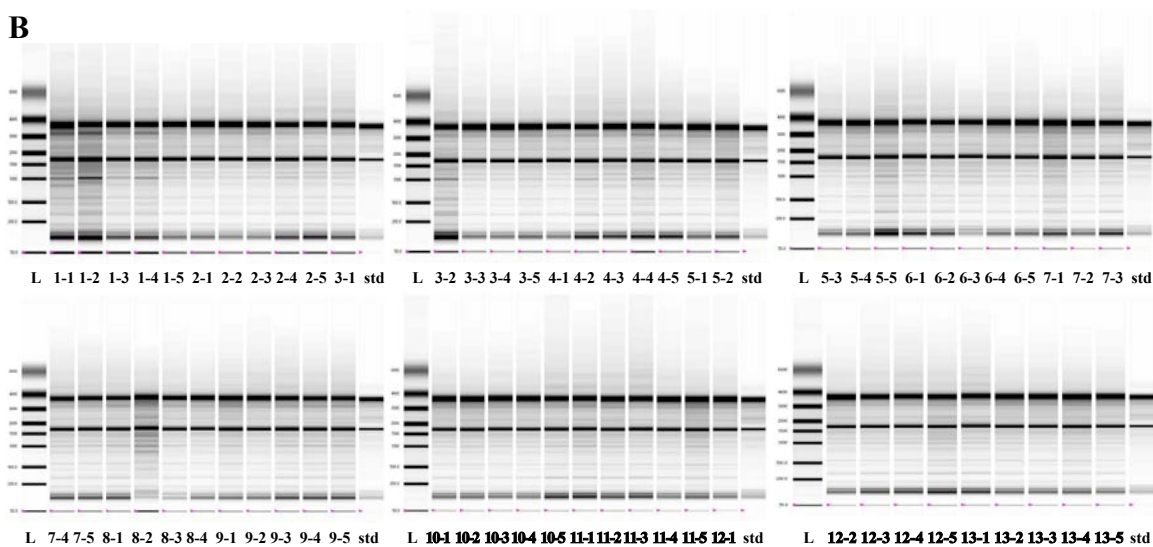


Figure 5-10: Analyzing the quality and quantity of the total RNA from the mouse organs administrated with the PLGA microparticles. A. gel electrophoresis of the total RNA samples from mouse spleen, B. gel electrophoresis of the total RNA samples from mouse lung, C. gel electrophoresis of the total RNA samples from mouse liver, D. gel electrophoresis of the total RNA samples from mouse kidney, E. gel electrophoresis of the total RNA samples from mouse heart. The numbers under the figures represent 'the number of the injection group – the number of mouse'. L represents ladder, and std represents standard RNA with a known concentration.

A



B



C

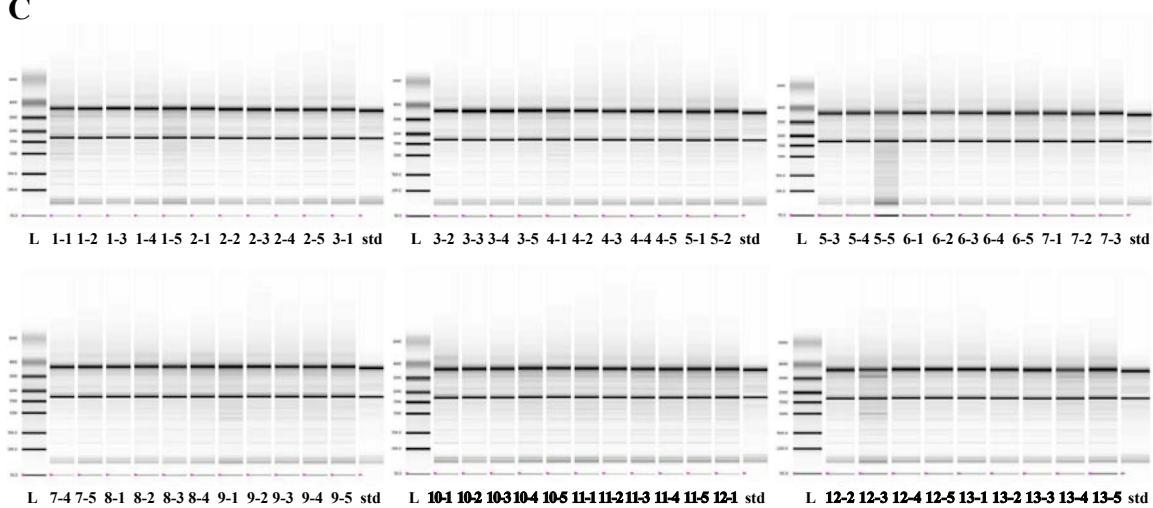
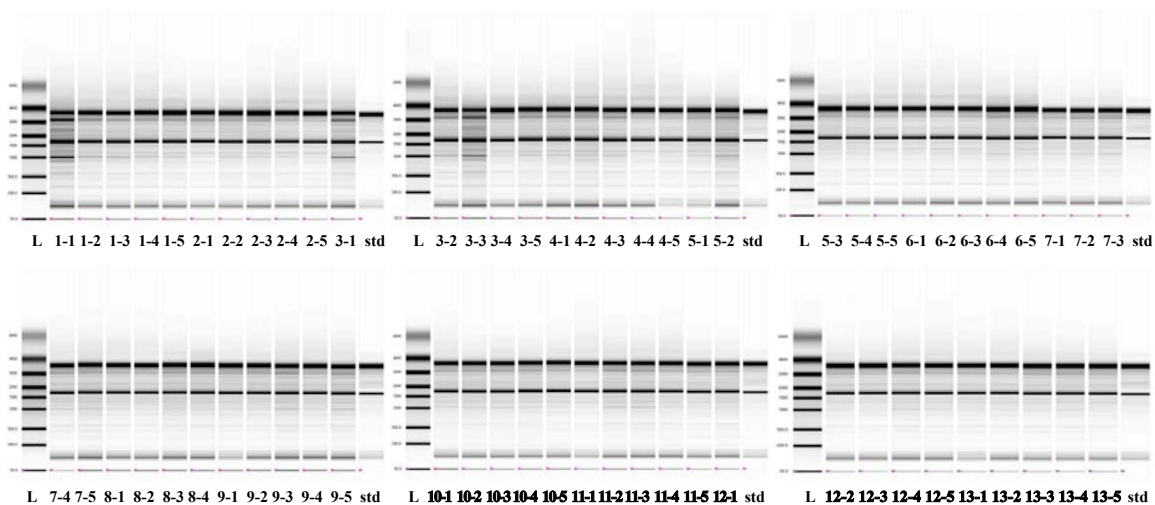
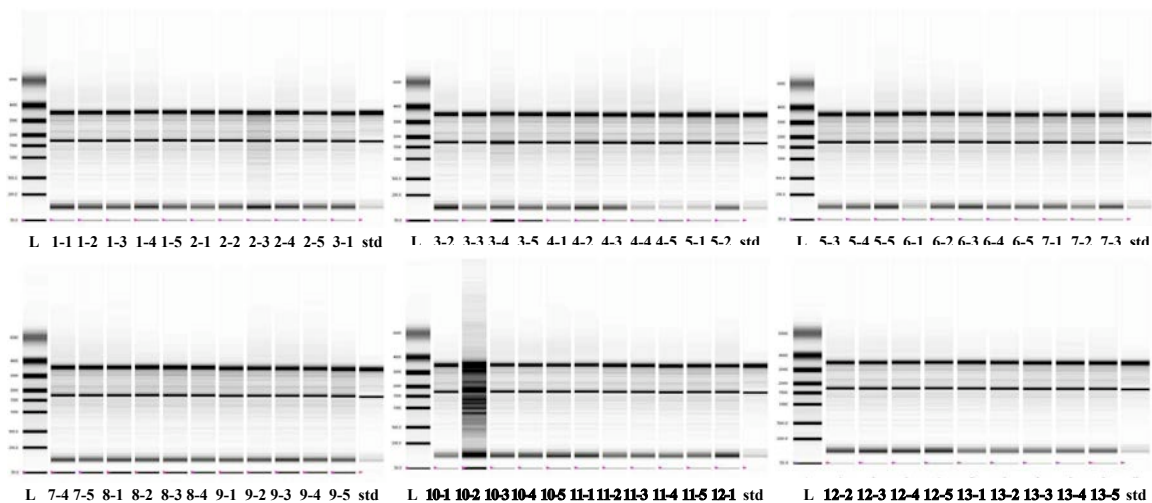


Figure 5-10 continued

D



E



Note: The numbers under the figures represents the number of injection group – the number of mouse. For example, 5-3 represents a sample from the third mouse from injection group 5 (PEI/siGAPDH). Table 5-2 shows the information on injection groups.

Figure 5-11: The effect of the modified PEI incorporation in PLGA microparticles on *in vivo* gene knockdown efficiency in mouse model. Three days after the injection of the various PLGA microparticle formulations (Table 5-2), five organs (liver, lung, heart, spleen, and kidney) were harvested. Total RNA was extracted from the organs and DNase treated. Its quality and quantity was assessed. The gene expression levels of GAPDH were analyzed using real-time PCR from each organ, normalized to that of NC1 injected groups. The data was reported as mean \pm standard deviation from triplicate RT-PCR reactions of each triplicate (n=5).

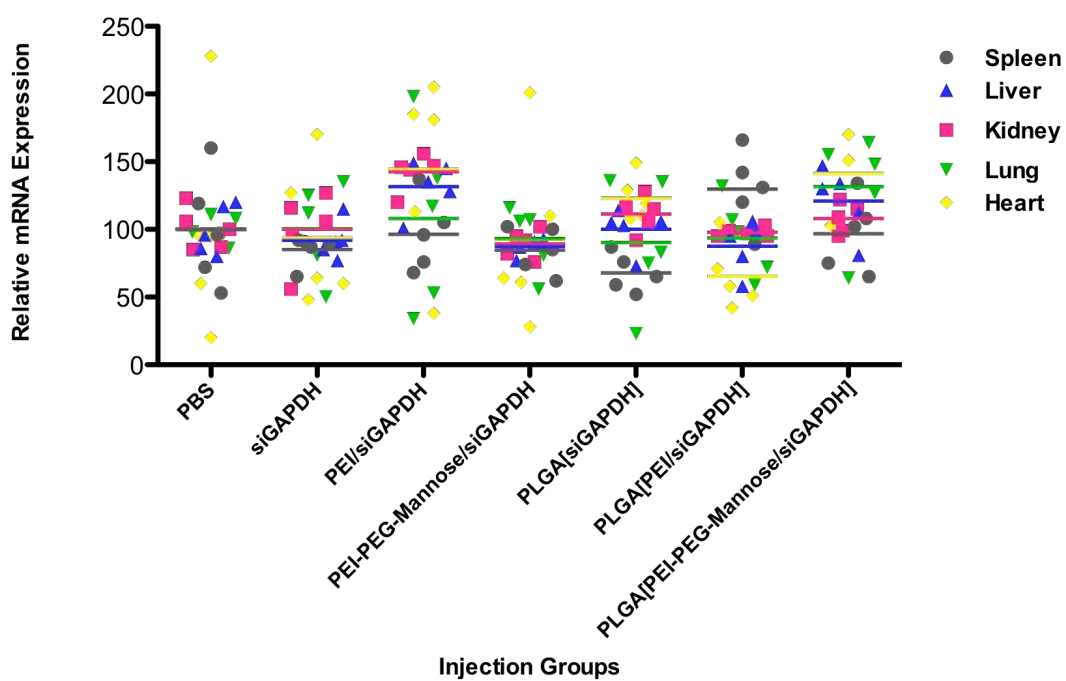
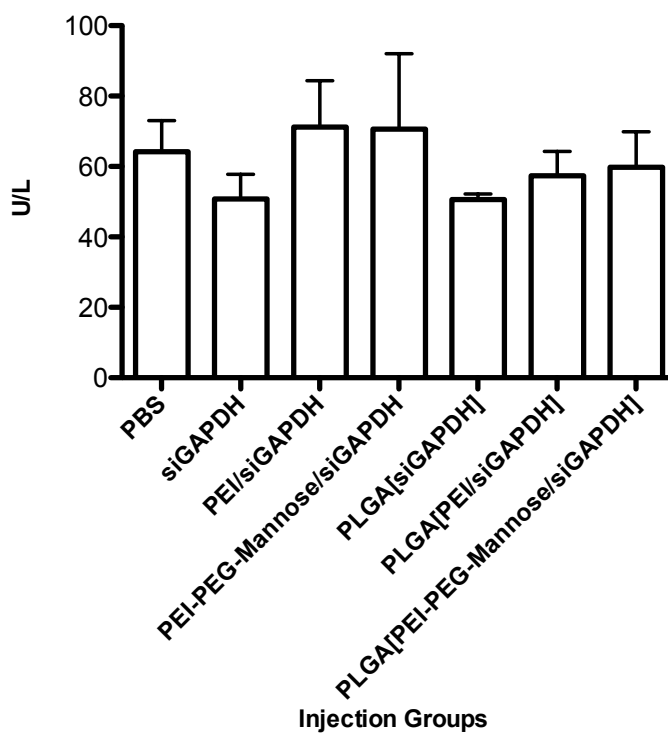
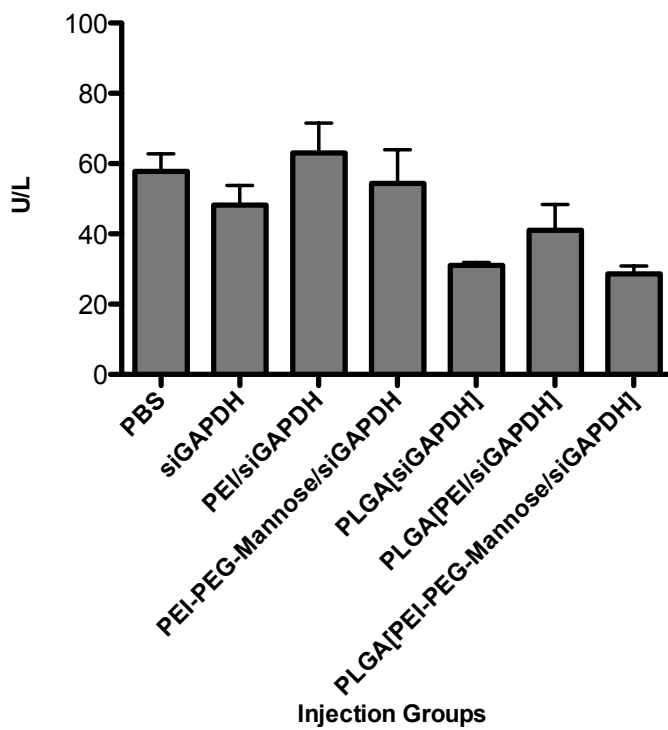


Figure 5-12: The effect of the modified PEI incorporation in PLGA microparticles on hepatotoxicity in mouse model. A. AST levels in plasma one day after the injection, B. ALT levels in plasma one day after the injection. The data was reported as mean \pm standard deviation (n=5).

A



B



CHAPTER 6: CONCLUSIONS AND FUTURE DIRECTIONS

The goal of this research has been developing an efficient siRNA delivery system using cationic polymers, PEG, mannose, and PLGA. These materials have been widely used in drug and gene delivery research. Cationic polymers, chitosan and PEI, were used to complex siRNA by electrostatic interactions, so that they condense and protect the siRNA during delivery.⁸² PEG were expected first, to increase serum half-life of a carrier by steric shielding effect and second, to decrease toxicity of cationic polymers.^{173,115, 116} Mannose ligand could promote receptor-mediated endocytosis by ligand-receptor specific interaction, which results in an increased delivery efficacy.¹²⁵ PLGA is a biodegradable polymer that has been widely used in drug delivery due to its controlled release property.^{219, 230} A delivery system consisted of cationic polymers, PEG, mannose, and PLGA has strong potential as an *in vivo* carrier of siRNA by exploiting the advantages of each component. We synthesized two different constructs of siRNA delivery system. The first construct has both mannose and PEG directly connected to the cationic backbone. The second construct has PEG connected to the backbone through one end and conjugated with mannose at the other end. Our goals are to build an efficacious delivery system for siRNA and also to investigate the effect of the location of the mannose in modified cationic polymer constructs.

We first synthesized a delivery system with chitosan as a cationic backbone and evaluated the potential as a siRNA carrier. Modified chitosans complexed and condensed siRNA successfully so that they retarded the migration of siRNA in the agarose gel electrophoresis. The chitosan polymers had minimal cytotoxicity showing near 100% cell viability at the high concentration of 1mg/ml. They formed nanoplexes small enough to be endocytosed, which were uptaken by mouse macrophage cells at 2 hours post-transfection. The second construct, chitosan-PEG-mannose, displayed enhanced siRNA retardation ability and cellular uptake when compared to the first construct, mannose-

chitosan-PEG. In the structure of chitosan-PEG-mannose, having mannose at the tip of PEG chain could expose the ligand and expedite ligand-receptor interactions. This resulted in an improved endocytosis of the nanoplexes. In contrast, PEG chains might shield the mannose ligand in the mannose-chitosan-PEG structure. This could interfere with ligand-receptor interactions. The modified chitosans did not significantly reduce *Renilla* luciferase gene expression. It might be correlated to the low lysosomal escape of siRNA. To induce RNAi, siRNA must escape from the lysosome to integrate with RISC. If it is held inside the lysosome, there is less chance to join the RISC thereby less induction of RNAi. Mannosylation and pegylation, alone or in combination, could not overcome the inherent low delivery efficacy of chitosan. Further study using a different cationic polymer would be recommended because both our modified chitosan and unmodified chitosan showed no significant gene silencing effect. A cationic polymer that has stronger siRNA condensation capacity could provide better protection to siRNA and lead to a better gene knockdown efficiency.

PEI was chosen next as a cationic backbone polymer in place of chitosan. PEI has proven gene delivery efficiency. We expected pegylation and mannosylation to reduce the cytotoxicity profile of PEI. The PEI formulations formed nanoplexes with siRNA strongly with or without modifications, so that the migration of siRNA was completely retarded at lower N/P ratios. The modified PEIs formed nano-sized complexes with siRNA. As a result, the modified PEI/siRNA nanoplexes were efficiently uptaken by RAW264.7 cells. PEI-PEG-mannose significantly enhanced siRNA delivery into the cells when compared to mannose-PEI-PEG. Furthermore, siRNA was separated from the lysosome and localized in the perinuclear region. It suggested that siRNA escaped from the lysosome and joined the RISC to initiate RNAi process. In real-time PCR analysis, the modified PEIs improved the siRNA delivery efficiency of PEI resulting in lower mRNA expressions relative to unmodified PEI. There was no significant difference between mannose-PEI-PEG and PEI-PEG-mannose.

To further study the gene silencing effect of polymer/siRNA nanoplexes on protein expression, dual-luciferase analysis was carried out. PEI-PEG-mannose demonstrated higher siRNA delivery efficiency than mannose-PEI-PEG. Mannosylation and pegylation significantly improved the cytotoxicity of PEI demonstrating increased cell viabilities relative to unmodified PEI. PEI-PEG-mannose resulted in higher cellular uptake and higher gene knockdown efficiency when compared to mannose-PEI-PEG. Increasing concentration of polymers elevated the cytotoxicity of polymers. PEI-PEG-mannose and mannose-PEI-PEG have great potential as an efficient siRNA delivery system. Adding PLGA excipient to the delivery system can further improve the toxicity profile of PEI and enhance *in vivo* gene knockdown efficiency of siRNA.

To further expand the delivery potential for *in vivo* applications, PLGA microparticle was utilized to encapsulate the modified PEI/siRNA nanoplexes. The PLGA microparticles can provide controlled release of the nanoplexes. We fabricated the PLGA microparticles encapsulating unmodified and modified PEI/siRNA nanoplexes. The modified PEI/siRNA nanoplexes marginally increased porosity of the PLGA microparticles. The particles were formed with the 2-4 μ m size range. The modified PEIs significantly improved the encapsulation efficiency of siRNA into the microparticles. The PLGA microparticles loaded with PEI-PEG-mannose/siRNA and mannose-PEI-PEG/siRNA nanoplexes displayed significantly lower initial burst and overall sustained release profile when compared to the PLGA microparticles loaded with siRNA only or unmodified PEI/siRNA nanoplexes. The PLGA microparticles incorporated with PEI-PEG-mannose resulted in higher cellular uptake than the PLGA particles loaded with PEI/siRNA or mannose-PEI-PEG/siRNA nanoplexes. The PLGA microparticles encapsulating the modified PEI/siRNA nanoplexes exhibited very low cytotoxicity at the high concentration of 1mg/ml. The PLGA particle formulations loaded with siEGFP did not significantly reduce the gene expression. There are two potential reasons why they did not show strong *in vitro* knockdown. First, the PLGA

particles have sustained release characteristics that can be difficult to analyze *in vitro*. Second, the cells are difficult to maintain for over 3 day period. In order to further investigate *in vivo* gene knockdown efficiency of the PLGA microparticles, we utilized the mouse model. The PLGA microparticles loaded with PEI/siGAPDH nanoplexes showed significant knockdown in the heart. The PLGA microparticles encapsulating siGAPDH showed efficient knockdown in the spleen. The PLGA microparticles incorporating PEI-PEG-mannose/siGAPDH nanoplexes resulted in no significant gene silencing. This result could be explained by the depot formation at the injection sight. The microparticles loaded with PEI-PEG-mannose/siGAPDH nanoplexes were held inside the depot at the injection site and could not efficiently deliver siRNA to the organs. In summery, the PLGA microparticles encapsulating the modified PEI/siRNA nanoplexes demonstrated low gene silencing effect. It can be explained by two potential reasons. First, the amount of siRNA might be too small for intraperitoneal administration. Second, the harvesting time might be too early to detect siRNA knockdown considering the sustained release property of the PLGA microparticles. Intraperitoneal route of administration requires higher dose of siRNA than other administration routes. Optimization of siRNA dose, particle size, administration route, and time point of harvesting organs may aid in development of siRNA delivery system for *in vivo* gene knockdown applications. The PLGA microparticles did not increase the level of hepatotoxicity markers such as AST and ALT relative to PBS, which is beneficial for *in vivo* gene delivery. In this study, pegylated and mannosylated PEIs reduced cytotoxicity of PEI without compromising delivery efficiency, improved loading of siRNA into microparticles, and increased cellular uptake of the siRNA. These findings have potential to lead to an improved long-acting efficacious siRNA delivery system.

REFERENCES

1. Anderson, W. F.; Blaese, R. M.; Culver, K., The ADA human gene therapy clinical protocol: Points to Consider response with clinical protocol, July 6, 1990. *Human Gene Therapy* **1990**, *1* (3), 331-62.
2. Rosenberg, S. A.; Aebersold, P.; Cornetta, K.; Kasid, A.; Morgan, R. A.; Moen, R.; Karson, E. M.; Lotze, M. T.; Yang, J. C.; Topalian, S. L.; et al., Gene transfer into humans--immunotherapy of patients with advanced melanoma, using tumor-infiltrating lymphocytes modified by retroviral gene transduction. *The New England Journal of Medicine* **1990**, *323* (9), 570-8.
3. Osanto, S.; Brouwenstyn, N.; Vaessen, N.; Figdor, C. G.; Melief, C. J.; Schrier, P. I., Immunization with interleukin-2 transfected melanoma cells. A phase I-II study in patients with metastatic melanoma. *Human Gene Therapy* **1993**, *4* (3), 323-30.
4. Arienti, F.; Sule-Suso, J.; Belli, F.; Mascheroni, L.; Rivoltini, L.; Melani, C.; Maio, M.; Cascinelli, N.; Colombo, M. P.; Parmiani, G., Limited antitumor T cell response in melanoma patients vaccinated with interleukin-2 gene-transduced allogeneic melanoma cells. *Human Gene Therapy* **1996**, *7* (16), 1955-63.
5. Nabel, G. J.; Gordon, D.; Bishop, D. K.; Nickoloff, B. J.; Yang, Z. Y.; Aruga, A.; Cameron, M. J.; Nabel, E. G.; Chang, A. E., Immune response in human melanoma after transfer of an allogeneic class I major histocompatibility complex gene with DNA-liposome complexes. *Proceedings of the National Academy of Sciences of the United States of America* **1996**, *93* (26), 15388-93.
6. Stopeck, A. T.; Hersh, E. M.; Akporiaye, E. T.; Harris, D. T.; Grogan, T.; Unger, E.; Warneke, J.; Schluter, S. F.; Stahl, S., Phase I study of direct gene transfer of an allogeneic histocompatibility antigen, HLA-B7, in patients with metastatic melanoma. *Journal of Clinical Oncology* **1997**, *15* (1), 341-9.
7. Mahvi, D. M.; Sondel, P. M.; Yang, N. S.; Albertini, M. R.; Schiller, J. H.; Hank, J.; Heiner, J.; Gan, J.; Swain, W.; Logrono, R., Phase I/IB study of immunization with autologous tumor cells transfected with the GM-CSF gene by particle-mediated transfer in patients with melanoma or sarcoma. *Human Gene Therapy* **1997**, *8* (7), 875-91.
8. Deshane, J.; Siegal, G. P.; Wang, M.; Wright, M.; Bucy, R. P.; Alvarez, R. D.; Curiel, D. T., Transductional efficacy and safety of an intraperitoneally delivered adenovirus encoding an anti-erbB-2 intracellular single-chain antibody for ovarian cancer gene therapy. *Gynecologic Oncology* **1997**, *64* (3), 378-85.
9. Kun, L. E.; Gajjar, A.; Muhlbauer, M.; Heideman, R. L.; Sanford, R.; Brenner, M.; Walter, A.; Langston, J.; Jenkins, J.; Facchini, S., Stereotactic injection of herpes simplex thymidine kinase vector producer cells (PA317-G1Tk1SvNa.7) and intravenous ganciclovir for the treatment of progressive or recurrent primary supratentorial pediatric malignant brain tumors. *Human Gene Therapy* **1995**, *6* (9), 1231-55.
10. Nguyen, D. M.; Spitz, F. R.; Yen, N.; Cristiano, R. J.; Roth, J. A., Gene therapy for lung cancer: enhancement of tumor suppression by a combination of

- sequential systemic cisplatin and adenovirus-mediated p53 gene transfer. *The Journal of Thoracic and Cardiovascular Surgery* **1996**, *112* (5), 1372-6; discussion 1376-7.
11. Romano, G.; Pacilio, C.; Giordano, A., Gene transfer technology in therapy: current applications and future goals. *Stem Cells* **1999**, *17* (4), 191-202.
 12. Gabhann, F. M.; Annex, B. H.; Popel, A. S., Gene therapy from the perspective of systems biology. *Current Opinion in Molecular Therapeutics* **2010**, *12* (5), 570-7.
 13. Behlke, M. A., Progress towards in vivo use of siRNAs. *Molecular Therapy* **2006**, *13* (4), 644-70.
 14. Kinoshita, M.; Hynynen, K., A novel method for the intracellular delivery of siRNA using microbubble-enhanced focused ultrasound. *Biochemical and Biophysical Research Communications* **2005**, *335* (2), 393-9.
 15. Akhtar, S.; Benter, I. F., Nonviral delivery of synthetic siRNAs in vivo. *The Journal of clinical investigation* **2007**, *117* (12), 3623-32.
 16. Aigner, A., Applications of RNA interference: current state and prospects for siRNA-based strategies in vivo. *Applied microbiology and biotechnology* **2007**, *76* (1), 9-21.
 17. Fire, A.; Xu, S.; Montgomery, M. K.; Kostas, S. A.; Driver, S. E.; Mello, C. C., Potent and specific genetic interference by double-stranded RNA in *Caenorhabditis elegans*. *Nature* **1998**, *391* (6669), 806-11.
 18. Gan, L.; Anton, K. E.; Masterson, B. A.; Vincent, V. A.; Ye, S.; Gonzalez-Zulueta, M., Specific interference with gene expression and gene function mediated by long dsRNA in neural cells. *Journal of Neuroscience Methods* **2002**, *121* (2), 151-7.
 19. Caplen, N. J.; Fleenor, J.; Fire, A.; Morgan, R. A., dsRNA-mediated gene silencing in cultured *Drosophila* cells: a tissue culture model for the analysis of RNA interference. *Gene* **2000**, *252* (1-2), 95-105.
 20. Karpala, A. J.; Doran, T. J.; Bean, A. G., Immune responses to dsRNA: implications for gene silencing technologies. *Immunology and Cell Biology* **2005**, *83* (3), 211-6.
 21. Elbashir, S. M.; Harborth, J.; Lendeckel, W.; Yalcin, A.; Weber, K.; Tuschl, T., Duplexes of 21-nucleotide RNAs mediate RNA interference in cultured mammalian cells. *Nature* **2001**, *411* (6836), 494-8.
 22. Cheng, J. C.; Sakamoto, K. M., The emerging role of RNA interference in the design of novel therapeutics in oncology. *Cell Cycle* **2004**, *3* (11), 1398-1401.
 23. Nieth, C.; Priebisch, A.; Stege, A.; Lage, H., Modulation of the classical multidrug resistance (MDR) phenotype by RNA interference (RNAi). *FEBS Letters* **2003**, *545* (2-3), 144-50.

24. Bernstein, E.; Caudy, A. A.; Hammond, S. M.; Hannon, G. J., Role for a bidentate ribonuclease in the initiation step of RNA interference. *Nature* **2001**, *409* (6818), 363-6.
25. Collins, R. E.; Cheng, X., Structural domains in RNAi. *FEBS Letters* **2005**, *579* (26), 5841-9.
26. Hammond, S. M.; Boettcher, S.; Caudy, A. A.; Kobayashi, R.; Hannon, G. J., Argonaute2, a link between genetic and biochemical analyses of RNAi. *Science* **2001**, *293* (5532), 1146-50.
27. Matranga, C.; Tomari, Y.; Shin, C.; Bartel, D. P.; Zamore, P. D., Passenger-strand cleavage facilitates assembly of siRNA into Ago2-containing RNAi enzyme complexes. *Cell* **2005**, *123* (4), 607-20.
28. Nykanen, A.; Haley, B.; Zamore, P. D., ATP requirements and small interfering RNA structure in the RNA interference pathway. *Cell* **2001**, *107* (3), 309-21.
29. Martinez, J.; Patkaniowska, A.; Urlaub, H.; Luhrmann, R.; Tuschl, T., Single-stranded antisense siRNAs guide target RNA cleavage in RNAi. *Cell* **2002**, *110* (5), 563-74.
30. Liu, J.; Carmell, M. A.; Rivas, F. V.; Marsden, C. G.; Thomson, J. M.; Song, J. J.; Hammond, S. M.; Joshua-Tor, L.; Hannon, G. J., Argonaute2 is the catalytic engine of mammalian RNAi. *Science* **2004**, *305* (5689), 1437-41.
31. Rand, T. A.; Ginalski, K.; Grishin, N. V.; Wang, X., Biochemical identification of Argonaute 2 as the sole protein required for RNA-induced silencing complex activity. *Proceedings of the National Academy of Sciences of the United States of America* **2004**, *101* (40), 14385-9.
32. Rivas, F. V.; Tolia, N. H.; Song, J. J.; Aragon, J. P.; Liu, J.; Hannon, G. J.; Joshua-Tor, L., Purified Argonaute2 and an siRNA form recombinant human RISC. *Nature Structural & Molecular Biology* **2005**, *12* (4), 340-9.
33. Caplen, N. J.; Parrish, S.; Imani, F.; Fire, A.; Morgan, R. A., Specific inhibition of gene expression by small double-stranded RNAs in invertebrate and vertebrate systems. *Proceedings of the National Academy of Sciences of the United States of America* **2001**, *98* (17), 9742-7.
34. Elbashir, S. M.; Lendeckel, W.; Tuschl, T., RNA interference is mediated by 21- and 22-nucleotide RNAs. *Genes & Development* **2001**, *15* (2), 188-200.
35. John, M.; Constien, R.; Akinc, A.; Goldberg, M.; Moon, Y. A.; Spranger, M.; Hadwiger, P.; Soutschek, J.; Vornlocher, H. P.; Manoharan, M.; Stoffel, M.; Langer, R.; Anderson, D. G.; Horton, J. D.; Kotliansky, V.; Bumcrot, D., Effective RNAi-mediated gene silencing without interruption of the endogenous microRNA pathway. *Nature* **2007**, *449* (7163), 745-7.
36. Grimm, D.; Streetz, K. L.; Jopling, C. L.; Storm, T. A.; Pandey, K.; Davis, C. R.; Marion, P.; Salazar, F.; Kay, M. A., Fatality in mice due to oversaturation of cellular microRNA/short hairpin RNA pathways. *Nature* **2006**, *441* (7092), 537-41.

37. Banan, M.; Puri, N., The ins and outs of RNAi in mammalian cells. *Current Pharmaceutical Biotechnology* **2004**, 5 (5), 441-50.
38. Sioud, M., On the delivery of small interfering RNAs into mammalian cells. *Expert Opinion on Drug Delivery* **2005**, 2 (4), 639-51.
39. Abe, T.; Goda, K.; Futami, K.; Furuichi, Y., Detection of siRNA administered to cells and animals by using a fluorescence intensity distribution analysis polarization system. *Nucleic Acids Research* **2009**, 37 (7).
40. Chiu, Y. L.; Ali, A.; Chu, C. Y.; Cao, H.; Rana, T. M., Visualizing a correlation between siRNA localization, cellular uptake, and RNAi in living cells. *Chemistry & Biology* **2004**, 11 (8), 1165-75.
41. Soutschek, J.; Akinc, A.; Bramlage, B.; Charisse, K.; Constien, R.; Donoghue, M.; Elbashir, S.; Geick, A.; Hadwiger, P.; Harborth, J.; John, M.; Kesavan, V.; Lavine, G.; Pandey, R. K.; Racie, T.; Rajeev, K. G.; Rohl, I.; Toudjarska, I.; Wang, G.; Wuschko, S.; Bumcrot, D.; Koteliansky, V.; Limmer, S.; Manoharan, M.; Vornlocher, H. P., Therapeutic silencing of an endogenous gene by systemic administration of modified siRNAs. *Nature* **2004**, 432 (7014), 173-8.
42. Zhang, S.; Zhao, B.; Jiang, H.; Wang, B.; Ma, B., Cationic lipids and polymers mediated vectors for delivery of siRNA. *Journal of Controlled Release* **2007**, 123 (1), 1-10.
43. Elmen, J.; Thonberg, H.; Ljungberg, K.; Frieden, M.; Westergaard, M.; Xu, Y.; Wahren, B.; Liang, Z.; Orum, H.; Koch, T.; Wahlestedt, C., Locked nucleic acid (LNA) mediated improvements in siRNA stability and functionality. *Nucleic Acids Research* **2005**, 33 (1), 439-47.
44. Nimesh, S.; Chandra, R., Polyethylenimine nanoparticles as an efficient in vitro siRNA delivery system. *European Journal of Pharmaceutics and Biopharmaceutics* **2009**.
45. Kim, W. J.; Kim, S. W., Efficient siRNA delivery with non-viral polymeric vehicles. *Pharmaceutical research* **2009**, 26 (3), 657-66.
46. Kawamata, Y.; Nagayama, Y.; Nakao, K.; Mizuguchi, H.; Hayakawa, T.; Sato, T.; Ishii, N., Receptor-independent augmentation of adenovirus-mediated gene transfer with chitosan in vitro. *Biomaterials* **2002**, 23 (23), 4573-4579.
47. Mao, S.; Sun, W.; Kissel, T., Chitosan-based formulations for delivery of DNA and siRNA. *Advanced drug delivery reviews* **2010**, 62 (1), 12-27.
48. Abdallah, B.; Sachs, L.; Demeneix, B. A., Non-viral gene transfer: applications in developmental biology and gene therapy. *Biology of the Cell* **1995**, 85 (1), 1-7.
49. Goff, S. P.; Berg, P., Construction of hybrid viruses containing SV40 and a phage DNA segments and their propagation in cultured monkey cells. *Cell* **1976**, 9 (4), 695-705.
50. Haynes, B. F., HIV vaccines: where we are and where we are going. *Lancet* **1996**, 348 (9032), 933-7.

51. Weber, J., Distinguishing between response to HIV vaccine and response to HIV. *Lancet* **1997**, *350* (9073), 230-1.
52. Romano, G.; Massi, D.; Giordano, A., The standpoint of AIDS research and therapy programs. *Anticancer Research* **1998**, *18* (4B), 2763-78.
53. Boyer, J. D.; Ugen, K. E.; Wang, B.; Agadjanyan, M.; Gilbert, L.; Bagarazzi, M. L.; Chattergoon, M.; Frost, P.; Javadian, A.; Williams, W. V.; Refaeli, Y.; Ciccarelli, R. B.; McCallus, D.; Coney, L.; Weiner, D. B., Protection of chimpanzees from high-dose heterologous HIV-1 challenge by DNA vaccination. *Nature Medicine* **1997**, *3* (5), 526-32.
54. Rowland-Jones, S. L.; Pinheiro, S.; Kaul, R.; Hansasuta, P.; Gillespie, G.; Dong, T.; Plummer, F. A.; Bwayo, J. B.; Fidler, S.; Weber, J.; McMichael, A.; Appay, V., How important is the 'quality' of the cytotoxic T lymphocyte (CTL) response in protection against HIV infection? *Immunology Letters* **2001**, *79* (1-2), 15-20.
55. Maier, P.; von Kalle, C.; Laufs, S., Retroviral vectors for gene therapy. *Future Microbiology* **2010**, *5*, 1507-23.
56. Zhang, X.; Godbey, W. T., Viral vectors for gene delivery in tissue engineering. *Advanced drug delivery reviews* **2006**, *58* (4), 515-34.
57. Stefaan C. De Smedt, J. D. a. W. E. H., Cationic Polymer Based Gene Delivery Systems **2000**, *17* (2), 113-126.
58. Martin, S. E.; Caplen, N. J., Applications of RNA interference in mammalian systems. *Annual review of genomics and human genetics* **2007**, *8*, 81-108.
59. Aiman, O. A.; Maureen, D. D.; Aliasger, K. S., Formulating poly(lactide-co-glycolide) particles for plasmid DNA delivery. *Journal of pharmaceutical sciences* **2008**, *97* (7), 2448-2461.
60. Ruponen, M.; Honkakoski, P.; Ronkko, S.; Pelkonen, J.; Tammi, M.; Urtti, A., Extracellular and intracellular barriers in non-viral gene delivery. *Journal of Controlled Release* **2003**, *93* (2), 213-7.
61. Onishi, H.; Machida, Y., Biodegradation and distribution of water-soluble chitosan in mice. *Biomaterials* **1999**, *20* (2), 175-82.
62. Aiba, S., Studies on chitosan: 4. Lysozymic hydrolysis of partially N-acetylated chitosans. *International Journal of Biological Macromolecules* **1992**, *14* (4), 225-8.
63. Escott, G. M.; Adams, D. J., Chitinase activity in human serum and leukocytes. *Infection and Immunity* **1995**, *63* (12), 4770-3.
64. Zhang, H.; Neau, S. H., In vitro degradation of chitosan by bacterial enzymes from rat cecal and colonic contents. *Biomaterials* **2002**, *23* (13), 2761-6.
65. Huang, M.; Fong, C. W.; Khor, E.; Lim, L. Y., Transfection efficiency of chitosan vectors: effect of polymer molecular weight and degree of deacetylation. *Journal of Controlled Release* **2005**, *106* (3), 391-406.

66. Mao, H. Q.; Roy, K.; Troung-Le, V. L.; Janes, K. A.; Lin, K. Y.; Wang, Y.; August, J. T.; Leong, K. W., Chitosan-DNA nanoparticles as gene carriers: synthesis, characterization and transfection efficiency. *Journal of Controlled Release* **2001**, *70* (3), 399-421.
67. Truong-Le, V. L.; Walsh, S. M.; Schweibert, E.; Mao, H. Q.; Guggino, W. B.; August, J. T.; Leong, K. W., Gene transfer by DNA-gelatin nanospheres. *Archives of Biochemistry and Biophysics* **1999**, *361* (1), 47-56.
68. Mhurchu, C. N.; Dunshea-Mooij, C.; Bennett, D.; Rodgers, A., Effect of chitosan on weight loss in overweight and obese individuals: a systematic review of randomized controlled trials. *Obesity Reviews* **2005**, *6* (1), 35-42.
69. Xu, C.; Pan, H.; Jiang, H.; Tang, G.; Chen, W., Biocompatibility evaluation of N,O-hexanoyl chitosan as a biodegradable hydrophobic polycation for controlled drug release. *Journal of Materials Science. Materials in Medicine* **2008**, *19* (6), 2525-32.
70. Mansouri, S.; Cuie, Y.; Winnik, F.; Shi, Q.; Lavigne, P.; Benderdour, M.; Beaumont, E.; Fernandes, J. C., Characterization of folate-chitosan-DNA nanoparticles for gene therapy. *Biomaterials* **2006**, *27* (9), 2060-5.
71. Borchard, G., Chitosans for gene delivery. *Advanced Drug Delivery Reviews* **2001**, *52*, 145-150.
72. Heo, S. H.; Jang, M. J.; Kim, D. G.; Jeong, Y. I.; Jang, M. K.; Nah, J. W., Characterization and preparation of low molecular weight water soluble chitosan nanoparticle modified with cell targeting ligand for efficient gene delivery. *Polymer-Korea* **2007**, *31* (5), 454-459.
73. Koping-Hoggard, M.; Tubulekas, I.; Guan, H.; Edwards, K.; Nilsson, M.; Varum, K. M.; Artursson, P., Chitosan as a nonviral gene delivery system. Structure-property relationships and characteristics compared with polyethylenimine in vitro and after lung administration in vivo. *Gene Therapy* **2001**, *8* (14), 1108-21.
74. Katas, H.; Alpar, H. O., Development and characterisation of chitosan nanoparticles for siRNA delivery. *Journal of Controlled Release* **2006**, *115* (2), 216-25.
75. Liu, X.; Howard, K. A.; Dong, M.; Andersen, M. O.; Rahbek, U. L.; Johnsen, M. G.; Hansen, O. C.; Besenbacher, F.; Kjems, J., The influence of polymeric properties on chitosan/siRNA nanoparticle formulation and gene silencing. *Biomaterials* **2007**, *28* (6), 1280-8.
76. Howard, K. A.; Rahbek, U. L.; Liu, X.; Damgaard, C. K.; Glud, S. Z.; Andersen, M. O.; Hovgaard, M. B.; Schmitz, A.; Nyengaard, J. R.; Besenbacher, F.; Kjems, J., RNA interference in vitro and in vivo using a novel chitosan/siRNA nanoparticle system. *Molecular Therapy* **2006**, *14* (4), 476-84.
77. Tang, M. X.; Szoka, F. C., The influence of polymer structure on the interactions of cationic polymers with DNA and morphology of the resulting complexes. *Gene therapy* **1997**, *4* (8), 823-32.

78. Godbey, W. T.; Wu, K. K.; Mikos, A. G., Size matters: molecular weight affects the efficiency of poly(ethylenimine) as a gene delivery vehicle. *Journal of biomedical materials research* **1999**, *45* (3), 268-75.
79. Aigner, A.; Fischer, D.; Merdan, T.; Brus, C.; Kissel, T.; Czubayko, F., Delivery of unmodified bioactive ribozymes by an RNA-stabilizing polyethylenimine (LMW-PEI) efficiently down-regulates gene expression. *Gene Therapy* **2002**, *9* (24), 1700-7.
80. Boussif, O.; Lezoualc'h, F.; Zanta, M. A.; Mergny, M. D.; Scherman, D.; Demeneix, B.; Behr, J. P., A versatile vector for gene and oligonucleotide transfer into cells in culture and in vivo: polyethylenimine. *Proceedings of the National Academy of Sciences of the United States of America* **1995**, *92* (16), 7297-301.
81. Hobel, S.; Aigner, A., Polyethylenimine (PEI)/siRNA-mediated gene knockdown in vitro and in vivo. *Methods in Molecular Biology* **2010**, *623*, 283-97.
82. Intra, J.; Salem, A. K., Characterization of the transgene expression generated by branched and linear polyethylenimine-plasmid DNA nanoparticles in vitro and after intraperitoneal injection in vivo. *Journal of Controlled Release* **2008**, *130* (2), 129-38.
83. Petersen, H.; Fechner, P. M.; Martin, A. L.; Kunath, K.; Stolnik, S.; Roberts, C. J.; Fischer, D.; Davies, M. C.; Kissel, T., Polyethylenimine-graft-Poly(ethylene glycol) Copolymers: Influence of Copolymer Block Structure on DNA Complexation and Biological Activities as Gene Delivery System. *Bioconjugate chemistry* **2002**, *13* (4), 845-854.
84. Zintchenko, A.; Philipp, A.; Dehshahri, A.; Wagner, E., Simple modifications of branched PEI lead to highly efficient siRNA carriers with low toxicity. *Bioconjugate chemistry* **2008**, *19* (7), 1448-55.
85. Sun, Y.-X.; Zeng, X.; Meng, Q.-F.; Zhang, X.-Z.; Cheng, S.-X.; Zhuo, R.-X., The influence of RGD addition on the gene transfer characteristics of disulfide-containing polyethyleneimine/DNA complexes. *Biomaterials* **2008**, *29* (32), 4356-4365.
86. Urban-Klein, B.; Werth, S.; Abuharbeid, S.; Czubayko, F.; Aigner, A., RNAi-mediated gene-targeting through systemic application of polyethylenimine (PEI)-complexed siRNA in vivo. *Gene therapy* **2005**, *12* (5), 461-6.
87. Goula D, B. C., Mantero S, Merlo G, Levi G, Demeneix BA., Polyethylenimine-based intravenous delivery of transgenes to mouse lung. *Gene Therapy* **1998**, *5*, 1291-1295.
88. Wightman, L.; Kircheis, R.; Rossler, V.; Carotta, S.; Ruzicka, R.; Kurs, M.; Wagner, E., Different behavior of branched and linear polyethylenimine for gene delivery in vitro and in vivo. *The Journal of Gene Medicine* **2001**, *3* (4), 362-72.
89. Gao, X.; Kim, K. S.; Liu, D., Nonviral gene delivery: what we know and what is next. *The AAPS Journal* **2007**, *9* (1), E92-104.

90. von Harpe, A.; Petersen, H.; Li, Y.; Kissel, T., Characterization of commercially available and synthesized polyethylenimines for gene delivery. *Journal of Controlled Release* **2000**, *69* (2), 309-22.
91. Godbey, W. T.; Wu, K. K.; Mikos, A. G., Poly(ethylenimine) and its role in gene delivery. *Journal of Controlled Release* **1999**, *60* (2-3), 149-160.
92. Godbey, W. T.; Wu, K. K.; Mikos, A. G., Poly(ethylenimine) and its role in gene delivery. *Journal of Controlled Release* **1999**, *60* (2-3), 149-60.
93. Werth, S.; Urban-Klein, B.; Dai, L.; Hobel, S.; Grzelinski, M.; Bakowsky, U.; Czubayko, F.; Aigner, A., A low molecular weight fraction of polyethylenimine (PEI) displays increased transfection efficiency of DNA and siRNA in fresh or lyophilized complexes. *Journal of Controlled Release* **2006**, *112* (2), 257-70.
94. Fischer, D.; Li, Y.; Ahlemeyer, B.; Krieglstein, J.; Kissel, T., In vitro cytotoxicity testing of polycations: influence of polymer structure on cell viability and hemolysis. *Biomaterials* **2003**, *24* (7), 1121-31.
95. Swami, A.; Kurupati, R. K.; Pathak, A.; Singh, Y.; Kumar, P.; Gupta, K. C., A unique and highly efficient non-viral DNA/siRNA delivery system based on PEI-bisepoxide nanoparticles. *Biochemical and Biophysical Research Communications* **2007**, *362* (4), 835-41.
96. Hassani, Z.; Lemkine, G. F.; Erbacher, P.; Palmier, K.; Alfama, G.; Giovannangeli, C.; Behr, J. P.; Demeneix, B. A., Lipid-mediated siRNA delivery down-regulates exogenous gene expression in the mouse brain at picomolar levels. *The Journal of Gene Medicine* **2005**, *7* (2), 198-207.
97. Zhang, C.; Yadava, P.; Hughes, J., Polyethylenimine strategies for plasmid delivery to brain-derived cells. *Methods* **2004**, *33* (2), 144-50.
98. Abdallah, B.; Hassan, A.; Benoist, C.; Goula, D.; Behr, J. P.; Demeneix, B. A., A powerful nonviral vector for in vivo gene transfer into the adult mammalian brain: polyethylenimine. *Human gene therapy* **1996**, *7* (16), 1947-54.
99. Schaffer, D. V.; Fidelman, N. A.; Dan, N.; Lauffenburger, D. A., Vector unpacking as a potential barrier for receptor-mediated polyplex gene delivery. *Biotechnology and bioengineering* **2000**, *67* (5), 598-606.
100. Plank, C.; Tang, M. X.; Wolfe, A. R.; Szoka, F. C., Jr., Branched cationic peptides for gene delivery: role of type and number of cationic residues in formation and in vitro activity of DNA polyplexes. *Human gene therapy* **1999**, *10* (2), 319-32.
101. Lee, Y.; Mo, H.; Koo, H.; Park, J. Y.; Cho, M. Y.; Jin, G. W.; Park, J. S., Visualization of the degradation of a disulfide polymer, linear poly(ethylenimine sulfide), for gene delivery. *Bioconjugate chemistry* **2007**, *18* (1), 13-8.
102. Hunter, A. C., Molecular hurdles in polyfectin design and mechanistic background to polycation induced cytotoxicity. *Advanced drug delivery reviews* **2006**, *58* (14), 1523-31.

103. Lingor, P.; Koeberle, P.; Kugler, S.; Bahr, M., Down-regulation of apoptosis mediators by RNAi inhibits axotomy-induced retinal ganglion cell death in vivo. *Brain* **2005**, *128* (Pt 3), 550-8.
104. Neu, M.; Fischer, D.; Kissel, T., Recent advances in rational gene transfer vector design based on poly(ethylene imine) and its derivatives. *The journal of gene medicine* **2005**, *7* (8), 992-1009.
105. Thomas, M.; Klivanov, A. M., Enhancing polyethylenimine's delivery of plasmid DNA into mammalian cells. *Proceedings of the National Academy of Sciences of the United States of America* **2002**, *99* (23), 14640-5.
106. Kim, S. H.; Jeong, J. H.; Lee, S. H.; Kim, S. W.; Park, T. G., LHRH receptor-mediated delivery of siRNA using polyelectrolyte complex micelles self-assembled from siRNA-PEG-LHRH conjugate and PEI. *Bioconjugate chemistry* **2008**, *19* (11), 2156-62.
107. Merkel, O. M.; Librizzi, D.; Pfestroff, A.; Schurrat, T.; Buyens, K.; Sanders, N. N.; De Smedt, S. C.; BÉHÉ, M.; Kissel, T., Stability of siRNA polyplexes from poly(ethylenimine) and poly(ethylenimine)-g-poly(ethylene glycol) under in vivo conditions: Effects on pharmacokinetics and biodistribution measured by Fluorescence Fluctuation Spectroscopy and Single Photon Emission Computed Tomography (SPECT) imaging. *Journal of Controlled Release* **2009**, *138* (2), 148-159.
108. Ogris M, B. S., Schüller S, Kircheis R, Wagner E, PEGylated DNA/transferrin-PEI complexes: reduced interaction with blood components, extended circulation in blood and potential for systemic gene delivery. *Gene Therapy* **1999**, *6* (4), 595-605.
109. Diebold, S. S.; Lehrmann, H.; Kursa, M.; Wagner, E.; Cotton, M.; Zenke, M., Efficient Gene Delivery into Human Dendritic Cells by Adenovirus Polyethylenimine and Mannose Polyethylenimine Transfection. *Human Gene Therapy* **1999**, *10*, 775.
110. K.W. Leong, H.-Q. M., V.L. Truong-Leb, K. Roy, S.M. Walsh, J.T. August, DNA-polycation nanospheres as non-viral gene delivery vehicles. *Journal of Controlled Release* **1998**, *53*, 183-193.
111. Bonsted, A.; Wagner, E.; Prasmickaite, L.; Hogset, A.; Berg, K., Photochemical enhancement of DNA delivery by EGF receptor targeted polyplexes. *Methods in Molecular Biology* **2008**, *434*, 171-81.
112. Moore, N. M.; Barbour, T. R.; Sakiyama-Elbert, S. E., Synthesis and Characterization of Four-Arm Poly(ethylene glycol)-Based Gene Delivery Vehicles Coupled to Integrin and DNA-Binding Peptides. *Molecular Pharmaceutics* **2008**, *5* (1), 140-150.
113. Mao, S.; Neu, M.; Germershaus, O.; Merkel, O.; Sitterberg, J.; Bakowsky, U.; Kissel, T., Influence of polyethylene glycol chain length on the physicochemical and biological properties of poly(ethylene imine)-graft-poly(ethylene glycol) block copolymer/SiRNA polyplexes. *Bioconjugate chemistry* **2006**, *17* (5), 1209-18.

114. Schiffelers, R. M.; Ansari, A.; Xu, J.; Zhou, Q.; Tang, Q.; Storm, G.; Molema, G.; Lu, P. Y.; Scaria, P. V.; Woodle, M. C., Cancer siRNA therapy by tumor selective delivery with ligand-targeted sterically stabilized nanoparticle. *Nucleic Acids Research* **2004**, *32* (19), e149.
115. Owens, D. E., 3rd; Peppas, N. A., Opsonization, biodistribution, and pharmacokinetics of polymeric nanoparticles. *International journal of pharmaceutics* **2006**, *307* (1), 93-102.
116. Peracchia, M. T.; Harnisch, S.; Pinto-Alphandary, H.; Gulik, A.; Dedieu, J. C.; Desmaele, D.; d'Angelo, J.; Muller, R. H.; Couvreur, P., Visualization of in vitro protein-rejecting properties of PEGylated stealth polycyanoacrylate nanoparticles. *Biomaterials* **1999**, *20* (14), 1269-75.
117. Peracchia, M. T.; Vauthier, C.; Passirani, C.; Couvreur, P.; Labarre, D., Complement consumption by poly(ethylene glycol) in different conformations chemically coupled to poly(isobutyl 2-cyanoacrylate) nanoparticles. *Life Science* **1997**, *61* (7), 749-61.
118. Leroux, J. C.; De Jaeghere, F.; Anner, B.; Doelker, E.; Gurny, R., An investigation on the role of plasma and serum opsonins on the internalization of biodegradable poly(D,L-lactic acid) nanoparticles by human monocytes. *Life Science* **1995**, *57* (7), 695-703.
119. Gref, R.; Minamitake, Y.; Peracchia, M. T.; Trubetskoy, V.; Torchilin, V.; Langer, R., Biodegradable long-circulating polymeric nanospheres. *Science* **1994**, *263* (5153), 1600-3.
120. Owens, D. E., 3rd; Peppas, N. A., Opsonization, biodistribution, and pharmacokinetics of polymeric nanoparticles. *International journal of pharmaceutics* **2006**, *307* (1), 93-102.
121. Fishburn, C. S., The pharmacology of PEGylation: balancing PD with PK to generate novel therapeutics. *Journal of pharmaceutical sciences* **2008**, *97* (10), 4167-83.
122. Webster, R.; Didier, E.; Harris, P.; Siegel, N.; Stadler, J.; Tilbury, L.; Smith, D., PEGylated proteins: evaluation of their safety in the absence of definitive metabolism studies. *Drug Metabolism and Disposition* **2007**, *35* (1), 9-16.
123. Pang, S.; Fiume, M. Z., Final report on the safety assessment of Ammonium, Potassium, and Sodium Persulfate. *International journal of toxicology* **2001**, *20* Suppl 3, 7-21.
124. Park, I. Y.; Kim, I. Y.; Yoo, M. K.; Choi, Y. J.; Cho, M. H.; Cho, C. S., Mannosylated polyethylenimine coupled mesoporous silica nanoparticles for receptor-mediated gene delivery. *International journal of pharmaceutics* **2008**, *359* (1-2), 280-7.
125. Diebold, S. S.; Kurs, M.; Wagner, E.; Cotten, M.; Zenke, M., Mannose polyethylenimine conjugates for targeted DNA delivery into dendritic cells. *The Journal of biological chemistry* **1999**, *274* (27), 19087-94.

126. Diebold, S. S.; Plank, C.; Cotten, M.; Wagner, E.; Zenke, M., Mannose receptor-mediated gene delivery into antigen presenting dendritic cells. *Somatic cell and molecular genetics* **2002**, *27* (1-6), 65-74.
127. Diebold, S. S.; Kurs, M.; Wagner, E.; Cotten, M.; Zenke, M., Mannose polyethylenimine conjugates for targeted DNA delivery into dendritic cells. *The Journal of biological chemistry* **1999**, *274* (27), 19087-94.
128. Diebold, S. S.; Plank, C.; Cotten, M.; Wagner, E.; Zenke, M., Mannose receptor-mediated gene delivery into antigen presenting dendritic cells. *Somatic cell and molecular genetics* **2002**, *27* (1-6), 65-74.
129. Keler, T.; Ramakrishna, V.; Fanger, M. W., Mannose receptor-targeted vaccines. *Expert opinion on biological therapy* **2004**, *4* (12), 1953-62.
130. Allavena, P.; Chieppa, M.; Monti, P.; Piemonti, L., From pattern recognition receptor to regulator of homeostasis: the double-faced macrophage mannose receptor. *Critical reviews in immunology* **2004**, *24* (3), 179-92.
131. Apostolopoulos, V.; McKenzie, I. F., Role of the mannose receptor in the immune response. *Current molecular medicine* **2001**, *1* (4), 469-74.
132. Regnier-Vigouroux, A., The mannose receptor in the brain. *International review of cytology* **2003**, *226*, 321-42.
133. Jiang, H.-L.; Kim, Y.-K.; Arote, R.; Jere, D.; Quan, J.-S.; Yu, J.-H.; Choi, Y.-J.; Nah, J.-W.; Cho, M.-H.; Cho, C.-S., Mannosylated chitosan-graft-polyethylenimine as a gene carrier for Raw 264.7 cell targeting. *International journal of pharmaceutics* **2009**, *375* (1-2), 133-139.
134. Kim, T. H.; Jin, H.; Kim, H. W.; Cho, M. H.; Cho, C. S., Mannosylated chitosan nanoparticle-based cytokine gene therapy suppressed cancer growth in BALB/c mice bearing CT-26 carcinoma cells. *Molecular Cancer Therapeutics* **2006**, *5* (7), 1723-32.
135. Zhou, X.; Liu, B.; Yu, X.; Zha, X.; Zhang, X.; Chen, Y.; Wang, X.; Jin, Y.; Wu, Y.; Shan, Y.; Liu, J.; Kong, W.; Shen, J., Controlled release of PEI/DNA complexes from mannose-bearing chitosan microspheres as a potent delivery system to enhance immune response to HBV DNA vaccine. *Journal of Controlled Release* **2007**, *121* (3), 200-7.
136. Diebold, S. S.; Lehrmann, H.; Kurs, M.; Wagner, E.; Cotten, M.; Zenke, M., Efficient gene delivery into human dendritic cells by adenovirus polyethylenimine and mannose polyethylenimine transfection. *Human gene therapy* **1999**, *10* (5), 775-86.
137. Zhou, X.; Liu, B.; Yu, X.; Zha, X.; Zhang, X.; Chen, Y.; Wang, X.; Jin, Y.; Wu, Y.; Chen, Y.; Shan, Y.; Chen, Y.; Liu, J.; Kong, W.; Shen, J., Controlled release of PEI/DNA complexes from mannose-bearing chitosan microspheres as a potent delivery system to enhance immune response to HBV DNA vaccine. *Journal of Controlled Release* **2007**, *121* (3), 200-7.

138. Hashimoto, M.; Morimoto, M.; Saimoto, H.; Shigemasa, Y.; Yanagie, H.; Eriguchi, M.; Sato, T., Gene transfer by DNA/mannosylated chitosan complexes into mouse peritoneal macrophages. *Biotechnology letters* **2006**, *28* (11), 815-21.
139. Kim, T. H.; Nah, J. W.; Cho, M. H.; Park, T. G.; Cho, C. S., Receptor-mediated gene delivery into antigen presenting cells using mannosylated chitosan/DNA nanoparticles. *Journal of nanoscience and nanotechnology* **2006**, *6* (9-10), 2796-803.
140. Intra, J.; Salem, A. K., Fabrication, characterization and in vitro evaluation of poly(D,L-lactide-co-glycolide) microparticles loaded with polyamidoamine-plasmid DNA dendriplexes for applications in nonviral gene delivery. *Journal of pharmaceutical sciences* **2009**, *99* (1), 368-84.
141. Okada, H., One- and three-month release injectable microspheres of the LH-RH superagonist leuprorelin acetate. *Advanced drug delivery reviews* **1997**, *28* (1), 43-70.
142. Barrow, E. L.; Winchester, G. A.; Staas, J. K.; Quenelle, D. C.; Barrow, W. W., Use of microsphere technology for targeted delivery of rifampin to Mycobacterium tuberculosis-infected macrophages. *Antimicrobial Agents and Chemotherapy* **1998**, *42* (10), 2682-9.
143. Luten, J.; van Nostrum, C. F.; De Smedt, S. C.; Hennink, W. E., Biodegradable polymers as non-viral carriers for plasmid DNA delivery. *Journal of Controlled Release* **2008**, *126* (2), 97-110.
144. Bilati, U.; Allemann, E.; Doelker, E., Poly(D,L-lactide-co-glycolide) protein-loaded nanoparticles prepared by the double emulsion method--processing and formulation issues for enhanced entrapment efficiency. *Journal of Microencapsulation* **2005**, *22* (2), 205-14.
145. Kanchan, V.; Panda, A. K., Interactions of antigen-loaded polylactide particles with macrophages and their correlation with the immune response. *Biomaterials* **2007**, *28* (35), 5344-57.
146. Gary, D. J.; Puri, N.; Won, Y. Y., Polymer-based siRNA delivery: perspectives on the fundamental and phenomenological distinctions from polymer-based DNA delivery. *Journal of Controlled Release* **2007**, *121* (1-2), 64-73.
147. Yuan, X.; Li, L.; Rathinavelu, A.; Hao, J.; Narasimhan, M.; He, M.; Heitlage, V.; Tam, L.; Viqar, S.; Salehi, M., SiRNA drug delivery by biodegradable polymeric nanoparticles. *Journal of Nanoscience and Nanotechnology* **2006**, *6* (9-10), 2821-8.
148. Cun, D.; Foged, C.; Yang, M.; Fr̄kjÊr, S.; Nielsen, H. M. r., Preparation and characterization of poly(dl-lactide-co-glycolide) nanoparticles for siRNA delivery. *International journal of pharmaceutics* **2010**, *390* (1), 70-75.
149. Tahara, K.; Sakai, T.; Yamamoto, H.; Takeuchi, H.; Kawashima, Y., Establishing chitosan coated PLGA nanosphere platform loaded with wide variety of nucleic acid by complexation with cationic compound for gene delivery. *International journal of pharmaceutics* **2008**, *354* (1-2), 210-6.

150. Takeshita, F.; Ochiya, T., Therapeutic potential of RNA interference against cancer. *Cancer Science* **2006**, *97* (8), 689-696.
151. Ikeda, Y.; Taira, K., Ligand-targeted delivery of therapeutic siRNA. *Pharmaceutical Research* **2006**, *23* (8), 1631-40.
152. Liu, B., Exploring cell type-specific internalizing antibodies for targeted delivery of siRNA. *Briefings in Functional Genomics and Proteomics* **2007**, *6* (2), 112-9.
153. Koch, A. M.; Reynolds, F.; Merkle, H. P.; Weissleder, R.; Josephson, L., Transport Of Surface-Modified Nanoparticles Through Cell Monolayers. *ChemBioChem* **2005**, *6* (2), 337-345.
154. Dunlap, D. D.; Maggi, A.; Soria, M. R.; Monaco, L., Nanoscopic structure of DNA condensed for gene delivery. *Nucleic Acids Research* **1997**, *25* (15), 3095-101.
155. Toncheva, V.; Wolfert, M. A.; Dash, P. R.; Oupicky, D.; Ulbrich, K.; Seymour, L. W.; Schacht, E. H., Novel vectors for gene delivery formed by self-assembly of DNA with poly(L-lysine) grafted with hydrophilic polymers. *Biochimica et Biophysica Acta* **1998**, *1380* (3), 354-68.
156. Minagawa, K.; Matsuzawa, Y.; Yoshikawa, K.; Matsumoto, M.; Doi, M., Direct observation of the biphasic conformational change of DNA induced by cationic polymers. *FEBS Letters* **1991**, *295* (1-3), 67-9.
157. Borchard, G., Chitosans for gene delivery. *Advanced drug delivery reviews* **2001**, *52* (2), 145-50.
158. Stellwagen, N. C., Electrophoresis of DNA in agarose gels, polyacrylamide gels and in free solution. *Electrophoresis* **2009**, *30* (S1), S188-S195.
159. Smith, L. E.; Smallwood, R.; Macneil, S., A comparison of imaging methodologies for 3D tissue engineering. *Microscopy Research and Technique* **2010**, *73* (12), 1123-1133.
160. Nehal, K. S.; Gareau, D.; Rajadhyaksha, M., Skin Imaging With Reflectance Confocal Microscopy. *Seminars in Cutaneous Medicine and Surgery* **2008**, *27* (1), 37-43.
161. VanGuilder, H. D.; Vrana, K. E.; Freeman, W. M., Twenty-five years of quantitative PCR for gene expression analysis. *Biotechniques* **2008**, *44* (5), 619-26.
162. Berridge, M. V.; Herst, P. M.; Tan, A. S.; El-Gewely, M. R., Tetrazolium dyes as tools in cell biology: New insights into their cellular reduction. *Biotechnology Annual Review* **2005**, *Volume 11*, 127-152.
163. University of Iowa Office of Animal Resources.
<http://research.uiowa.edu/animal/>.
164. 2007. *Current Protocols in Immunology*.
165. Janeway, C., *Immunobiology*. 5 ed.; Garland Science: 2005.

166. Gorner, T.; Gref, R.; Michenot, D.; Sommer, F.; Tran, M. N.; Dellacherie, E., Lidocaine-loaded biodegradable nanospheres. I. Optimization Of the drug incorporation into the polymer matrix. *Journal of Controlled Release* **1999**, *57* (3), 259-68.
167. Hobel, S.; Koburger, I.; John, M.; Czubayko, F.; Hadwiger, P.; Vornlocher, H. P.; Aigner, A., Polyethylenimine/small interfering RNA-mediated knockdown of vascular endothelial growth factor in vivo exerts anti-tumor effects synergistically with Bevacizumab. *The Journal of Gene Medicine* **2010**, *12* (3), 287-300.
168. Soppimath, K. S.; Aminabhavi, T. M.; Kulkarni, A. R.; Rudzinski, W. E., Biodegradable polymeric nanoparticles as drug delivery devices. *Journal of Controlled Release* **2001**, *70* (1-2), 1-20.
169. Promega *siCHECKTM Vectors: Technical Bulletin*; Promega: 2005.
170. User:Braindamaged TaqMan probe chemistry mechanism. <http://en.wikipedia.org/wiki/File:Taqman.png>.
171. Rudzinski, W. E.; Aminabhavi, T. M., Chitosan as a carrier for targeted delivery of small interfering RNA. *International journal of pharmaceutics* **2010**, *399* (1-2), 1-11.
172. Noh, S. M.; Park, M. O.; Shim, G.; Han, S. E.; Lee, H. Y.; Huh, J. H.; Kim, M. S.; Choi, J. J.; Kim, K.; Kwon, I. C.; Kim, J.-S.; Baek, K.-H.; Oh, Y.-K., Pegylated poly-l-arginine derivatives of chitosan for effective delivery of siRNA. *Journal of Controlled Release* **2010**, *145* (2), 159-164.
173. Fernandez-Megia, E.; Novoa-Carballal, R. n.; Quijón, E.; Riguera, R., Conjugation of Bioactive Ligands to PEG-Grafted Chitosan at the Distal End of PEG. *Biomacromolecules* **2007**, *8* (3), 833-842.
174. Vyas, S. P.; Singh, A.; Sihorkar, V., Ligand-receptor-mediated drug delivery: an emerging paradigm in cellular drug targeting. *Critical Reviews in Therapeutic Drug Carrier Systems* **2001**, *18* (1), 1-76.
175. Diebold, S. S.; Lehrmann, H.; Kursa, M.; Wagner, E.; Cotten, M.; Zenke, M., Efficient Gene Delivery into Human Dendritic Cells by Adenovirus Polyethylenimine and Mannose Polyethylenimine Transfection. *Human Gene Therapy* **1999**, *10* (5), 775-786.
176. Hashimoto, M.; Morimoto, M.; Saimoto, H.; Shigemasa, Y.; Yanagie, H.; Eriguchi, M.; Sato, T., Gene Transfer by DNA/mannosylated Chitosan Complexes into Mouse Peritoneal Macrophages. *Biotechnology Letters* **2006**, *28* (11), 815-821.
177. Brus, C.; Petersen, H.; Aigner, A.; Czubayko, F.; Kissel, T., Physicochemical and biological characterization of polyethylenimine-graft-poly(ethylene glycol) block copolymers as a delivery system for oligonucleotides and ribozymes. *Bioconjugate chemistry* **2004**, *15* (4), 677-84.
178. Yamaoka, T.; Tabata, Y.; Ikada, Y., Distribution and tissue uptake of poly(ethylene glycol) with different molecular weights after intravenous administration to mice. *Journal of pharmaceutical sciences* **1994**, *83* (4), 601-6.

179. Handwerker, R. G.; Diamond, S. L., Biotinylated Photocleavable Polyethylenimine: Capture and Triggered Release of Nucleic Acids from Solid Supports. *Bioconjugate chemistry* **2007**, *18* (3), 717-723.
180. Sagara, K.; Kim, S. W., A new synthesis of galactose-poly(ethylene glycol)-polyethylenimine for gene delivery to hepatocytes. *Journal of Controlled Release* **2002**, *79* (1-3), 271-281.
181. Storm, G.; Belliot, S. O.; Daemen, T.; Lasic, D. D., Surface modification of nanoparticles to oppose uptake by the mononuclear phagocyte system. *Advanced drug delivery reviews* **1995**, *17* (1), 31-48.
182. Howard, K. A.; Paludan, S. R.; Behlke, M. A.; Besenbacher, F.; Deleuran, B.; Kjems, J., Chitosan/siRNA Nanoparticle-mediated TNF-[alpha] Knockdown in Peritoneal Macrophages for Anti-inflammatory Treatment in a Murine Arthritis Model. *Molecular Therapy* **2008**, *17* (1), 162-168.
183. Kim, T. H.; Park, I. K.; Nah, J. W.; Choi, Y. J.; Cho, C. S., Galactosylated chitosan/DNA nanoparticles prepared using water-soluble chitosan as a gene carrier. *Biomaterials* **2004**, *25* (17), 3783-3792.
184. Opanasopit, P.; Techaarpornkul, S.; Rojanarata, T.; Ngawhirunpat, T.; Ruktanonchai, U., Nucleic Acid Delivery with Chitosan Hydroxybenzotriazole. *Oligonucleotides* **2010**, *20* (3), 127-136.
185. Techaarpornkul, S.; Wongkupasert, S.; Opanasopit, P.; Apirakaramwong, A.; Nunthanid, J.; Ruktanonchai, U., Chitosan-Mediated siRNA Delivery In Vitro - Effect of Polymer Molecular Weight, Concentration and Salt Forms. *AAPS PharmSciTech* **2010**, *11* (1), 64-72.
186. Kunath, K.; Merdan, T.; Hegener, O.; Häberlein, H.; Kissel, T., Integrin targeting using RGD-PEI conjugates for in vitro gene transfer. *The Journal of Gene Medicine* **2003**, *5* (7), 588-599.
187. Lu, B.; Wang, C.-F.; Wu, D.-Q.; Li, C.; Zhang, X.-Z.; Zhuo, R.-X., Chitosan based oligoamine polymers: Synthesis, characterization, and gene delivery. *Journal of Controlled Release* **2009**, *137* (1), 54-62.
188. Jen, K. Y.; Gewirtz, A. M., Suppression of gene expression by targeted disruption of messenger RNA: available options and current strategies. *Stem Cells* **2000**, *18* (5), 307-19.
189. Beyerle, A.; Merkel, O.; Stoeger, T.; Kissel, T., PEGylation affects cytotoxicity and cell-compatibility of poly(ethylene imine) for lung application: Structure-function relationships. *Toxicology and Applied Pharmacology* **2010**, *242* (2), 146-154.
190. Yamaoka, T.; Tabata, Y.; Ikada, Y., Comparison of body distribution of poly(vinyl alcohol) with other water-soluble polymers after intravenous administration. *The Journal of pharmacy and pharmacology* **1995**, *47* (6), 479-86.
191. Lee, S. H.; Kim, S. H.; Park, T. G., Intracellular siRNA delivery system using polyelectrolyte complex micelles prepared from VEGF siRNA-PEG conjugate

- and cationic fusogenic peptide. *Biochemical and Biophysical Research Communications* **2007**, *357* (2), 511-6.
192. Clements, B.; Bai, J.; Kucharski, C.; Farrell, L.; Lavasanifar, A.; Ritchie, B.; Ghahary, A.; Uludağ, H., RGD Conjugation to Polyethyleneimine Does Not Improve DNA Delivery to Bone Marrow Stromal Cells. *Biomacromolecules* **2006**, *7* (5), 1481-1488.
 193. Biswal, B. K.; Debata, N. B.; Verma, R. S., Development of a targeted siRNA delivery system using FOL-PEG-PEI conjugate. *Molecular Biology Reports* **2010**, *37* (6), 2919-2926.
 194. Breunig, M.; Hozsa, C.; Lungwitz, U.; Watanabe, K.; Umeda, I.; Kato, H.; Goepferich, A., Mechanistic investigation of poly(ethylene imine)-based siRNA delivery: disulfide bonds boost intracellular release of the cargo. *Journal of Controlled Release* **2008**, *130* (1), 57-63.
 195. Kang, J. H.; Tachibana, Y.; Kamata, W.; Mahara, A.; Harada-Shiba, M.; Yamaoka, T., Liver-targeted siRNA delivery by polyethylenimine (PEI)-pullulan carrier. *Bioorganic & Medicinal Chemistry* **2010**, *18* (11), 3946-3950.
 196. Patnaik, S.; Arif, M.; Pathak, A.; Singh, N.; Gupta, K. C., PEI-alginate nanocomposites: Efficient non-viral vectors for nucleic acids. *International journal of pharmaceutics* **2010**, *385* (1-2), 194-202.
 197. Kawakami, S.; Hashida, M., Targeted delivery systems of small interfering RNA by systemic administration. *Drug metabolism and pharmacokinetics* **2007**, *22* (3), 142-51.
 198. Katayose, S.; Kataoka, K., Water-soluble polyion complex associates of DNA and poly(ethylene glycol)-poly(L-lysine) block copolymer. *Bioconjugate chemistry* **1997**, *8* (5), 702-7.
 199. Merkel, O. M.; Beyerle, A.; Librizzi, D.; Pfestroff, A.; Behr, T. M.; Sproat, B.; Barth, P. J.; Kissel, T., Nonviral siRNA Delivery to the Lung: Investigation of PEG-PEI Polyplexes and Their In Vivo Performance. *Molecular Pharmaceutics* **2009**, *6* (4), 1246-1260.
 200. Kunath, K.; von Harpe, A.; Fischer, D.; Kissel, T., Galactose-PEI-DNA complexes for targeted gene delivery: degree of substitution affects complex size and transfection efficiency. *Journal of Controlled Release* **2003**, *88* (1), 159-72.
 201. Lecocq, M.; Wattiaux-De Coninck, S.; Laurent, N.; Wattiaux, R.; Jadot, M., Uptake and Intracellular Fate of Polyethylenimine in Vivo. *Biochemical and Biophysical Research Communications* **2000**, *278* (2), 414-418.
 202. Barber, R. D.; Harmer, D. W.; Coleman, R. A.; Clark, B. J., GAPDH as a housekeeping gene: analysis of GAPDH mRNA expression in a panel of 72 human tissues. *Physiological Genomics* **2005**, *21* (3), 389-395.
 203. Thomasin, C.; Corradin, G.; Men, Y.; Merkle, H. P.; Gander, B., Tetanus toxoid and synthetic malaria antigen containing poly(lactide)/poly(lactide-co-glycolide) microspheres: importance of polymer degradation and antigen release for immune response. *Journal of Controlled Release* **1996**, *41* (1-2), 131-145.

204. Walter, E.; Dreher, D.; Kok, M.; Thiele, L.; Kiama, S. G.; Gehr, P.; Merkle, H. P., Hydrophilic poly(dl-lactide-co-glycolide) microspheres for the delivery of DNA to human-derived macrophages and dendritic cells. *Journal of Controlled Release* **2001**, *76* (1-2), 149-168.
205. Prior, S.; Gander, B.; Blarer, N.; Merkle, H. P.; Subir, M. L.; Irache, J. M.; Gamazo, C., In vitro phagocytosis and monocyte-macrophage activation with poly(lactide) and poly(lactide-co-glycolide) microspheres. *European Journal of Pharmaceutical Sciences* **2002**, *15* (2), 197-207.
206. Newman, K. D.; Elamanchili, P.; Kwon, G. S.; Samuel, J., Uptake of poly(D,L-lactic-co-glycolic acid) microspheres by antigen-presenting cells in vivo. *Journal of Biomedical Materials Research* **2002**, *60* (3), 480-486.
207. Perlstein, I.; Connolly, J. M.; Cui, X.; Song, C.; Li, Q.; Jones, P. L.; Lu, Z.; DeFelice, S.; Klugherz, B.; Wilensky, R.; Levy, R. J., DNA delivery from an intravascular stent with a denatured collagen-poly(lactic-co-glycolic acid)-controlled release coating: mechanisms of enhanced transfection. *Gene Therapy* **2003**, *10* (17), 1420-1428.
208. Cohen, H., Levy, R.J., Gao, J., Fishbein, I., Kousaev, V., Sosnowski, S., Slomkowski, S., and Golomb, G., Sustained delivery and expression of DNA encapsulated in polymeric nanoparticles. *Gene Therapy* **2000**, *7* (22), 1896-1905.
209. Panyam, J.; Sahoo, S. K.; Prabha, S.; Bargar, T.; Labhasetwar, V., Fluorescence and electron microscopy probes for cellular and tissue uptake of poly(-lactide-co-glycolide) nanoparticles. *International journal of pharmaceutics* **2003**, *262* (1-2), 1-11.
210. Panyam, J.; Zhou, W.-Z.; Prabha, S.; Sahoo, S. K.; Labhasetwar, V., Rapid endo-lysosomal escape of poly(DL-lactide-co-glycolide) nanoparticles: implications for drug and gene delivery. *The FASEB Journal* **2002**, *16* (10), 1217-1226.
211. Malek, A.; Czubayko, F.; Aigner, A., PEG grafting of polyethylenimine (PEI) exerts different effects on DNA transfection and siRNA-induced gene targeting efficacy. *Journal of Drug Targeting* **2008**, *16* (2), 124-39.
212. Carrasquillo, K. G.; Ricker, J. A.; Rigas, I. K.; Miller, J. W.; Gragoudas, E. S.; Adamis, A. P., Controlled Delivery of the Anti-VEGF Aptamer EYE001 with Poly(lactic-co-glycolic)Acid Microspheres. *Investigative Ophthalmology & Visual Science* **2003**, *44* (1), 290-299.
213. De Rosa, G.; Quaglia, F.; La Rotonda, M. I.; Appel, M.; Alphandary, H.; Fattal, E., Poly(lactide-co-glycolide) microspheres for the controlled release of oligonucleotide/polyethylenimine complexes. *Journal of pharmaceutical sciences* **2002**, *91* (3), 790-9.
214. Pistel, K. F.; Kissel, T., Effects of salt addition on the microencapsulation of proteins using W/O/W double emulsion technique. *Journal of Microencapsulation* **2000**, *17* (4), 467-83.
215. Freytag, T.; Dashevsky, A.; Tillman, L.; Hardee, G. E.; Bodmeier, R., Improvement of the encapsulation efficiency of oligonucleotide-containing

- biodegradable microspheres. *Journal of Controlled Release* **2000**, *69* (1), 197-207.
216. Florence, A. T.; Whitehill, D., Stabilization of water/oil/water multiple emulsions by polymerization of the aqueous phases. *The Journal of pharmacy and pharmacology* **1982**, *34* (11), 687-91.
217. Crotts, G.; Park, T. G., Preparation of porous and nonporous biodegradable polymeric hollow microspheres. *Journal of Controlled Release* **1995**, *35* (2-3), 91-105.
218. Barman, S. P.; Lunsford, L.; Chambers, P.; Hedley, M. L., Two methods for quantifying DNA extracted from poly(lactide-co-glycolide) microspheres. *Journal of Controlled Release* **2000**, *69* (3), 337-344.
219. Patil, Y.; Panyam, J., Polymeric nanoparticles for siRNA delivery and gene silencing. *International journal of pharmaceutics* **2009**, *367* (1-2), 195-203.
220. Bivas-Benita, M.; Romeijn, S.; Junginger, H. E.; Borchard, G., PLGA-PEI nanoparticles for gene delivery to pulmonary epithelium. *European Journal of Pharmaceutics and Biopharmaceutics* **2004**, *58* (1), 1-6.
221. Gwak, S. J.; Kim, B. S., Poly(lactic-co-glycolic acid) nanosphere as a vehicle for gene delivery to human cord blood-derived mesenchymal stem cells: comparison with polyethylenimine. *Biotechnology Letters* **2008**, *30* (7), 1177-82.
222. Murata, N.; Takashima, Y.; Toyoshima, K.; Yamamoto, M.; Okada, H., Anti-tumor effects of anti-VEGF siRNA encapsulated with PLGA microspheres in mice. *Journal of Controlled Release* **2008**, *126* (3), 246-254.
223. Khan, A.; Benboubetra, M.; Sayyed, P. Z.; Wooi Ng, K.; Fox, S.; Beck, G.; Benter, I. F.; Akhtar, S., Sustained Polymeric Delivery of Gene Silencing Antisense ODNs, siRNA, DNazymes and Ribozymes: In Vitro and In Vivo Studies. *Journal of Drug Targeting* **2004**, *12* (6), 393-404.
224. Chollet, P.; Favrot, M. C.; Hurbin, A.; Coll, J. L., Side-effects of a systemic injection of linear polyethylenimine-DNA complexes. *The Journal of Gene Medicine* **2002**, *4* (1), 84-91.
225. Jain, A. K.; Swarnakar, N. K.; Godugu, C.; Singh, R. P.; Jain, S., The effect of the oral administration of polymeric nanoparticles on the efficacy and toxicity of tamoxifen. *Biomaterials* **2011**, *32* (2), 503-515.
226. Ozer, J.; Ratner, M.; Shaw, M.; Bailey, W.; Schomaker, S., The current state of serum biomarkers of hepatotoxicity. *Toxicology* **2008**, *245* (3), 194-205.
227. Nathwani, R. A.; Pais, S.; Reynolds, T. B.; Kaplowitz, N., Serum alanine aminotransferase in skeletal muscle diseases. *Hepatology* **2005**, *41* (2), 380-2.
228. Dhamelincourt, P., Barbillat, J., and Delhaye, M., Laser confocal Raman microspectrometry. *Spectroscopy Europe* **1993**, *5* (2), 16.
229. Clontech *pEGFP-C1 Vector Information*; Clontech: 2002.

230. Woodrow, K. A.; Cu, Y.; Booth, C. J.; Saucier-Sawyer, J. K.; Wood, M. J.; Mark Saltzman, W., Intravaginal gene silencing using biodegradable polymer nanoparticles densely loaded with small-interfering RNA. *Nature Materials* **2009**, *8* (6), 526-533.